



Universidade de Brasília – UnB
Instituto de Geociências – IG
Programa de Pós-graduação em Geologia

**Variação do tamanho corporal em répteis marinhos e sua relação com as extinções do
Mesozoico**

Lucila Monteiro de Souza



Brasília, agosto de 2018
Universidade de Brasília – UnB
Instituto de Geociências – IG
Programa de Pós-graduação em Geologia

**Variação do tamanho corporal em répteis marinhos e sua relação com as extinções do
Mesozoico**

Lucila Monteiro de Souza

Orientador: Prof. Dr. Rodrigo Miloni Santucci

Tese de Doutorado apresentada ao Instituto de Geociências da Universidade de Brasília como requisito parcial para obtenção do título de Doutor em Geologia, na área de concentração em Bioestratigrafia e Paleoecologia.

Brasília, agosto de 2018

Tese apresentada na forma de artigo conforme Art. 34 do Regimento da Pós-graduação do Instituto de Geociências da Universidade de Brasília.

RESUMO

Os répteis predadores marinhos desenvolveram-se na Era Mesozoica e tornaram-se componentes dominantes dos ecossistemas marinhos mundiais. Ao longo do Mesozoico vários grupos com afinidades filogenéticas distintas apresentaram sucesso evolutivo como predadores de topo e estiveram expostos a flutuações ambientais, stress climático e extinções em massa. O tamanho corporal é uma das propriedades biológicas mais básicas e significantes para a compreensão da história evolutiva de um grupo. Identificar padrões de tamanho corporal de grupos extintos como os répteis marinhos pode ampliar a interpretação sobre a estruturação dos ecossistemas marinhos atuais, auxiliando na diferenciação entre perturbações antropológicas e padrões resultantes de processos ecológicos e evolutivos em um grande espaço de tempo. Os répteis marinhos têm sido estudados com foco na descrição de novas espécies, revisão taxonômica e análises cladísticas. A busca por padrões paleoecológicos em larga escala tem sido de interesse recente entre os biólogos/paleontólogos, porém ainda pouco estudada. Este trabalho integra pela primeira vez dados de tamanhos corporais de plesiossauros, mosassauros e notossauros, juntamente com os ictiossauros, sob a óptica tanto de fatores biológicos (e.g. variação do tamanho corporal, morfologia dentária e preferências alimentares), como fatores abióticos relacionados aos eventos de extinção e variações do nível do mar, carbono, oxigênio, temperatura e distribuição geográfica das espécies de cada grupo. Nós testamos para Ichthyosauria, Nothosauria, Mosasauroidea e Plesiosauria mudanças direcionais do tamanho corporal usando análises filogenéticas e não filogenéticas, para verificar se estes grupos possuem uma tendência para a mudança evolutiva do tamanho corporal ao longo do tempo (aumento ou diminuição) e como os tamanhos variaram (ou foram afetados) através das extinções em massa. As análises não filogenéticas não indicaram nenhuma correlação entre aumento ou diminuição de tamanho e tempo para Ichthyosauria, Plesiosauria, Nothosauria e Mosasauroidea. Por outro lado, verificou-se uma tendência de seleção de espécies de tamanhos médios para Ichthyosauria e Plesiosauria, sendo estes tamanhos os sobreviventes frente aos eventos de extinção. As estratégias alimentares e a competição entre os grupos são fatores determinantes para compreender este padrão evolutivo.

Palavras-chave: Ichthyosauria, Plesiosauria, Nothosauria, Mosasauroidea, tamanho corporal, Mesozoico, extinções em massa.

SUMÁRIO

1- Apresentação	1
Capítulo 1- Variação do tamanho corporal em ictiossauros e sua relação com as extinções do Mesozoico	2
ABSTRACT.....	3
1-Introduction.....	4
2- Materials and Methods	6
Taxa.....	6
Body size estimate	7
Directional body size changes	8
Feeding habits.....	10
3- Results	12
4- Discussion.....	24
5- Conclusions.....	28
6- References.....	29
Supplementary Information S1	
Supplementary Information S2	
Supplementary Information S3	
Capítulo 2- Variação do tamanho corporal em répteis marinhos e sua relação com as extinções do Mesozoico	76
RESUMO.....	77
1- Introdução	78
2- Materiais e Métodos	81
Estimativa do tamanho corporal	81
Mudanças direcionais para o tamanho corporal	83
3- Resultados.....	85
4- Discussão	933
5- Conclusões	100

6- Referências	1022
Supplementary Information S1	
Supplementary Information S2	
Supplementary Information S3	

1- Apresentação

O formato dessa tese segue o Regulamento do Programa de Pós-graduação em Geologia da Universidade de Brasília, conforme o Art. 35 do Regimento, sendo apresentada na forma de artigos.

São analisados tamanhos corporais de espécies pertencentes a quatro grupos de répteis marinhos predadores extintos, incluindo: ictiossauros, plesiossauros, mosassauros e notossauros, e como estes tamanhos variaram frente aos eventos de extinção ao longo do Mesozoico. Elementos abióticos que oscilam frente a eventos de extinção como nível do mar, flutuações dos níveis de oxigênio, carbono e temperatura possuem grande influência nos ecossistemas marinhos mundiais e foram avaliados de forma integrada aos aspectos evolutivos e paleoecológicos. Este trabalho é estruturado em dois capítulos, ambos em forma de artigo. O Capítulo 1 discute a variação do tamanho corporal em espécies de ictiossauros frente ao impacto dos eventos de extinção na história evolutiva do grupo. Este artigo foi aceito para publicação na revista “*Palaeogeography, Palaeoclimatology, Palaeoecology*” e será citado no capítulo 2 como “Souza and Santucci (no prelo)” em virtude da necessidade de integração dos dados. Ressalta-se que esse artigo ainda se encontra em fase de revisão final e que as sugestões da banca examinadora serão incorporadas à versão final antes da publicação. O capítulo 2 discute a variação do tamanho corporal em espécies de plesiossauros, mosassauros e notossauros frente aos eventos de extinção, correlacionando os resultados com os dados encontrados para ictiossauros.

Cada um dos capítulos contém resumo, introdução, justificativa, objetivo, materiais e métodos, resultados, discussão, conclusões e referências bibliográficas. O capítulo 1 está escrito em inglês, segundo as normas do periódico internacional “*Palaeogeography, Palaeoclimatology, Palaeoecology*”. O capítulo 2 foi elaborado seguindo os padrões de periódicos internacionais e ainda se encontra em português.

Capítulo 1

Variação do tamanho corporal em ictiossauros e sua relação com as extinções do Mesozoico

ABSTRACT

Ichthyosauria is a group of marine reptiles that ruled Mesozoic seas for about 150 Ma until their extinction during the Cenomanian (30 Ma before the K-Pg mass extinction event). Their high diversity ranges from small eel-like to giant bodied species, which qualifies them as good candidates for studies on body size trends such as the Cope's rule, the tendency towards an increase in body size in an evolutionary lineage. In this work, we tested Ichthyosauria for directional changes in body size (within-lineage trend) using both, phylogenetic and non-phylogenetic approaches, to verify whether they have a tendency for body size change over time and how it varied (or has been affected) by mass extinctions events. Femoral, humeral, and skull lengths were collected (or estimated from humeral length) from 83 ichthyosaur species and were used as a proxy for body size. Palaeoenvironmental data as sea level, oxygen and carbon dioxide levels, and temperature, as well as feeding habits, were used to compose a more integrated global analysis. Despite both giant and small body sizes are present in the evolutionary history of the group, our data do not support a body size increase trend over evolutionary time in Ichthyosauria. However, the relative average-sized species became predominant, being the survivors over the environmental fluctuations. The Pangea breakup and dramatic changes on oceanic basins would probably have more influence in ichthyosaur feeding strategies and body size patterns than previously thought.

Key-words: Ichthyosauria, body size, mass extinctions, feeding habits

1-Introduction

Ichthyosauria is a group of diapsid marine reptiles that ruled global seas during most of the Mesozoic, specifically, from the Early Triassic (Olenekian) to the Late Cretaceous (Cenomanian) (Motani, 2005; Fischer *et al.*, 2014a). They are a diverse and successful clade of predators with a complex evolutionary history, a “land to sea” transition resulting in a fish- or dolphin-like body well-adapted to dive, which allowed them to occupy the highest trophic levels (Motani, 2001; Fischer *et al.*, 2016). Ichthyosaurs were the first marine reptiles (mosasaurs, plesiosaurs, and nothosaurs) to attain large sizes (Motani, 2005). Body size changes in ichthyosaurs were quite debated due to their intriguing extinction 30 million years before the Cretaceous-Paleogene mass extinction event and remains poorly understood. Their body size varies greatly, ranging from *Chaohusaurus geishanensis*, which reached only 0,7 m in length (Motani & You, 1998) to *Shonisaurus sikanniensis*, which is estimated to be approximately 21,0 m in length (Nicholls & Manabe, 2004). This qualifies them as a unique group for body size evaluation through time.

Body size is a key variable to understand ecological and physiological processes due to the benefits and side effects associated to larger sizes. The tendency of size increase over geological time, known as Cope’s Rule, and the influence on increasing body size by low temperatures reconized as Bergmann’s Rule is documented in many groups (Colbert, 1993; Atkinson, 1994; Arnold *et al.*, 1995; Alroy, 1998; Ashton *et al.*, 2000; Ashton, 2002). Ichthyosaurs were successful predators and, during the Mesozoic, they developed different diet styles (Motani, 2009), where the prey preference and the feeding strategy may be associated to competition success, predation,

and resources demand. Thus, significant changes in their food supply may have caused major changes on their body size and susceptibility to extinction (Hone & Benton, 2005).

Understanding body size variation in the history of biological groups is essential to disclose patterns and processes related to the evolution of extinct clades (Benson *et al.*, 2014). The ichthyosaur fossil record provides an abundant material, ensuring the accuracy of evolutionary change estimates over geologic time (Thorne *et al.*, 2011). Thus, they may reveal processes at the macro- and microevolutionary scales that are essential for the understanding of Mesozoic marine biological community structures. Some studies have analysed the high degree of ichthyosaur species survivorship across the Triassic-Jurassic boundary (201,3 My) and their reduction in disparity (Thorne *et al.*, 2011; Marek *et al.*, 2015; Fischer *et al.*, 2016) or the consequences of the Jurassic-Cretaceous mass extinction event on their diversity (Fischer *et al.*, 2012; Tennant *et al.*, 2016). Temperature, oxygen, carbon dioxide fluctuations, and sea-level changes are also considered as putative drivers for the evolutionary history of marine reptiles (Benson & Butler, 2011; Scheyer *et al.*, 2014; Fischer *et al.*, 2016).

Ichthyosaurs can not only clarify biological process that affected extinct marine reptiles, but they also can disclose important evolutionary information about the open ocean biota, revealing past environmental transitions (Fischer *et al.*, 2016). Additionally, during their evolutionary history, ichthyosaurs have faced two important mass extinctions (which delimitated the Triassic-Jurassic and Jurassic-Cretaceous boundaries, respectively) until their final demise during the Late Cretaceous. Considering their importance as a component of Mesozoic marine ecosystems, we tested the Ichthyosuria body size variation over time and how it varied (or has been

affected) across mass extinctions events. We use both phylogenetic and non-phylogenetic approaches to verify whether ichthyosaurs have an increase/decrease tendency for evolutionary body size change. Additionally, feeding habits, determined by teeth morphology (Massare, 1987) and geographic distribution during the Mesozoic were reviewed for each ichthyosaur species considered in this analysis to verify how they varied through mass extinctions events.

2- Materials and Methods

Taxa

We compiled a dataset on the preserved body, femur, and humerus lengths for 193 adult samples from 75 named ichthyosaur species, adding information of associated geological unit, age interval, geographic localities, and identification of the material. The adult individuals were identified by surface texture of the shaft of the humerus (i. e. smooth in mature animals) (Johnson, 1977), when available, and descriptive anatomical information (completely ossified epiphyses of long bones and fused cranial sutures of the dorsal skull roof) (Maxwell *et al.*, 2012) (Supplementary Information S1). Taxa and/or specimens represented by badly preserved materials, immature individuals, and lacking both femoral and humeral size information were not considered.

Ichthyosaurs have a broad geographic distribution, comprising taxa collected from Canada (McGowan, 1995; Nicholls & Manabe, 2004; Maxwell & Caldwell, 2006; Druckenmiller & Maxwell, 2010), USA, including Alaska (McGowan, 1972; Schmitz *et al.*, 2004; Massare *et al.*, 2006; Maxwell & Kear, 2010; Adams & Fiorillo, 2011; Druckenmiller *et al.*, 2014), Argentina (Fernández & Aguirre-Urreta,

2005; Fernández, 2007; Fernández & Maxwell, 2012), Chile (Stinnesbeck *et al.*, 2014), Norway (Motani, 1998; Druckenmiller *et al.*, 2012; Roberts *et al.*, 2014), Switzerland (Sander, 1989; Maisch & Reisdorf, 2006), England (McGowan, 1974, 1995b, 1996, 2003), Germany (McGowan, 1996; Maisch, 2008; Maxwell *et al.*, 2012), France (Motani, 2005; Fischer *et al.*, 2014b), Italy (Dal Sasso & Pinna, 1996), Russia (Arkhangelsky *et al.*, 2008, 2014; Fischer *et al.*, 2011), Iraq (Fischer *et al.*, 2013), China (Maisch & Hungerbühler, 2001; Nicholls *et al.*, 2003; Rieppel *et al.*, 2003; Jiang *et al.*, 2005; Ji *et al.*, 2013; Motani *et al.*, 2015), Japan (Motani, 1997), Thailand (Mazin *et al.*, 1991), and Australia (McGowan, 1972; Zammit, 2010; Zammit *et al.*, 2010), for example.

Body size estimate

Ichthyosaur specimens are generally well preserved, many of them in three dimensions and articulated, showing, in some instances, body outlines and other rarely preserved anatomical details (Marek *et al.*, 2015). Despite these rich and well-preserved materials, some specimens are not complete enough for a more accurate body size estimation. Long bones as humerus and femur have positive correlation with body size in extant birds (Butler & Goswami, 2008; Field *et al.*, 2013), mammals (Christiansen, 1999; Egi, 2001), terrestrial tetrapods (Campione & Evans, 2012), and dinosaurs (Carrano, 2006; Therrien *et al.*, 2007; Souza & Santucci, 2014). Skull length also has a positive correlation with body length in Mesozoic mammals (Pyenson & Sponberg, 2011) and archosauromorphs (Hurlburt *et al.*, 2003). Thus, correlations between humerus and femur were assessed to test their validity for ichthyosaurs.

To estimate body size variation within ichthyosaurs, different body plans must be considered. Basal Late Triassic lizard-like ichthyosaurs are related to the rise of derived parvipelvians (Fischer *et al.*, 2014b), for example. Taking these differences in body size patterns into account, we divided Ichthyopterygia into two distinct groups according to their morphological evolutionary history: the lizard-like Ichthyopterygia, ranging from the most basal Ichthyopterygia to Euichthyosauria and the thunniform parvipelvians. This arrangement was applied to improve the accuracy of body size estimations.

The large amount of fossil material described ensures robust experimental regression equations to find out possible linear relations among body length and other skeletal element measurements (e.g. humerus and femur), which maximizes the number of taxa with information about body length. Thus, Shapiro Wilk's test was applied to all femur and humerus measurements. After checking the normal distribution of the data (Supplementary Information S2A), we tested the presence of linear correlation between humerus and femur for the species that have both elements preserved (Supplementary Information S2B). The resulting equation was applied to estimate the humerus length in taxa that only have the femur preserved. Finally, we created a data set comprising humerus and femur lengths for all studied taxa and the humerus length was used as a proxy for the entire body size.

Directional body size changes

The age, in Ma, assigned to each taxon was obtained by calculating the average age of the total time span of the taxon available in the literature. We assigned absolute geochronological ages to the chronostratigraphic boundaries by using the

International Chronostratigraphic Chart (Cohen *et al.*, 2013). Thus, parametric statistics have been employed in nonphylogenetic approaches and carried out in PAST (Hammer *et al.*, 2001). Our nonphylogenetic approach assessed body size trends by adjusting humerus lengths against stratigraphic ages of each taxon in a linear regression to test for body size increase/decrease trends through time in Ichthyopterygia and its subclades (Ichthyosauria, Hueneosauria, Merriamosauria, Euichthyosauria, Parvipelvia, Thunnosauria, Baracromia, Ophtalmosauridae, and Platypterygiinae) (Supplementary Information S2C) because Cope's rule is rarely tested in a variety of taxonomic levels (Klompmaker *et al.*, 2015).

We calculated the mean and standard deviation of humerus length for the geological time intervals, Triassic (251,2-201,3 My), Lower Jurassic (201,3-174,1 My), Middle/Upper Jurassic (174,1-145), and Early Cretaceous (145,0-100,3 My) to test if the 75 species included in the nonphylogenetic approach have any increase or decrease trend in body size variation.

Most ichthyosaur phylogenies generally encompass the same taxa and have compatible topologies (Motani, 1999; Maisch & Matzke, 2000). Because of that, we select three well-resolved ichthyosaur phylogenies encompassing high number of taxa: 1) Jiang *et al.* (2016), 2) Ji *et al.* (2015) because they considered several basal taxa, and 3) Fischer *et al.* (2016), because they depicted well-resolved apical taxa. The monophyletic subclades Ichthyosauria, Hueneosauria, Merriamosauria, were taken from Jiang *et al.* (2016) and Euichthyosauria and Parvipelvia were taken from Ji *et al.* (2015), whereas the most derived subclades, such as Thunnosauria, Baracromia, Ophtalmosauridae, and Platypterygiinae were taken from Fischer *et al.* (2016).

The compiled tree was used to calculate the ancestor-pairwise comparison using weighted squared-change parsimony (SCP) in Mesquite 3.2 (Maddison & Maddison, 2017). This method was used to compare traits within species lineages in each branch to calculate ancestral states for the 53 Ichthyopterygia species. Ancestral states algorithm calculates the ancestral values for humerus length for a given node by considering the distance, in millions of years, from its direct descendants in the tree and the humerus length of these descendants. We used log humerus lengths as a proxy of body size. A 3 My interval was inferred for the internodes, as proposed in Laurin (2004) and Butler & Goswami (2008) in previous studies of this nature.

Trends within lineages were based on a time calibrated tree, comparisons among terminal taxa, ancestral nodes, and among internal nodes provided the body size change trends that occurred within the clades Ichthyopterygia, Ichthyosauria, Hueneosauria, Merriamosauria, Euichthyosauria, Parvipelvia, Thunnosauria, Baracromia, Ophthalmosauridae, and Platypterygiinae. We used chi-square test to verify if body increase and decrease changes within clades occurred at equal rates (null hypothesis) or if they follow any directional trend (Supplementary Information S3).

Feeding habits

The 75 species were classified into different ecological feeding habits by considering teeth morphology and gut contents previously available in literature (Massare, 1987; Dick & Maxwell, 2015b; Fischer *et al.*, 2016). Triassic ichthyosaurs present a wide range of ecological feeding habits, the generalist ambush genera feed on hard shelled prey in circalittoral zones (Massare, 1988; Dick & Maxwell, 2015b) and were present from the east to the northwest of Pangea. The crunch genera emerged in

the Anisian and occupied regions equivalent to China, Italy, Canada, and USA territories in Pangea. They are characterized by fairly robust, blunt teeth to crush hard prey items such as armoured fish, crustaceans, and, possibly, thin-shelled ammonite (Massare, 1987; Jiang *et al.*, 2008). Gut contents of a crunch species, *Ichthyosaurus communis*, include *Pholidophorus* fish scales and cephalopod hooklets (Pollard, 1968; Massare, 1987). The smash genera also appeared in the Anisian and occupied the regions equivalent to China, Italy, and North America territories in Pangea. Their acute but rounded apex teeth (Fischer *et al.*, 2011) were used to grasp soft prey such as belemnoids and soft cephalopod (Massare, 1987). For instance, *Stenopterygius* has gut contents consisting of cephalopod hooklets, fish remains, and bits of wood (Pollard, 1968; Massare, 1987; Dick & Maxwell, 2015a). The complete loss or reduction of teeth in some adult species is referred to, in the literature (e.g. Nicholls & Manabe, 2004), as edentulous and we treated this feature as a particular feeding habit given its widespread use in the literature. Due to this peculiar trait, a filter feeding was suggested for some taxa (Nicholls & Manabe, 2004) as well as the preference for slow moving soft body prey (Motani *et al.*, 2013). This includes giant species such as *Shonisaurus*, which inhabited the regions equivalent to China, Canada, and North America territories of Pangea.

Feeding habits were quite diverse during the Jurassic and many of them persisted until the Cretaceous. The pierce genera are typified by having pointed teeth with long, delicate, sharply or smooth morphology, used for piercing preferably small fish and soft cephalopod (Massare, 1987). They are mainly found on European deposits such as England and Germany. The cut genera are present in European (England and Germany) sedimentary rocks; the preference for vertebrate prey is evidenced by the preserved gut contents of *Temnodontosaurs*, which comprise marine reptile remains and

large fish (Martin *et al.*, 2012). They are characterized morphologically by large sized species with sharp, robust, cutting, and large teeth that exhibits well-marked carinae (Massare, 1987).

3- Results

We used linear regressions to estimate femur and humerus lengths for apical taxa (thunniform) which lack these elements. Linear correlations were initially used to test if humerus and femur lengths are correlated. Linear correlation for derived taxa (Supplementary Information S2B) were tested for 19 species with both femur and humerus resulting in the equation, $y = 1,2985x + 1,3075$ (Pearson's $r^2 = 0,94$ and $P<0.05$), which was used to estimate humerus length for those species in which only the femur is preserved. The taxa *Ophthalmosaurus icenicus*, *Stenopterygius quadriscissus*, *S. uniter*, and *S. triscissus* have more than one specimen reported in the literature and the mean values for humerus length were used.

Linear correlation was also tested in basal taxa where seven species were used and one of these, *Guanlingsaurus liangae* has more than one specimen reported in the literature. We used the mean of femur and humerus lengths in this case. Seven species have both femur and humerus belonging to the same specimen. The resulting correlation is described by the following equation, $y = 1,3297x - 2,5992$ (Pearson's $r^2 = 0,97$ and $P<0.05$), which was used to estimate the humerus length for basal species that only have the femur preserved. Finally, humerus lengths were used as a proxy to assess increase and decrease trends in body size.

The nonphylogenetic approach includes a total of 75 species, where 55 of them have information regarding the humerus dimensions available. For the remaining 20 species, the humerus length was estimated by linear regressions. The regression analysis of log transformed humerus lengths and mean stratigraphic age furnished the regression line $y = -0,0026x + 1,4447$ ($r^2 = 0,1429$ and $P < 0,01$) for the correlation between humerus length and mean age intervals for Ichthyopterygia (Figure 5). The regression line (Supplementary Information 2C) depicts a tendency toward body size increasing during the evolution of the group, but the x-axis (time) explains only 14,29% of the y-axis (log humerus length) variance, suggesting a weak correlation between body size and time. The correlation between log humerus length and stratigraphic age does not support a body size increase trend in ichthyosaurs. All subclades (Ichthyosauria, Hueneosauria, Merriamosauria, Euichthyosauria, Parvipelvia, Thunnosauria, Baracromia, Ophthalmosauridae, and Platypterygiinae) also show the same weak correlation between humerus length and age (Supplementary Information 2C), being that Euichthyosauria presents the highest correlation value ($r^2 = 0,22$) among all subclades analysed, with a significant relationship $P = 0,004$ and Baracromia presents the weakest correlation ($r^2 = 0,001$) among all subclades with nonsignificant relationship $P = 0,86$. Despite nonphylogenetic analysis provide no support for any significant positive/negative relationship between body size and stratigraphic age, a tendency for increasing body size is observed in some Ichthyopterygia clades (Supplementary Information 2C).

A second nonphylogenetic analysis was made by using the log humerus mean length, rather than the largest length, for all 75 species to test (increase/decrease tendency) in body size (Table 1) for a given time interval. Triassic taxa present the highest standard deviation, with species ranging in size from *Chaohusaurus*

geishanensis (0,7 m) to *Shonisaurus sikanniensis* (21,0 m). Body size mean increases from the Triassic to the Early Cretaceous showing an increase in average size in Ichthyopterygia. But, on the other hand, as body size increases, standard deviation decreases abruptly between the Triassic and the Late Jurassic (Table 1).

Time interval	n	Minimum humerus	Maximum humerus	Mean	Standard deviation
Triassic (251,2 Ma-201,3 Ma)	25	1,7	56,75	11,1	13,57
EoJurassic (201,3 Ma-174,1 Ma)	19	5,15	30,93	10,66	5,96
NeoJurassic (174,1 Ma-145 Ma)	21	5,08	20,51	13,01	3,59
Cretaceous (145 Ma-100,3 Ma)	10	7,5	16,70	11,91	3,41

Table 1. Standard deviation of Ichthyopterygia body size for four time intervals (Triassic 251,2 Ma-201,3 Ma; EoJurassic 201,3 Ma- 174,1 Ma; NeoJurassic 174,1 Ma- 145 Ma; Cretaceous 145 Ma- 100,3 Ma).

The phylogenetic approach encompasses 52 taxa (Figure 2) that were included in at least one of the three chosen cladograms (Ji *et al.*, 2015, 2016; Fischer *et al.*, 2016). Other 21 taxa used in the nonphylogenetic approach were excluded because their phylogenetic relationships are not well established. The calibrated tree has been used to calculate ancestor-descendent changes (see Supplementary Information S3) for Ichthyopterygia, Ichthyosauria, Hueneosauria, Merriamosauria, Euichthyosauria, Parvipelvia, Thunnosauria, Baracromia, Ophthalmosauridae, and Platynptyeriinae. The ancestor-descendent body size comparison shows more positive changes than negative ones for all these ten subclades and for Ichthyopterygia, Ichthyosauria, Hueneosauria, Merriamosauria, Euichthyosauria subclades positive changes are statistically significant. The sum, mean, median, and skew were positive for all subclades (Table 2).

The ancestral humerus lengths (node values) were compared with changes along branches. It can be noted that positive changes exceed negative ones ranging from -0,4 to 0,3 (Figure 1 and Table 2). According to chi-square goodness-of-fit tests, the null hypothesis cannot be rejected and despite positive/negative changes in Ichthyopterygia do not occur at equal rates, this pattern is not out of a random pattern of 50% increases or decreases. Thus, ichthyosaurs do not seem to present a tendency to increase in body size over time.

	Sum	Mean	Median	Skew	N	Positive changes	Negative changes	χ^2	P
Ichthyopterygia	1,31	0,01	0,02	0,13	93	60	33	3,98	0,04
Ichthyosauria	1,56	0,01	0,02	0,13	85	56	29	4,37	0,03
Hueneosauria	1,16	0,01	0,02	0,13	81	54	27	4,60	0,03
Merriamosauria	1,61	0,02	0,02	0,12	76	52	26	5,33	0,02
Euichthyosauria	0,47	0,007	0,01	0,12	64	42	21	3,57	0,05
Parvipelvia	0,72	0,01	0,01	0,11	53	35	18	2,77	0,09
Thunnosauria	0,56	0,01	0,01	0,06	37	24	13	1,65	1,19
Baracromia	0,43	0,01	0,01	0,06	33	22	11	1,85	0,17
Ophthalmosauridae	0,40	0,01	0,01	0,06	28	19	9	1,84	0,17
Platypterygiinae	-0,06	-0,003	0	0,06	16	10	6	0,50	0,47

Table 2. Ancestor-descendent pairwise comparison results for Ichthyopterygia based on the phylogenetic data available in the supertree (52 taxa). The values of sum, mean, median, skew, positive and negative changes were calculated from the differences between log10 skull length of the terminal taxa and ancestral states (internal nodes) and differences between internal nodes for each clade. Chi-squared tests the null hypothesis that body size increases and decreases are equally likely.

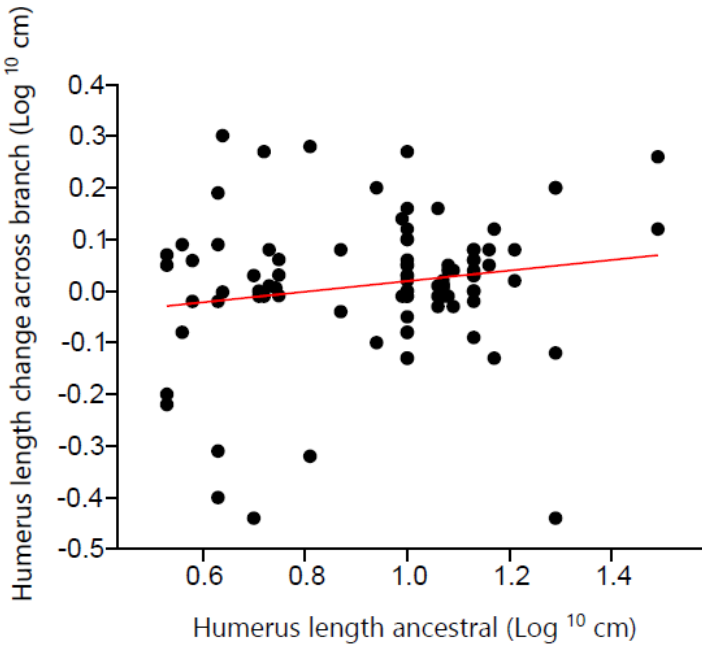


Fig. 1 Changes between ancestor and descendants. Scatter plot comparing ancestral size at nodes in the supertree (log₁₀ humerus length, y-axis) against calculated changes through the branches (log₁₀ humerus length, x-axis).

All species depicted in the calibrated phylogeny were assigned to some feeding habit to test if they are associated to monophyletic groups (Figure 2). The sharing of morphological characteristics such as skull size and tooth shape could define feeding strategies and prey preferences within a lineage.

Figure 3 depicts the age (Ma) and humerus size (Log10) for the 75 species used in the non-phylogenetic approach. To each species a colour representing the feeding habits were assigned. In this way, it shows the ichthyosaur feeding habit arrangement through time and how they were affected by mass extinctions events across the Mesozoic. The ambush-generalist specimens (red dots) with facultative durophagy (Dick & Maxwell, 2015b) comprises 5 species. They have been restricted to the Early Triassic and disappeared from the geological record since then. The crunch specimens (blue dots) used to feed on hard prey such as armoured fish (Dick & Maxwell, 2015b)

and are represented by eight species that appeared in the Early Triassic surviving until the Late Jurassic (Massare, 1987; Dick & Maxwell, 2015b). The dark green dots represent the smash feeding habit, it is characterized by the preference for hunt on soft prey such as belemnoids and soft cephalopod (Dick & Maxwell, 2015b). They encompasses 24 species and appear during the Early Triassic facing the Tr-J bottleneck successfully, surviving until the Cretaceous with a life span of 146,5 My (Massare, 1987; Dick & Maxwell, 2015b). The yellow dots comprise edentulous species (mainly shastasaurids) which had preference for soft body prey (Nicholls & Manabe, 2004). They are represented by 7 species that emerged during the Late Triassic and were registered until the Early Jurassic-Middle Jurassic transition.

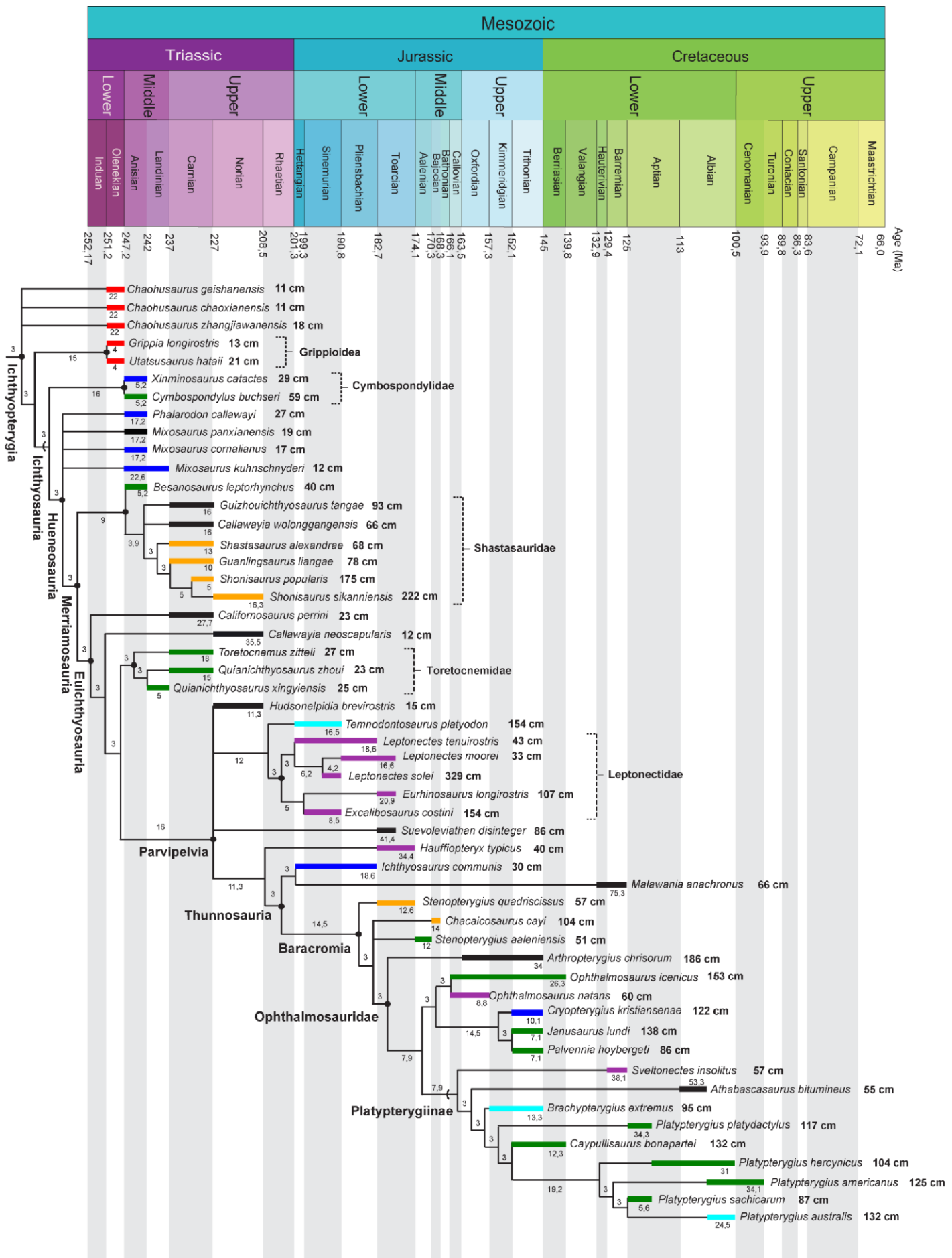


Fig. 2 Calibrated supertree depicting the phylogenetic relationships for Ichthyopterygia. The clades used in ancestral-descendant comparisons (Ichthyosauria, Hueneosauria, Merriamosauria, Euichthyosuria, Parvipelvia, Thunnosauria, Baracromia, Ophthalmosauridae, and Platypterygiinae) are indicated by black dots (node based) or by curved lines (stem based). The number beside each taxon indicates their temporal range. The measurement (cm) above each species indicates their respective size based on the humerus length. The color of the bars indicates the ecological feeding habits as suggested by Massare (1987) and Dick & Maxwell (2015). See the color key in the Fig. 3.

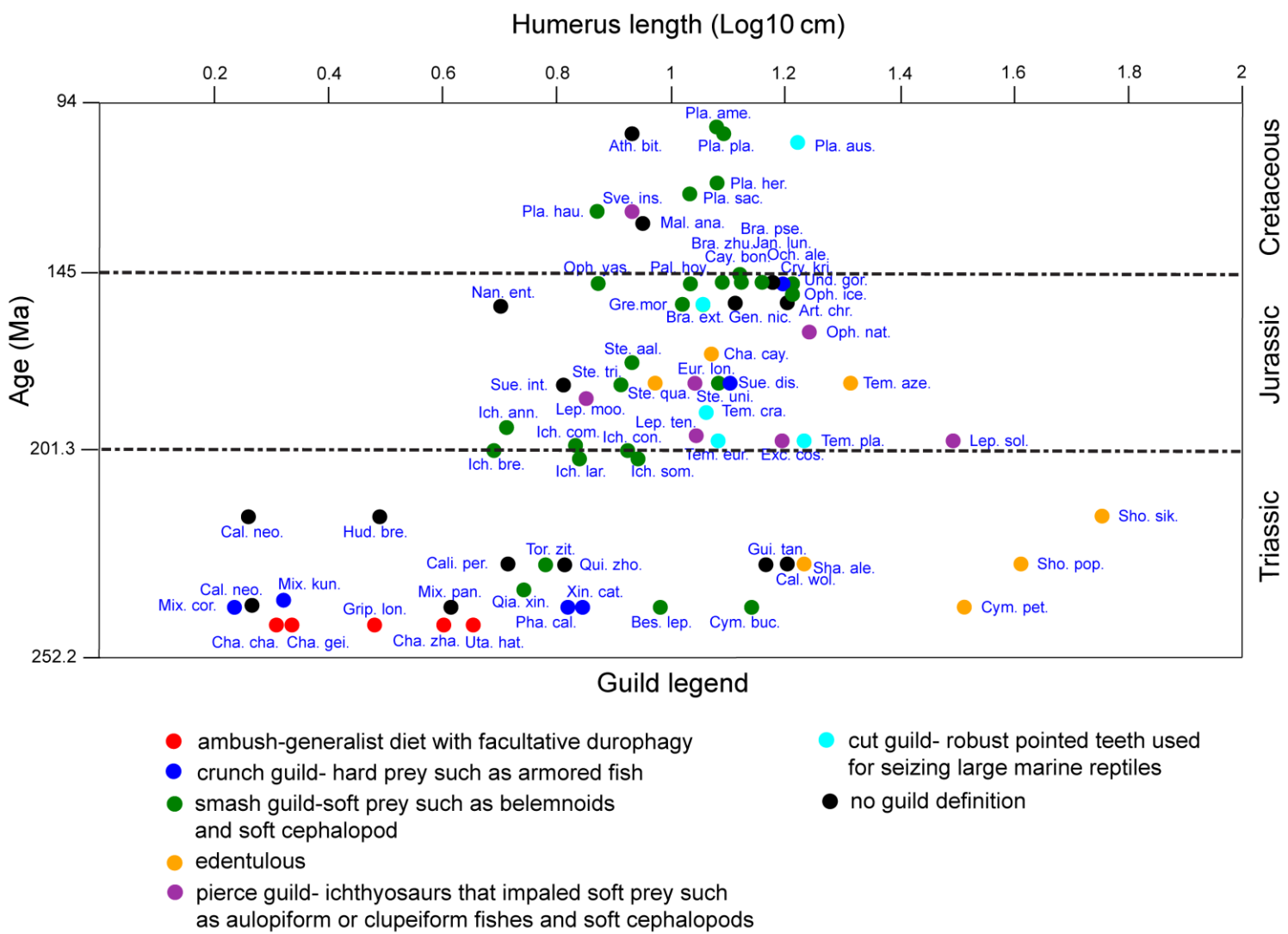
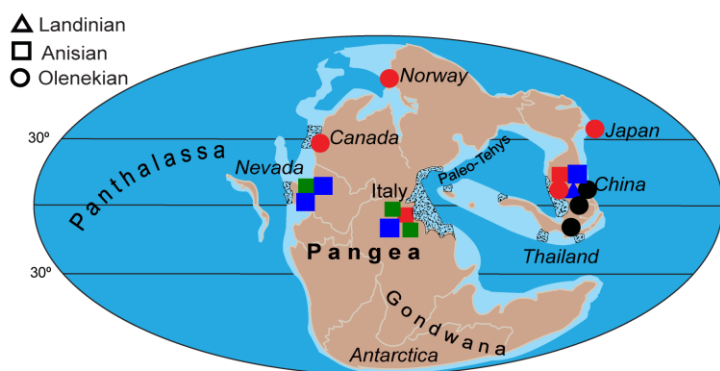
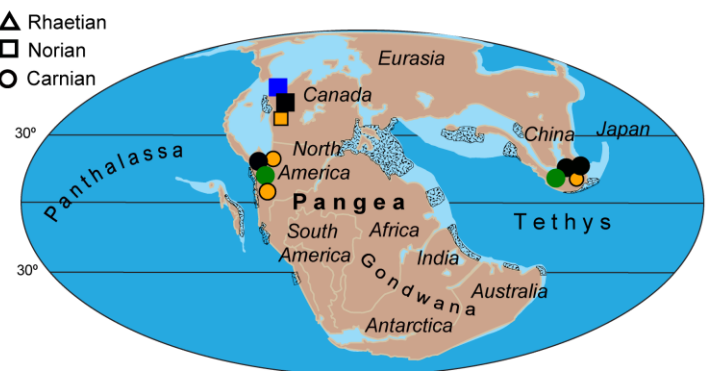


Fig. 3 Scatter plot comparing age (y-axis, My) and humerus length (Log 10, x-axis, proxy for body mass) for Ichthyopterygia. The age assigned to each taxon was calculated as the mid-point of its total stratigraphic range. Each point (species) is represented by its respective ecological feeding habit color. Six ecological feeding habits are used according to Massare (1987) and Dick & Maxwell (2015).

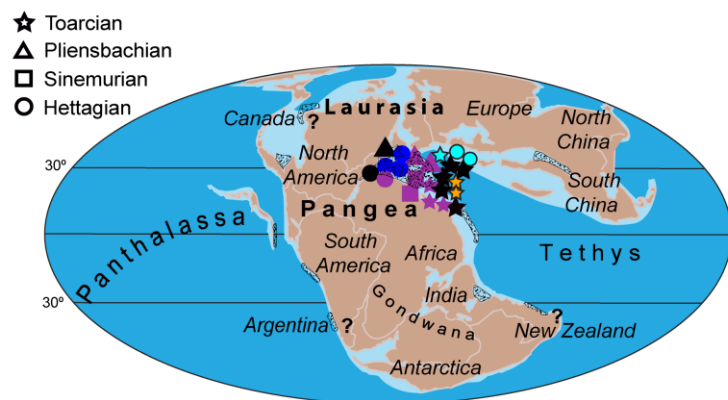
Early/Middle Triassic



Late Triassic



Early Jurassic



Middle/Late Jurassic



Early Cretaceous



Cenomanian

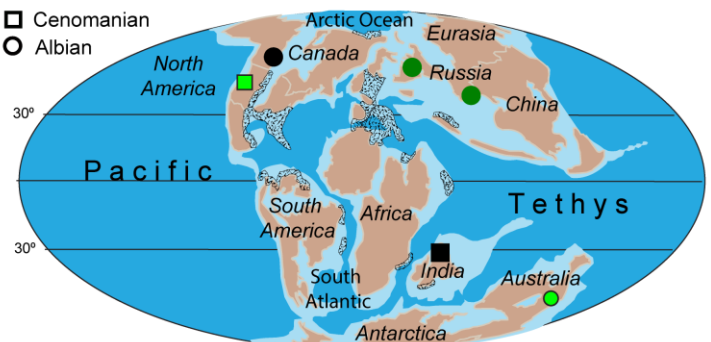


Fig. 4 Mesozoic palaeobiogeographical distribution of Ichthyopterygia. Paleogeographic maps were modified from Scotese (2014a,b). The color of the symbols represents the ichthyosaur species included in this study (AppendixS1). See the color key in the Fig. 3.

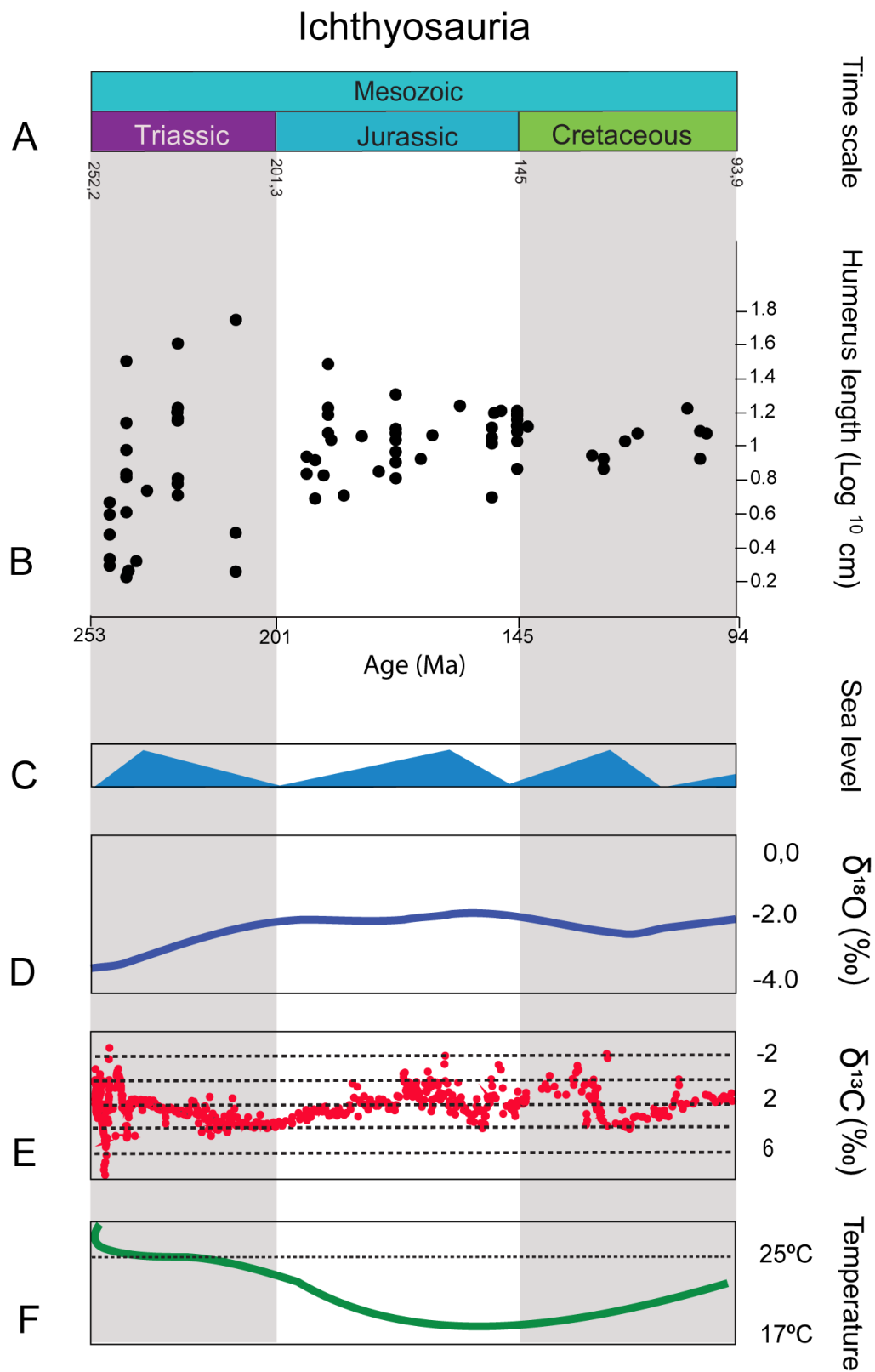


Fig. 5- A and B) Stratigraphic chart (Cohen et al., 2013) and humerus size (Log₁₀) of Ichthyopterygia(including all 73 taxa) correlated with, C) Eustatic sea level (Gradstein et al., 2012), D) Oxygen variation ($\delta^{18}\text{O}$) (Price et al., 2013), E) Carbon variation (Saltzman & Thomas, 2012) and F) Global climatic variations through Mesozoic (Scotese, 2015).

The pierce feeding habit, represented by purple dots, emerged in the Early Jurassic and is characterized by piercing teeth that impaled soft prey such as aulopiform or clupeiform fishes and soft cephalopods (Massare, 1987). The light blue colour illustrates cut feeding habit genera which are characterized by robust cutting teeth specimens that preferably prey on vertebrates (Massare, 1987). Pierce and cut habits comprise 7 species and 5 species, respectively, and both ecotypes appeared just after the Triassic-Jurassic boundary and persisted until Cretaceous.

Considering these feeding habits described above, the 25 species of ichthyosaurs recorded for the Triassic can be assigned to four different ecological groups, the 38 species of the Jurassic are distributed into five ecological groups, and the 10 Cretaceous species can be assigned to three different groups. According to this distribution, the Early Jurassic is the time interval where the ichthyosaurs reached their greatest diversity in terms of feeding strategies (Figure 4). Some feeding habits are more related to certain time interval and/or body size (e. g., ambush-generalist predators, which are represented by small Early Triassic ichthyosaurs, and cut predators, which comprise large Jurassic/Cretaceous species). On the other hand, the smash ichthyosaurs are present throughout the Mesozoic and in all types of body size.

The paraphyletic group which encompasses *Chaohusaurus* and Grippoidea are mainly ambush-generalist predators. The other non-monophyletic group composed by *Mixosaurus* and Cymbospondylidae are predominantly crunch feeders. Three monophyletic groups show specific feeding strategies: Shastasauridae, as edentulous forms; Toretocnemidae, as smash predators; and Leptocnetidae, as pierce feeders.

The most basal subclades present an apparent compartmentalization of feeding habits distribution across the basal branches of the phylogeny until the origin of

the Parvipelvia subclade. In Thunnosauria (and its subclades) this distribution pattern has been altered by the development of new feeding habits within the same monophyletic groups (e. g. Platypterygiine).

To evaluate the behaviour of different feeding habits over time, we made geographic distribution paleomaps depicting all ichthyosaur species and their respective feeding habits. Tectonics has major influence in paleogeography and worldwide distribution of marine reptiles (Bardet *et al.*, 2014). The opening and closure of paleo-oceans as a result of global tectonics partially controlled ichthyosaur dispersion routes (Bardet *et al.*, 2014). The decrease of coastal habitats in Middle to Late Triassic is correlated with a geographical large-scale distribution of tuna-shaped ichthyosaurs (Figure 4), the evolution of a unique body plan adaptation that allowed them to attain an almost global distribution (Motani, 2010; Scheyer *et al.*, 2014).

Early Triassic ichthyosaurs are represented by 17 species geographically distributed over Thailand, China, Japan, Norway, Canada, Europe, and North America, comprising three ecological feeding habits: ambush, smash, and crunch predators. Their initial evolutive acquirements in swimming styles and body proportions enabled them to disperse through Northern coast of Pangea. However, in Ladinian the ambush predators went extinct and this feeding habit has never been recorded again for Ichthyopterygia. The Late Triassic is characterized for a more restricted ichthyosaur geographic distribution, with records in China, Canada, and USA. The Late Triassic also marks the irradiation of the Parvipelvia. The Early Jurassic was the most critical period concerning the Ichthyopterygia geographical distribution, all species used in this study inhabited the European Tethys sea, presenting five different feeding habits. During the Hettangian four feeding habits can be found: crunch, smash, pierce, and cut habits. The pierce feeding habit is the only one present in the Sinemurian and the Pliensbachian. During

the Toarcian, however, four different feeding styles are present: smash, pierce, cut, and edentulous (Figures 3 and 4).

Late Jurassic ichthyosaurs exhibit a widespread geographic distribution (Figure 4), 19 species are divided into five ecological feeding habits: crunch, smash, edentulous, pierce, and cut specialists that inhabited Russia, Europe, Norway, Canada, USA, and South America. The Cretaceous Ichthyopterygia are globally widespread, but during the transition to the Cretaceous, the edentulous (Bajocian) and crunch (Tithonian) species went extinct so that in the Cretaceous three feeding habits are found, being reduced to only two in the Cenomanian.

4- Discussion

Increase and decrease body size tendency was tested in 10 Ichthyopterygia clades under both nonphylogenetic and phylogenetic viewpoints. Nonphylogenetic results detected mild size increase trend and no significant correlation between body length and age (Figure 5a). The phylogenetic results show a tendency towards body size increase in ichthyosaurs across the entire Mesozoic, as the ancestor-descendent pairwise comparisons show higher number of positive changes in all subclades, so that positive body size changes (increase) in Ichthyopterygia are more frequent than the negative ones, but not statistically significant for Parvipelvia, Thunnosauria, Baracromia, Ophthalmosauridae and Platypterigiinae (Figure 1 and Table 2). Therefore, these results show that Cope's rule was not an evolutionary driver for body size variation in Ichthyopterygia.

The results are intriguing once more basal members of Ichthyopterygia are small bodied species, such as *Chaohusaurus geishanensis*, *Grippia longirostris*, and *Utatsusaurus hataii*. Thus, there would be a high probability in achieving larger body sizes through evolutive time as predicted by the Cope's rule. Humerus size values for Early Jurassic range from the small *Ichthyosaurus breviceps* (5,15 cm humerus length) to the large *Teniodontosaurus platyodon* (17 cm humerus length). The small sizes previously found in the Triassic are not present in the Early Jurassic and the data show an increase in the minimum humerus size values (Table 1). Similarly, a decrease in the maximum sizes is followed by the absence of the giant sizes in the Early Jurassic.

Our analysis suggests that as body size increases, standard deviation decreases abruptly between the Triassic and the Late Jurassic. This is in line with the Early Cretaceous Ichthyopterygia low disparity mentioned by previous authors (Thorne *et al.*, 2011; Martin *et al.*, 2012; Fischer *et al.*, 2014b, 2016) and shows how critical the Tr-J event was for ichthyosaur evolution. This pattern is followed by a restriction on the Early Jurassic ecospace diversity (Dick & Maxwell, 2015b; Fischer *et al.*, 2016) probably due to the ecological structure reorganization of a transitional Triassic-Jurassic environment. In this way, paleoenvironmental factors must be considered for a more global analysis. The breakup of Pangea, at least in part, affected the global sea level, CO₂, O₂, and temperature (Figure 5) (Schoene *et al.*, 2010; Ogg *et al.*, 2012) and changed the configuration of oceanic basins (Höfling *et al.*, 2002).

Minimum log humerus lengths increase and maximum log humerus lengths decrease, this suggests a pruning of extreme sizes for both, larger and smaller ones, associated with the decreasing of standard deviation values. The Triassic-Jurassic boundary marks the progressive demise of both large and small sized ichthyosaurs (Figure 5a). Giant sizes as such those represented by shastasaursids and small-bodied

forms, as the basal groups were no longer present in the evolutionary history of the ichthyosaurs after the Tr-J extinction. Other groups such as Thalattosauria, Nothosauria, Pachypleurosauria, Pistosauroidea, and Placodontia also went extinct at this period (Benson *et al.*, 2010).

The extinction of 95% of Rhaetian reef-related forms (McLeod, 2015) indicates the decline of previous well-established Triassic ecosystems and, accordingly, many top predators such as ichthyosaurs were affected. Additionally, 69% of Radiolaria genera, 90% of bivalved mollusc's species, 80% of brachiopods species, and 60% of ammonite species also vanished at that time (McLeod, 2015). The severe environmental changes, because of the Tr-J mass extinction, caused the decline and the rise of different groups of marine reptiles during the Triassic-Jurassic turnover and changed ichthyosauroid feeding habits. The emergence of new ecological feeding habits such as pierce and cut ones in the Early Jurassic and the disappearance of ambush predators can be seen in the Figure 3.

The marine environmental changes during the Triassic-Jurassic transition must have restructured ichthyosaurs feeding habits but, apparently, they did not diminish their diversity. However, while the Early Jurassic ichthyosauroid species developed new feeding habits, the Late Jurassic species seem to be geographically restricted to the most interior portion of the Tethys Ocean and apparently associated to the coral reef occurrences (Figure 4). The coral reefs are reliable paleoclimatic indicators and their distribution patterns give trace of environmental fluctuations, nutrient regimes, biotic interactions, and mass extinctions (Flugel, 2002; Höfling *et al.*, 2002; Leinfelder *et al.*, 2002; Pandolfi & Kiessling, 2014). The Early Jurassic extinction (Toarcian) seems to have been decisive for the group (Richoz *et al.*, 2012, Song *et al.*, 2016). A faunal turnover event, after the Toarcian crisis, explains the new

areas filled by the fast thunniform swimmers (Figure 4), this radiation following migration suggests the filling of new niches and the partial discard of precedent ones (Dick *et al.*, 2015) (Figure 3). The colours indicating the feeding habits in the Figure 3 show different food preference unrestricted to belemnites as previously thought (Fischer *et al.*, 2016). The reef biota encompasses a diverse fauna (Flugel, 2002; Leinfelder *et al.*, 2002) that may have been a source of potential prey for ichthyosaurs (Selden & Nudds, 2012).

The figure 2 shows the compartmentalization of feeding habits in monophyletic groups from Grippoidea to Leptocnetidae during the Triassic. This pattern of guild arrangement seems to have changed within Thunnosauria during the Triassic-Jurassic transition. Furthermore, a generalist prey preference such as cut and smash feeding habits prevailed until the end of Cretaceous. *Platypterygius australis* feed on diverse prey like birds, turtles, and fish (Kear, 2003). Although feeding habit guild diversity diminished during the Cretaceous, the diversity of prey types did not disappear from the menu of the last ichthyosaurs. The top predator ichthyosaurs that present body and dental configurations that allowed the hunting diversified prey types were predominant at the end of Cretaceous.

The smash predators were the most common forms in the Cenomanian and this was the longer-lasting feeding habit in the whole ichthyosaur evolutive history. They emerged during the Anisian and persisted until the Cenomanian, surviving through two severe mass extinctions events along the Mesozoic (Tr-J, J-K). Their acute teeth with rounded apex, used to grasp soft prey such as belemnoids and soft cephalopod (Massare, 1987), represent the most successful feeding habit of Ichthyopterygia. The range of variation of the corporal sizes suggests a relationship between the smash feeding habit and medium body size (Figure 3), teeth morphologies

and feeding strategies that enable feeding on a wide variety of food items may have been a positive advantage for a worldwide dispersion of the group and for the long evolutionary success of ichthyosaurs.

5- Conclusions

- 1-The data provide no evidence for significant body size decrease or increase (Cope's rule) over evolutionary time in Ichthyopterygia or Ichthyosauria.
- 2-The average-sized species became dominant, being the survivors over the environmental fluctuations.
- 3-Most ichthyosaur species were found in the equatorial north-western Europe in the opening of Tethys Sea (Early Jurassic) period. The occurrence of diversified feeding habits in a relatively restricted area and the maintenance of feeding habits diversity post Triassic-Jurassic extinction event may indicate a period of intense competition among different ichthyosauroid groups.
- 4-The Triassic species had feeding habits mainly restricted to monophyletic groups until Parvipelvia in the Triassic. On the other hand, after the Triassic-Jurassic transition, the Thunnosauria feeding habits have been restructured among lineages.

6- References

- Adams, T.L. & Fiorillo, A.R. 2011. *Platypterygius* Huene, 1922 (Ichthyosauria, Ophthalmosauridae) from the Late Cretaceous of Texas, USA. *Paleontol. Electron.* 14: 1-12.
- Alroy, J. 2000. Understanding the dynamics of trends within evolving lineages. *Paleobiology*. 26: 319–329.
- Arkhangelsky, M.S., Averianov, A. O., Pervushov, E.M., Ratnikov, V.Y. & Zozrev, N.Y. 2008. On ichthyosaur remains from the Cretaceous of the Voronezh Region. *Paleontol. J.* 42: 287–291.
- Arkhangelsky, M.S., Zverkov, N.G., Архангельский, М.С. & Зверьков, Н.Г. 2014. On a new Ichthyosaur of the genus *Undorosaurus*. *Proc. Zool. Inst. RAS.* 318: 187–196.
- Arnold, A.J., Kelly, D.C. & Parker, W.C. 1995. Causality and Cope's rule: evidence from the planktonic foraminifera. *J. Paleontol.* 69: 203–210.
- Arnold, C. & Nunn, C.L. 2010. Phylogenetic Targeting of Research Effort in Evolutionary Biology. *Am. Nat.* 176: 601–612.
- Ashton, K.G., Tracy, M.C. & de Queiroz, A., 2000. Is Bergmann's Rule valid for mammals? *Am. Nat.* 156: 390–415.
- Ashton, K. G. 2002. Patterns of within-species body size variation of birds: Strong evidence for Bergmann's rule. *Gl. Ecol. and Biog.* 11: 505–523.
- Atkinson, D. 1994. Temperature and organism size a biological law for ectotherms? *Adv. in Ecol. Res.* 25: 1-58.

- Bardet, N., Falconnet, J., Fischer, V., Houssaye, A., Jouve, S., Pereda Suberbiola, X. et al. 2014. Mesozoic marine reptile palaeobiogeography in response to drifting plates. *Gondwana Res.* 26: 869–887.
- Benson, R.B.J. & Butler, R.J. 2011. Uncovering the diversification history of marine tetrapods: ecology influences the effect of geological sampling biases. *Geol. Soc. London, Spec. Publ.* 358: 191–208.
- Benson, R.B.J., Butler, R.J., Lindgren, J. & Smith, A.S. 2010. Mesozoic marine tetrapod diversity: mass extinctions and temporal heterogeneity in geological megabiases affecting vertebrates. *Proc. R. Soc. B Biol. Sci.* 277: 829–834.
- Benson, R.B.J., Frigot, R. A., Goswami, A., Andres, B. & Butler, R.J. 2014. Competition and constraint drove Cope's rule in the evolution of giant flying reptiles. *Nat. Commun.* 5: 1-8.
- Butler, R.J. & Goswami, A. 2008. Body size evolution in Mesozoic birds: Little evidence for Cope's rule. *J. Evol. Biol.* 21: 1673–1682.
- Campione, N.E. & Evans, D.C. 2012. A universal scaling relationship between body mass and proximal limb bone dimensions in quadrupedal terrestrial tetrapods. *BMC Biol.* 10: 1-21.
- Carrano, M.T. 2006. Body-size evolution in the dinosauria. In: Amniote Paleobiology: Perspectives on the Evolution of Mammals, Birds and Reptiles (M.T. Carrano, T.J. Gaudin, R.W. Blob & J.R. Wible, eds), pp. 225–257. University of Chicago Press, Chicago. Christiansen, P. 1999. Scaling of mammalian long bones: small and large mammals compared. *J. Zool.* 247: 333–348.

- Cohen, K.M., Finney, S.C., Gibbard, P.L. & Fan, J.-X. (2013; updated) The ICS International Chronostratigraphic Chart. *Episodes* 36: 199–204.
- Colbert, E.H. 1993. Feeding strategies and metabolism in elephants and sauropod dinosaurs. *Am. J. Sci.* 293: 1–19.
- Dal Sasso, C. & Pinna, G. 1996. *Besanosaurus leptorhynchus* n. gen. n. sp., a new shastasaurid ichthyosaur from the Middle Triassic of Besano (Lombardy, N. Italy). *Paleontol. Lomb. New Ser.* 4: 1–22.
- Dick, D.G. & Maxwell, E.E. 2015a. Ontogenetic tooth reduction in *Stenopterygius quadriscissus* (Reptilia: Ichthyosauria): Negative allometry, changes in growth rate, and early senescence of the dental lamina. *PLoS One* 10: 1–14.
- Dick, D.G. & Maxwell, E.E. 2015b. The evolution and extinction of the ichthyosaurs from the perspective of quantitative ecospace modelling. *Biol. Lett.* 11: 1–5.
- Druckenmiller, P.S., Hurum, J.H., Knutsen, E.M. & Nakrem, H.A. 2012. Two new ophthalmosaurids (Reptilia: Ichthyosauria) from the Agardhfjellet Formation (Upper Jurassic: Volgian/Tithonian), Svalbard, Norway. *Nor. Geol. Tidsskr.* 92: 311–339.
- Druckenmiller, P.S., Kelley, N., Whalen, M.T., McRoberts, C. & Carter, J.G. 2014. An Upper Triassic (Norian) ichthyosaur (Reptilia, Ichthyopterygia) from northern Alaska and dietary insight based on gut contents. *J. Vertebr. Paleontol.* 34: 1460–1465.
- Druckenmiller, P.S. & Maxwell, E.E. 2010. A new Lower Cretaceous (lower Albian) ichthyosaur genus from the Clearwater Formation, Alberta, Canada. *Can. J. Earth Sci.* 47(8): 1029–1036.

- Egi, N. 2001. Body mass estimates in extinct mammals from limb bone dimensions: the case of North American hyaenodontids. *Palaeontology* 44: 497–528.
- Nicholls, E.L. & Manabe, M. 2004. Giant ichthyosaurs of the Triassic—a new species of *Shonisaurus* from the Pardonet Formation (Norian: Late Triassic) of British Columbia. *J. Vertebr. Paleontol.* 24: 838–849.
- Felsenstein, J. 1985. Phylogenies and the Comparative Method. *Am. Nat.* 125: 1–15.
- Fernández, M. 2007. Redescription and phylogenetic position of *Caypullisaurus* (Ichthyosauria: Ophthalmosauridae). *J. Paleontol.* 81: 368–375.
- Fernández, M. & Aguirre-Urreta, M.B. 2005. von Huene, 1927 (Ichthyosauria: Ophthalmosauridae) from the Early Cretaceous of Patagonia, Argentina. *J. Vertebr. Paleontol.* 25: 583–587.
- Fernández, M.S. & Maxwell, E.E. 2012. The genus *Arthropterygius* Maxwell (Ichthyosauria: Ophthalmosauridae) in the Late Jurassic of the Neuquén Basin, Argentina. *Geobios* 45: 535–540.
- Field, D.J., Lynner, C., Brown, C. & Darroch, S.A.F. 2013. Skeletal correlates for body mass estimation in modern and fossil flying birds. *PLoS One* 8: 1–13.
- Fischer, V. 2016. Taxonomy of *Platypterygius campylodon* and the diversity of the last ichthyosaurs. *Peer J* 4:1-21.
- Fischer, V., Appleby, R.M., Naish, D., Liston, J., Riding, J.B., Brindley, S., et al. 2013. A basal thunnosaurian from Iraq reveals disparate phylogenetic origins for Cretaceous ichthyosaurs. *Biol. Lett.* 9: 1-6.

- Fischer, V., Bardet, N., Benson, R.B.J., Arkhangelsky, M.S. & Friedman, M. 2016. Extinction of fish-shaped marine reptiles associated with reduced evolutionary rates and global environmental volatility. *Nat. Commun.* 7: 1–11.
- Fischer, V., Bardet, N., Guiomar, M. & Godefroit, P. 2014a. High diversity in Cretaceous ichthyosaurs from Europe prior to their extinction. *PLoS One* 9:1-26.
- Fischer, V., Cappetta, H., Vincent, P., Garcia, G., Goolaerts, S. & Martin, J.E. et al. 2014b. Ichthyosaurs from the French Rhaetian indicate a severe turnover across the Triassic-Jurassic boundary. *Naturwissenschaften* 101: 1027–1040.
- Fischer, V., Maisch, M.W., Naish, D., Kosma, R., Liston, J. & Joger, U. et al. 2012. New ophthalmosaurid ichthyosaurs from the European lower Cretaceous demonstrate extensive ichthyosaur survival across the Jurassic-Cretaceous boundary. *PLoS One* 7:1-23.
- Fischer, V., Masure, E., Arkhangelsky, M.S. & Godefroit, P. 2011. A new Barremian (Early Cretaceous) ichthyosaur from western Russia. *J. Vertebr. Paleontol.* 31: 1010–1025.
- Flugel, E. 2002. Triassic reef patterns. In: *Phanerozoic Reef Patterns* (W. Kiessling, E. Flugel, J. Golonka, eds.), pp. 391-463. 2002. SEPM Society for Sedimentary Geology.
- Golonka, J. 2007. Late Triassic and Early Jurassic palaeogeography of the world. *Palaeogeogr. Palaeoclimatol. Palaeoecol.* 244: 297–307.
- Hammer, O., Harper, D.A.T. & Ryan, P.D. 2001. PAST: paleontological statistics software package for education and data analysis. *Paleontol. Electron.* 4: 4–9.

- Höfling, R., Erlangen, D. & Scott, R.W. 2002. Early and Mid-Cretaceous buildups. In: Phanerozoic Reef Patterns (W. Kiessling, E. Flugel, J. Golonka, eds.), pp. 391-463. 2002. SEPM Society for Sedimentary Geology.
- Hone, D.W.E. & Benton, M.J. 2005. The evolution of large size: how does Cope's rule work? *Trends Ecol. Evol.* 20: 4–6.
- Hunt, G., Hopkins, M.J. & Lidgard, S. 2015. Simple versus complex models of trait evolution and stasis as a response to environmental change. *Proc. Natl. Acad. Sci. U. S. A.* 112: 4885–4890.
- Hurlbut, G.R., Heckert, A.B. & Farlow, J.O. 2003. Body mass estimates of phytosaurs (Archosauria: Parasuchidae) from the Petrified Forest Formation (Chinle Group: Revueltian) based on skull and limb bone measurements. *Paleontology and Geology of the Snyder Quarry, New Mexico Museum of Natural History and Science. Bulletin No. 24.* pp,105-114.
- Ji, C., Jiang, D.-Y., Motani, R., Hao, W.-C., Sun, Z.-Y. & Cai, T. 2013. A new juvenile specimen of *Guanlingsaurus* (Ichthyosauria, Shastasauridae) from the Upper Triassic of southwestern China. *J. Vertebr. Paleontol.* 33: 340–348.
- Ji, C., Jiang, D., Motani, R., Rieppel, O.C., Hao, W. & Sun, Z. 2015. Phylogeny of the Ichthyopterygia incorporating recent discoveries from South China. *J. Vertebr. Paleontol.* 36: 1-19.
- Jiang, D.-Y., Motani, R., Huang, J.-D., Tintori, A., Hu, Y.-C., Rieppel, O., et al. 2016. A large aberrant stem ichthyosauromorph indicating early rise and demise of ichthyosauromorphs in the wake of the end-Permian extinction. *Sci. Rep.* 6: 1-9.

- Jiang, D., Hao, W., Maisch, M.W., Matzke, A.T. & Sun, Y. 2005. A basal mixosaurid ichthyosaur from the Middle Triassic of China. *Palaeontology* 48: 869–882.
- Jiang, D., Motani, R., Hao, W., Schmitz, L., Rieppel, O., Sun, Y., et al. 2008. New primitive ichthyosaurian (Reptilia, Diapsida) from the Middle Triassic of Panxian, Guizhou, southwestern China and its position in the Triassic biotic recovery. *Prog. Nat. Sci.* 18: 1315–1319.
- Johnson, R. 1977. Size independent criteria for estimating relative age and the relationships among growth parameters in a group of fossil reptiles (Reptilia: Ichthyosauria). *Can. J. Earth Sci.* 14: 1916-1924.
- Kear, B.P. 2003. Cretaceous marine reptiles of Australia: A review of taxonomy and distribution. *Cretac. Res.* 24: 277–303.
- Klompmaker, A., Schweitzer, C.E. & Feldmann, R.M. 2015. Environmental and scale-dependent evolutionary trends in the body size of crustaceans. *Proc. R. Soc. B-Biological Sci.* 282: 1-8.
- Laurin, M. 2004. The Evolution of Body Size, Cope's Rule and the Origin of Amniotes. *Syst. Biol.* 53: 594–622.
- Leinfelder, R.R., Schimid, D.U., Nose, M., Werner, W. 2002. Jurassic reef patterns—the expression of a changing globe. In: *Phanerozoic Reef Patterns* (W. Kiessling, E. Flugel, J. Golonka, eds.), pp. 391-463. 2002. SEPM Society for Sedimentary Geology.
- Maddison, W.P. & Maddison, D.R. 2017. Mesquite: a modular system for evolutionary analysis. Version 3.2. <http://mesquiteproject.org>.

- Maisch, M.W. 2008. Revision der Gattung *Stenopterygius* Jaekel, 1904 emend. Von Huene, 1922 (Reptilia: Ichthyosauria) aus dem unteren Jura Westeuropas. *Palaeodiversity* 1: 227–271.
- Maisch, M.W. & Hungerbühler, A. 2001. New evidence for a discrete supratemporal bone in the Jurassic ichthyosaur *Temnodontosaurus*. *Hist. Biol.* 15: 335–345.
- Maisch, M.W. & Reisdorf, A.G. 2006. Evidence for the longest stratigraphic range of a post-Triassic ichthyosaur: a *Leptonectes tenuirostris* from the Pliensbachian (Lower Jurassic) of Switzerland. *Geobios* 39: 491–505.
- Marek, R.D., Moon, B.C., Williams, M. & Benton, M.J. 2015. The skull and endocranum of a Lower Jurassic ichthyosaur based on digital reconstructions. *Palaeontology* 58: 723–742.
- Martin, J.E., Fischer, V., Vincent, P. & Suan, G. 2012. A longirostrine *Temnodontosaurus* (Ichthyosauria) with comments on Early Jurassic ichthyosaur niche partitioning and disparity. *Palaeontology* 55: 995–1005.
- Massare, J.A. 1988. Swimming capabilities of Mesozoic marine reptiles: Implications for method of predation. *Paleobiology* 14: 187–205.
- Massare, J.A. 1987. Tooth Morphology and Prey Preference of Mesozoic Marine Reptiles. *J. Vertebr. Paleontol.* 7: 121-137.
- Massare, J.A., Buchholtz, E.A., Kenney, J.M. & Chomat, A.M. 2006. Vertebral morphology of *Ophthalmosaurus natans* (Reptilia: Ichthyosauria) from the Jurassic Sundance Formation of Wyoming. *Paludicola* 5: 242–254.

Maxwell, E.E. & Caldwell, M.W. 2006. Evidence for a second species of the ichthyosaur *Platypterygius* in North America: a new record from the Loon River Formation (Lower Cretaceous) of northwestern Canada. *Can. J. Earth Sci.* 43: 1291–1295.

Maxwell, E.E., Fernández, M.S. & Schoch, R.R. 2012. First diagnostic marine reptile remains from the Aalenian (middle Jurassic): A new ichthyosaur from southwestern Germany. *PLoS One* 7:1-13.

Maxwell, E.E. & Kear, B.P. 2010. Article Postcranial Anatomy of *Platypterygius americanus* (Reptilia: Ichthyosauria) From the Cretaceous of Wyoming. *J. Vertebr. Paleontol.* 30: 1059–1068.

Maxwell, E.E., Scheyer, T.M. & Fowler, D.A. 2014. An evolutionary and developmental perspective on the loss of regionalization in the limbs of derived ichthyosaurs. *Geol. Mag.* 151: 29–40.

Mazin, J. M., Suteethorn, V., Buffetaut, E., Jaeger, J. J. & Helmcke-Ingavat, R. 1991. Preliminary description of *Thaisaurus chonglakmanii* n. g. n. sp. a new ichthyopterygian (Reptilia) from the Early Triassic of Thailand. *Acad. Sci. Paris.* 313: 1207–1212.

McGowan, C. 2003. A new specimen of *Excalibosaurus* from the English Lower Jurassic. *J. Vertebr. Paleontol.* 23: 950–956.

McGowan, C. 1995a. A remarkable small ichthyosaur from the Upper Triassic of British Columbia, representing a new genus and species. *Can. J. Earth Sci.* 32: 292–303.

McGowan, C. 1974. A Revision of the Latipinnate Ichthyosaurs of the Lower Jurassic of England (Reptilia: Ichthyosauria). *R. Ont. Mus. Life. Sci. Contrib.* 94: 1-44.

- McGowan, C. 1972a. Evolutionary trends in longipinnate ichthyosaurs with particular reference to the skull and fore fin. *Life Sci. Contr., R. Ont. Mus.* 83: 1–38.
- McGowan, C. 1996. Giant ichthyosaurs of the Early Jurassic. *Can. J. Earth Sci.* 3: 1011–1021.
- McGowan, C. 1995b. *Temnodontosaurus risor* is a juvenile of *T. platyodon* (Reptilia: Ichthyosauria). *J. Vertebr. Paleontol.* 14: 472–479.
- McGowan, C. 1972b. The systematics of Cretaceous ichthyosaurs with particular reference to the material from North America. *Contrib. to Geol.* 11: 9–29.
- McLeod, N. 2015. *The Great Extinctions What Causes Them & How They Shape Life*, 1st edn. Natural History Museum, London.
- Maisch, M. W. & Matzke, A. T. 2000a. The Ichthyosauria. *Stuttgarter Beiträge zur Naturkunde, Serie B* 298: 1–159.
- Maisch, M.W. & Matzke, A.T. 2000. The Ichthyosauria. *Stuttgarter Beiträge zur Naturkunde, Serie B* 298: 1-159.
- Motani, R. 2001. Estimating body mass from silhouettes: testing the assumption of elliptical body cross-sections. *Paleobiology* 27: 735–750.
- Motani, R. 2005. Evolution of fish-shaped reptiles (Reptilia: Ichthyopterygia) in their physical environments and constraints. *Annu. Rev. Earth Planet. Sci.* 33: 395–420.
- Motani, R. 1998. First complete forefin of the ichthyosaur *Grippia longirostris* from the Triassic of Spitsbergen. *Palaeontology* 41: 591–599.
- Motani, R. 1997. New information on the forefin of *Utatsusaurus Hataii* (Ichthyosauria). *J. Paleontol.* 71: 475–479.

- Motani, R. 1999. Phylogeny of the Ichthyopterygia. *J. Vertebr. Paleontol.* 19: 473–496.
- Motani, R. 2009. The Evolution of Marine Reptiles. *Evol. Educ. Outreach.* 2: 224–235.
- Motani, R. 2010. Warm-Blooded “Sea Dragons”? *Science* 328: 1361–1362.
- Motani, R., Ji, C., Tomita, T., Kelley, N., Maxwell, E., Jiang, D.Y. et al. 2013. Absence of suction feeding ichthyosaurs and its implications for Triassic mesopelagic paleoecology. *PLoS One* 8:1-11.
- Motani, R., Jiang, D.-Y., Chen, G.-B., Tintori, A., Rieppel, O., Ji, C. et al. 2015. A basal ichthyosauriform with a short snout from the Lower Triassic of China. *Nature* 517: 485–491.
- Motani, R. & You, H. 1998. Taxonomy and limb ontogeny of *Chaohusaurus* *geishanensis* (Ichthyosauria), with a note on the allometric equation. *J. Vertebr. Paleontol.* 18: 533–540.
- Nicholls, E.L., Wei, C. & Manabe, M. 2003. Li, 1999 (Reptilia, Ichthyosauria) from the Late Triassic of southern China, and implications for the distribution of Triassic ichthyosaurs. *J. Vertebr. Paleontol.* 22: 759–765.
- Ogg, J.G., Hinnov, L.A. & Huang, C. 2012. Jurassic. In: The Geologic Scale (F.M. Gradstein, J.G. Ogg, M. Schmitz, G. Ogg, eds.), pp. 731-791. Oxford, UK, 2012. Elsevier, UK.
- Pandolfi, J.M. & Kiessling, W. 2014. Gaining insights from past reefs to inform understanding of coral reef response to global climate change. *Curr. Opin. Environ. Sustain.* 7: 52–58.

- Pollard, J.E. 1968. The gastric contents of an ichthyosaur from the Lower Lias of Lyme Regis, Dorset. *Palaeontology* 11: 376-399.
- Price, G.D., Twitchett, R.J., Wheeley, J.R. & Buono, G. 2013. Isotopic evidence for long term warmth in the Mesozoic. *Sci. Rep.* 3: 1-5.
- Pyenson, N.D.; Sponberg, S.N. 2011. Reconstructing Body Size in Extinct Crown Cetacea (Neoceti) Using Allometry, Phylogenetic Methods and Tests from the Fossil Record. *J. Mammal. Evol.* 18: 269-288.
- Richoz, S., van de Schootbrugge, B., Pross, J., Püttmann, W., Quan, T.M., Lindström, S. et al. 2012. Hydrogen sulphide poisoning of shallow seas following the end-Triassic extinction. *Nat. Geosci.* 5: 662–667.
- Rieppel, O.C., Jinling, L. & Jun, L. 2003. *Lariosaurus xingyiensis* (Reptilia: Sauropterygia) from the Triassic of China. *Can. J. Earth Sci.* 40: 621–634.
- Roberts, A.J., Druckenmiller, P.S., Sætre, G.P. & Hurum, J.H. 2014. A new upper Jurassic ophthalmosaurid ichthyosaur from the Slottsmøya Member, Agardhfjellet Formation of central Spitsbergen. *PLoS One* 9:1-24.
- Saltzman, M.R. & Thomas, E. 2012. Carbon isotope stratigraphy. In: *The Geologic Scale* (F.M. Gradstein, J.G. Ogg, M. Schmitz, G. Ogg, eds.), pp. 207-232. Oxford, UK, 2012. Elsevier, UK.
- Sander, P.M. 1989. The large ichthyosaur *Cymbospondylus buchseri*, sp. nov., from the Middle Triassic of Monte San Giorgio (Switzerland), with a survey of the genus in Europe. *J. Vertebr. Paleontol.* 9: 163–173.

- Sander, P.M., Chen, X., Cheng, L. & Wang, X. 2011. Short-snouted toothless ichthyosaur from China suggests Late Triassic diversification of suction feeding ichthyosaurs. *PLoS One* 6:1-10.
- Scheyer, T.M., Romano, C., Jenks, J. & Bucher, H. 2014. Early Triassic marine biotic recovery: The predators' perspective. *PLoS One* 9:1-20.
- Schmitz, L., Sander, P.M., Storrs, G.W. & Rieppel, O.C. 2004. New Mixosauridae (Ichthyosauria) from the Middle Triassic of the Augusta Mountains (Nevada, USA) and their implications for mixosaur taxonomy. *Palaeontogr. Abteilung A Paläozoologie—Stratigraphie* 270: 133–162.
- Schoene, B., Guex, J., Bartolini, A., Schaltegger, U. & Blackburn, T.J. 2010. Correlating the end-Triassic mass extinction and flood basalt volcanism at the 100 ka level. *Geology* 38: 387–390.
- Scotese, C.R. 2014a. The PALEOMAP Project PaleoAtlas for ArcGIS, version 2, Volume 2, Cretaceous Plate Tectonic, Paleogeographic, and Paleoclimatic Reconstructions, Maps 16-32, Mollweide projection. PALEOMAP Project, Evanston, IL.
- Scotese, C.R. 2014b. The PALEOMAP Project PaleoAtlas for ArcGIS, version 2, Volume 3, Triassic and Jurassic Plate Tectonic, Paleogeographic, and Paleoclimatic Reconstructions, Map 33-48, Mollweide projection. PALEOMAP Project, Evanston, IL.
- Scotese, C.R. 2015. Some thoughts on Global Climate Change: The transition from icehouse to hothouse conditions. In: *Earth History: The Evolution of Earth System* (C.R. Scotese, edn), pp. 1-55. PALEOMAP Project.
- Selden, P. & Nudds, J. 2012. *Evolution of Fossil Ecosystems*, 2nd edn. Elsevier B.V.

- Song, J., Littke, R. & Weniger, P. 2016. Organic geochemistry of the Lower Toarcian Posidonia Shale in NW Europe. *Org. Geochem.* 106:76-92.
- Sookias, R.B., Benson, R.B.J. & Butler, R.J. 2012. Biology, not environment, drives major patterns in maximum tetrapod body size through time. *Biol. Lett.* 8: 674–677.
- Souza, L.M. & Santucci, R.M. 2014. Body size evolution in Titanosauriformes (Sauropoda, Macronaria). *J. Evol. Biol.* 27: 2001–2012.
- Stinnesbeck, W., Frey, E., Rivas, L., Pérez, J., Cartes, M., Soto, C., & Lobos, P. 2014. A Lower Cretaceous ichthyosaur graveyard in deep marine slope channel deposits at Torres del Paine National Park, southern Chile: Geological Society of America Bulletin, v.126, no. 9-10, p. 1317.
- Tennant, J.P., Mannion, P.D., Upchurch, P., Sutton, M.D. & Price, G.D. 2016. Biotic and environmental dynamics through the Late Jurassic-Early Cretaceous transition: Evidence for protracted faunal and ecological turnover. *Biol. Rev.* 92:776–814.
- Therrien, F., Henderson, D.M., Journal, S., Mar, N., Therrien, F.O.I.S. & Henderson, D.M. 2007. My theropod is bigger than yours...or not: Estimating body size from skull length in theropods. *J. Vert. Paleontol.* 27: 108-115.
- Thorne, P.M., Ruta, M. & Benton, M.J. 2011. Resetting the evolution of marine reptiles at the Triassic-Jurassic boundary. *Proc. Natl. Acad. Sci. U. S. A.* 108: 8339–8344.
- Yang, P., Jiang, D., Motani, R., Tintori, A., Sun, Y. & Sun, Z. 2013. A new species of Qianichthyosaurus (Reptilia: Ichthyosauria) from Xingyi Fauna (Ladinian, Middle Triassic) of Guizhou. *Acta Sci. Nat. Univ. Pekin.* 49: 1002–1008.

Zammit, M. 2010. A review of Australasian ichthyosaurs. *Alcheringa An Australas. J. Palaeontol.* 34: 281–292.

Zammit, M., Norris, R.M. & Kear, B.P. 2010. The Australian Cretaceous ichthyosaur *Platypterygius australis*: a description and review of postcranial remains. *J. Vertebr. Paleontol.* 30: 1726–1735.

Supplementary Information S1- Ichthyosauria

Taxa	Total (cm)	Skull (cm)	Femur (cm)	Humerus (cm)	Material	Time interval	Localization	Geologic Unit	References
<i>Arthropterygius chrisorum</i>		152,06*	13,36*	16,05	MOZ 6145	Kimmeridgian	Neuquén Province, Argentina	Vaca Muerta	(Fernandez & Maxwell, 2012)
<i>Athabascasaurus bitumineus</i>	350	58,73*	5,69	8,69*	TMP 2000.29.01	Early Albian	Alberta, Canada	Clearwater, Wabiskaw	(Druckenmiller & Maxwell, 2010)
<i>Besanosaurus leptorhynchus</i>	500	38,42*	8,3	9,6	BES SC 999	Anisian	Besano, Sasso Caldo quarry, Italy	Grenzbitumen- horizon, Besano Fm.	(Dal Sasso & Pinna, 1996)
<i>Brachypterygius extremus</i>		93,43*	9,8*	11,43	BMNH R3177	Kimmeridgian- Tithonian	Dorset, England	Kimmeridge Clay	(McGowan & Motani, 2003; Fischer <i>et al.</i> , 2016)
<i>Brachypterygius pseudoscylticus</i>		117,54*	11,27*	13,33	УПИМ No. 3/100	Tithonian	Ul'yanovsk Oblast, Russia		(Cleary <i>et al.</i> , 2015)
<i>Brachypterygius zhuravlevi</i>		105,74*	8,2	12,4	SRM Hb, no. 30192	Tithonian	Samara Oblast, Russia		(Arkhangelsky, 2001)
<i>Californosaurus perrini</i>	200	21,08*	5,5	5,22*	UP 9119	Carnian	Shasta County, California, USA	Hosselkus Limestone	(Merriam, 1902)
<i>Callawayia neoscacularis</i>		7,62*	3,33	1,82*	ROM 41993	Norian	British Columbia, Canada	Pardonet	(McGowan, 1994)
<i>Callawayia wolonggangensis</i>		66		16,55*	SPCV 10306	Carnian	China, Guizhou Province, Guanling County	Xiaowa Fm.	(Chen <i>et al.</i> , 2007)
<i>Caypullisaurus bonapartei</i>	470,73			12,6	MACN-N-32	Early Tithonian	Neuquén Province, Argentina	Vaca Muerta	(Cleary <i>et al.</i> , 2015)
	151,5				MOZ 6139	Berriasian	Neuquén Province, Argentina	Vaca Muerta	(Fernandez, 2007)

	112			MOZ 6067	Late Tithonian	Neuquén Province, Argentina	Vaca Muerta	(Fernandez, 2007)	
		8,2	14,2	MLP 83-XI-16-1	Early Tithonian	Neuquén Province, Argentina	Vaca Muerta	(Cleary <i>et al.</i> , 2015)	
<i>Chacaicosaurus cayi</i>	98	8,25	12,02*	MOZ 5803 PV	Bajocian	Chacaico Sur- Chara, Neuquén province, Argentina	Los Molles Fm.	(Fischer <i>et al.</i> , 2016; Fernández, 1994)	
<i>Chaohusaurus zhangjiawanensis</i>	16,23*	4,96*	4	WHGMR V26025	Olenekian	Hubei Province, China	Jialingjiang Fm.	(Chen <i>et al.</i> , 2013)	
		1,6		WHGMR V26001	Olenekian	Hubei Province, China	Jialingjiang Fm.	(Chen <i>et al.</i> , 2013)	
<i>Chaohusaurus chaoxianensis</i>	8,58*	3,51*	2,07	AGM-CH-628-19	Olenekian	China, Anhui Province, Maijishan	Nanlinghu	(Motani <i>et al.</i> , 2015)	
<i>Chaohusaurus geishanensis</i>	70	8,85*	3,56*	2,14	IVPP V4001	Olenekian	China, Anhui Province, Maijishan	Maijishan	(Motani & You, 1998)
<i>Cryopterygius kristiansenae</i>	122	11,2	15,5	PMO 214.578	Tithonian	Svalbard, Norway	Agardhfjellet, Slottsmøya	(Druckenmiller <i>et al.</i> , 2012)	
<i>Cymbospondylus petrinus</i>	116,6	25,5	32,5	UP No. 9950	Anisian	Nevada, USA		(Merriam, 1908)	
<i>Cymbospondylus buchseri</i>	500	55,86*	12,48*	14	PIMUZ T 4351	Anisian	Switzerland, Monte San Giorgio	Grenzbitumen- horizon, Besano Fm.	
<i>Eurhinosaurus longirostris</i>	107,5		11,2	MNHN- 1946-20	Early Toarcian	Whitby, Yorkshire, England	Upper Lias	(McGowan, 2003)	
<i>Excalibosaurus costini</i>	154	11,43	15,71	ROM 47697	Sinemurian	Somerset, England	Lower Lias	(McGowan, 2003)	
<i>Grendelius mordax</i>	82		10,52*	BRSMG Ce16696	Middle Kimmeridgian	Dorset, England	Kimmeridge Clay	(Cleary <i>et al.</i> , 2015)	
<i>Grippia longirostris</i>	100	3,42		PMU R448	Olenekian	Svalbard, Norway	Vikinghøgda Fm.	(Motani, 1998)	
		3,07		PMU R 472	Olenekian	Svalbard, Norway	Vikinghøgda Fm.	(Motani, 1998)	

<i>Guanlingsaurus liangae</i>	830	12,22	Gmr014	Carnian	China, Guizhou Province, Guanling County	Xiaowa Fm.	(Ji <i>et al.</i> , 2013)	
	78,42	14	15	YIGMR SPCV03107	Carnian	China, Guizhou Province, Guanling County	Xiaowa Fm.	(Sander <i>et al.</i> , 2011)
<i>Gengasaurus nicosiae</i>	114,11*	11,06*	13,06	MSVG 39617	Late Kimmeridgian – Earliest Tithonian	Marche, Italy	E. Calcareo aptici e Saccocoma Formation	(Paparella <i>et al.</i> , 2016)
<i>Guizhouichthyosaurus tangae</i>	730	93	DQ-41	Carnian	China, Guizhou Province, Guanling County	Wayao Mb., Falang Fm.	(Maisch <i>et al.</i> , 2006; Shang & Li, 2009)	
	550	65	11,5	14,5	IVPP V 11853	Carnian	Falang Fm.	(Shang & Li, 2009)
<i>Hauffiopteryx typicus</i>	235	31,63*	6,05*	6,56	MHH '9'	Early Toarcian	Holzmaden, Baden-Württemberg, Germany	Posidonia shale (Maisch, 2008)
<i>Hudsonelpidia brevirostris</i>	100	12,82*	3,71	3,14	ROM 41993	Norian	Canada, British Columbia, Williston Lake	Pardonet Fm. (McGowan, 1995)
<i>Ichthyosaurus anningae</i>		13,73*	2,88	5,15	DONMG:1983.98	Hettangian/Sinemurian–Pliensbachian	England, Dorset	(Lomax & Massare, 2015)
<i>Ichthyosaurus breviceps</i>	100	22,32		NHM 39263?	Upper Hettangian - Lower Sinemurian	Lyme Regis, Dorset, England	Lower Lias	(McGowan, 1974)
		27,27		BMNH R3367	Upper Hettangian - Lower Sinemurian	Lyme Regis, Dorset, England	Lower Lias	(McGowan, 1974)
		22,8		BMNH R216	Upper Hettangian - Lower Sinemurian	Lyme Regis, Dorset, England	Lower Lias	(McGowan, 1974)
	153	30,5	3,2	4,9	CAMSMX.50187	Hettangian	Lyme Regis, Dorset, England	Blue Lias (Cleary <i>et al.</i> , 2015)
<i>Ichthyosaurus</i>			5,8	NHMUK PV R	Hettangian	Axminster, Devon,	Lower Lias	(Cleary <i>et al.</i> , 2015)

<i>communis</i>				5787		England		
		6,3	NHMUK PV R 288	Hettangian	Street, Somerset, England	Lower Lias	(Cleary <i>et al.</i> , 2015)	
	52,5		BMNH 39492	Sinemurian	Lyme Regis, Dorset, England	Lower Lias	(McGowan, 1974)	
	28,2	5,5	BMNH R1162	Sinemurian	Lyme Regis, Dorset, England	Lower Lias	(McGowan, 1974)	
	210	9	BMNH 2013	Sinemurian	Street, Somerset, England	Lower Lias	(McGowan, 1974)	
		5,75	SCC 15	Sinemurian	Street, Somerset, England	Lower Lias	(McGowan, 1974)	
		9,5	OUM J13799	Sinemurian	Lyme Regis, Dorset, England	Lower Lias	(McGowan, 1974)	
	350	30	4	7,5	BRSUG 25300	Hettangian	Somerset, England	Blue Lias, pre- planorbis beds
	243,8			Plate 17	Hettangian	Street, Somerset, England	Blue Lias	(Cleary <i>et al.</i> , 2015)
		32	5	BRSU UKN	Late Sinemurian	Charmouth, Dorset, England	Lower Lias	(Cleary <i>et al.</i> , 2015)
<i>Ichthyosaurus</i> <i>conybearae</i>	23,03			IGS 956	Upper Hettangian - Lower Sinemurian	Lyme Regis, Dorset, England	Lower Lias	(McGowan, 1974)
		8,5	NHMUK PV R 10019	Hettangian	Lyme Regis, Dorset, England	Blue Lias	(Cleary <i>et al.</i> , 2015)	
	122,2	20		NHM 43006	Upper Hettangian - Lower Sinemurian	Lyme Regis, Dorset, England	Lower Lias	(McGowan, 1974)
<i>Ichthyosaurus</i> <i>larkini</i>	250	35,5	5,6	7,7	BRSUG 25300	Hettangian	Somerset, England	Blue Lias Formation
		32	5,4	AGC 11	Hettangian	Street, England	Blue Lias Formation	(Lomax & Massare, 2017)
			8	CAMSM J59575	Hettangian	Street, England	Blue Lias Formation	(Lomax & Massare, 2017)
<i>Ichthyosaurus</i> <i>somersetensis</i>	200- 300	43,8	6	8,8	ANSP 15766	Hettangian	Somerset, England	Blue Lias Formation
								(Lomax & Massare, 2017)

		6,3		AGC 16	Hettangian	Somerset, England	Blue Lias Formation	(Lomax & Massare, 2017)	
<i>Janusaurus lundi</i>	141,27*	10,3	15,2	PMO 222.654	Tithonian	Svalbard, Norway	Slottsmøya Mb., Agardhfjellet Fm.	(Roberts <i>et al.</i> , 2014; Fischer <i>et al.</i> , 2016)	
<i>Leptonectes moorei</i>	32,8		7,12	NHMUK PV R 14370	Early Pliensbachian	West of Seatown, Dorset, England	Belemnite Marls	(McGowan & Millner, 1999)	
	279			GPIT 328/4/5	Early Toarcian	Holzmaden, Baden-Württemberg, Germany	Posidonia Shale, Lias II 5/2	(Huene, 1922)	
<i>Leptonectes solei</i>	1000	340,89*	24,82*	30,93	BRSMG Ce9856	Late Sinemurian	Dorset, England	Lower Lias	
<i>Leptonectes tenuirostris</i>	135	35,25		BMNH R498	Lower Hettangian - Upper Sinemurian	Street, Somerset, England	Lower Lias	(McGowan, 1974)	
	283	58,33		IGS 51236,	Lower Hettangian - Upper Sinemurian	Street, Somerset, England		(McGowan, 1974)	
		34,29		NMO 26575	Late Pliensbachian	Hauenstein, Switzerland	Upper Lias	(Maisch & Reisdorf, 2006)	
			11,2	BGS 51235	Sinemurian			(McGowan, 2003)	
<i>Malawania anachronus</i>	62,59*	7,93*	9	NHMUK PV R6682.	Hauterivian-Barremian	Amadia, Kurdistan region, Iraq	'pre-Planorbis' beds of England	(Fischer <i>et al.</i> , 2013)	
<i>Mixosaurus cornalianus</i>	80	17,2	3,23*	1,7	NHMUK PV R5702	Anisian	Switzerland, Monte San Giorgio, Tre Fontane	Besano, Italy	(Cleary <i>et al.</i> , 2015)
<i>Mixosaurus kuhnschnyderi</i>		8,7*	3,53*	2,1	PIMUZ TI 324	Anisian/Ladinian	Switzerland, Monte San Giorgio	Besano, Italy	(Brinkmann, 1998)
<i>Mixosaurus panxianensis</i>	73	16,62*	5,03*	4,1	GMPKU-P-1033	Anisian	China, Guizhou Province, Panxian County, Yangjuan Village	Mb. II, Guanling Fm.	(Jiang <i>et al.</i> , 2006)
<i>Nannopterygius enthekiodon</i>	12,85*	6,86	5,08	NHMUK PV R 46497	Kimmeridgian	Dorset, England	Kimmeridge Clay	(Cleary <i>et al.</i> , 2015)	
		7,3		NHMUK PV R 1197	Kimmeridgian	UNK., England	Kimmeridge Clay	(Cleary <i>et al.</i> , 2015)	

		5,8		NHMUK PV R 47424	Kimmeridgian	Cambridgeshire, England	Kimmeridge Clay	(Cleary <i>et al.</i> , 2015)
<i>Ochevia alekseevi</i>	143,81*	12,86*	15,4	URM no. 56702	Tithonian	Ul'yanovsk Oblast, Russia		(Arkhangelsky, 2001)
<i>Ophthalmosaurus icenicus</i>	138,73*	9,2	15	NHMUK PV R 2160	Middle Callovian	Cambridgeshire, England	Oxford Clay, Peterborough	(Cleary <i>et al.</i> , 2015)
			22	NHMUK PV R 2133	Middle Callovian	Cambridgeshire, England	Oxford Clay, Peterborough	(Cleary <i>et al.</i> , 2015)
		10,6	13,8	NHMUK PV R 2132	Middle Callovian	Cambridgeshire, England	Oxford Clay, Peterborough	(Cleary <i>et al.</i> , 2015)
			14,1	NHMUK PV R 2152	Middle Callovian	Cambridgeshire, England	Oxford Clay, Peterborough	(Cleary <i>et al.</i> , 2015)
			14,5	Nº R 1307				(Cleary <i>et al.</i> , 2015)
			16	Nº 47885				(Cleary <i>et al.</i> , 2015)
<i>Ophthalmosaurus natans</i>	108,2			Nº 878	Oxfordian-Callovian	Wyoming, USA	Redwater Shale, Sundance Fm.	(Gilmore, 1905)
	102,8			Nº 603	Oxfordian-Callovian	Wyoming, USA	Redwater Shale, Sundance Fm.	(Gilmore, 1905)
			19	Nº S	Oxfordian-Callovian	Wyoming, USA	Redwater Shale, Sundance Fm.	(Gilmore, 1905)
			16,4	private collection	Oxfordian-Callovian	Wyoming, USA	Redwater Shale, Sundance Fm.	(Gilmore, 1905)
<i>Ophthalmosaurus yasykovi</i>	44,32*	6,82*	7,56	UPM No. EII-II- 7(1235)	Tithonian	Ul'yanovsk Oblast, Russia		(Cleary <i>et al.</i> , 2015)
<i>Palvennia hoybergeti</i>	86		10,84*	SVB 1451	Tithonian	Spitsbergen, Norway	Slottsmøya Mb., Agardhfjellet Fm.	(Druckenmiller <i>et al.</i> , 2012)
<i>Phalarodon callawayi</i>	150	26,7	6,64*	CNC VP 7275	Anisian	USA, Nevada, Augusta Mts, Pershing Co.	Fossil Hill, Favret Fm.	(Schmitz <i>et al.</i> , 2004)
<i>Platypterigius americanus</i>	85,76*	7,33	10,82*	UW5545	Cenomanian	Belle Fouche Shale		(Maxwell & Kear, 2010)

	125	14	UW2421	Upper Albian	Crook County, Wyoming, USA	Mowry Shale Mb. of the Graneros Fm.	(McGowan 1972; Maxwell & Kear, 2010)
	6,6	10,3	VP50	Upper Albian	Crook County, Wyoming, USA	Mowry Shale Mb. of the Graneros Fm.	(Nace, 1939)
<i>Platypterygius australis</i>	132	14	QMF 2453	Upper/Middle Albian	Galah Creek, Hughenden, Queensland, Australia	Tambo Fm.	(McGowan, 1972)
		15,33	F2453	Upper/Middle Albian	Flinders River, Queensland, Australia	Tambo Fm.	(McGowan, 1972)
		20,76	F3348/F3388	Upper Albian	Stewart Park, near Richmond, Queensland, Australia	Tambo Fm.	(Zammit, 2010)
		13	QM F18906	Upper Albian	Marathon Station, Queensland, Australia	Toolebuc Fm.	(Zammit <i>et al.</i> , 2010)
<i>Platypterygius campylodon</i>	107,01*	13,79*	16,6	UNKN - LOST 1	Late Albian	Kursk Oblast, Russia	Kursk Osteolite Mb, Seversk Sandstone Fm.
<i>Platypterygius hauthali</i>	43,56*	6,78*	7,5	MLP79-1-30-1	Barremian	Rio Belgrano, Santa Cruz province, Argentina	Rio Belgrano Fm.
<i>Platypterygius hercynicus</i>	103,2*	10,40*	12,2	SMSS "SGS"	Aptian	Lower Saxony, Germany	(Kolb & Sander, 2009)
<i>Platypterygius platydactylus</i>	500	117	12,5		Albian-Cenomanian	Aptian of northern Germany	(Broili, 1907)
<i>Platypterygius sachicarum</i>		87	10,92*	DON-19671	Lower Aptian	Boyaca, Colombia	Paja Fm.
<i>Quianichthysaurus</i>	121	24		IVPP V 11839	Carnian	Guizhou Province,	Xiaowa Fm.
							(Nicholls <i>et al.</i> , 2002)

<i>zhoui</i>							China, Asia		
	24	6,9	6,6	NH V1412/C1120	Carnian		Guizhou Province, China	Wayao Fm.	(Nicholls <i>et al.</i> , 2002)
	250			YIGMR XT _W Q-3	Carnian		Guizhou Province, China	Xiaowa Fm.	(Xiaofeng <i>et al.</i> , 2008)
		22		YIGMR TR00047	Carnian		Guizhou Province, China	Xiaowa Fm.	(Xiaofeng <i>et al.</i> , 2008)
<i>Qianichthyosaurus</i> <i>xingyiensis</i>	22,57*	5,27	5,6	WS2011-46-R1	Landinian		Xingyi, Guizhou	Wayao Mb., Falang Fm.	(Yang <i>et al.</i> , 2013)
<i>Shastasaurus</i> <i>alexandrae</i>	500	67,75*	14,73*	17	UP 9076	Carnian	Shasta County, limestones nr Smith's Cove, California, USA	Atractities beds, Hosselkus Limestone	(Merriam, 1902)
<i>Shonisaurus</i> <i>sikanniensis</i>	2100	224,95*	44,56*	56,66	TMP 94.378.2	Norian	British Columbia, Canada	Pardonet Fm.	(Nicholls & Manabe, 2004)
<i>Shonisaurus popularis</i>	1500	176,75*	35,42*	44,5	UNLV FZVE-1	Upper Carnian	West Union Canyon, Shoshone Mts, S of Ione, Nevada, USA	Luning	(Camp, 1981)
		37		UNLV FZVE-2	Upper Carnian		West Union Canyon, Shoshone Mts, S of Ione, Nevada, USA	Luning	(Camp, 1981)
<i>Stenopterygius</i> <i>aaleniensis</i>	216,67	47,11*	5,56	7,78	SMNS 90699	Aalenian	Baden- Wurttemberg, Germany	Opalinuston	(Maxwell <i>et al.</i> , 2012; Fischer <i>et al.</i> , 2016)
<i>Stenopterygius</i> <i>quadriscissus</i>	285	62,5	7,6	9,8	SMNS 50963	Toarcian	Germany	Lias εII3	(Maxwell, 2012)
		7,7		10,9	MHH 1981/33;	Toarcian	Germany	Lias εII9	(Maxwell, 2012)
	219	6	8,1		SMNS 6293	Toarcian	Holzmaden, Germany	Lower-Middle Posidonia Shale, Lias εII3	(Maisch, 2008; Maxwell, 2012)

285		PMUU R160	Toarcian	Holzmaden, Wiman's Exemplar No. III	Lower-Middle Posidonia Shale	(Maisch, 2008)		
220			Toarcian	Holzmaden, Zoologischer Garten Berlin	Lower-Middle Posidonia Shale	(Maisch, 2008)		
264			Toarcian	Ohmden, Deutsches Museum Munchen	Lower-Middle Posidonia Shale	(Maisch, 2008)		
340			Toarcian	Holzmaden, Zoologisches Museum Kiel	Lower-Middle Posidonia Shale	(Maisch, 2008)		
310		MHH 'Z 21'	Toarcian	Ohmden	Lower-Middle Posidonia Shale	(Maisch, 2008)		
245	7,4	9,9	GPIT 1491/8	Toarcian	Holzmaden, Germany	Lower-Middle Posidonia Shale	(Maisch, 2008; Maxwell, 2012)	
314	55,55	8	10,7	GPIT 1491/9	Toarcian	Ohmden	Lower-Middle Posidonia Shale	(Maisch, 2008; Maxwell, 2012)
260	7,4	9,3	SMNS 3775 lect	Toarcian	Holzmaden, Germany	Posidonia Shale, Lias εII3	(Maisch, 2008; Maxwell, 2012)	
290	54,12	6,47	10	S Museum of Szczecin, Poland	Early Toarcian	Baden- Wurttemberg, Holzmaden, Germany	Posidonia shale, Lias ε II 11	(Maisch, 2008)
270	54	7	10	Skeleton in Esslingen Museum, Germany	Early Toarcian	Baden- Wurttemberg, Holzmaden, Germany	Posidonia shale, Lias ε II 4	(Maisch, 2008)
317	52,43	7,03	10,81	SMNS 15033	Early Toarcian	Baden- Wurttemberg, Holzmaden, Germany	Posidonia shale, Lias ε II 6	(Maisch, 2008)

270	54,29	7,62	9,52	Skeleton '155' of Bernhard Hauff's album	Early Toarcian	Baden-Wurttemberg, Holzmaden, Germany	Posidonia shale, Lias ε II 3	(Maisch, 2008)
285		6,67	8,57	Museum of Kirchheim unter Teck, Germany	Early Toarcian	Baden-Wurttemberg, Holzmaden, Germany	Posidonia shale, Lias ε II 3	(Maisch, 2008)
235	44,17	6,25	8,34	Museo Pedagógico de Ciencias Naturales, Argentinien	Early Toarcian	Baden-Wurttemberg, Holzmaden, Germany	Posidonia shale, Lias ε II 3	(Maisch, 2008)
315	55,17		6,96	GPIT 43/0219-1	Toarcian	Baden-Wurttemberg, Holzmaden, Germany	Posidonia shale, Lias ε II 3/4	(Maisch, 2008)
	7	9,6	SMNS 7402	Toarcian	Germany	Lias εII6	(Maxwell, 2008)	
	6,8	8,7	SMNS 10460	Toarcian	Germany	Lias εII3	(Maxwell, 2008)	
317	8,3	10,4	SMNS 15033	Toarcian	Holzmaden, Germany	Posidonia Shale, Lias εII6	(Maisch, 2008; Maxwell, 2012)	
	8	10,5	SMNS 51142	Toarcian	Germany	Lias εII10	(Maxwell, 2012)	
	6,6	8,8	SMNS 51948	Toarcian	Germany	Lias εII3	(Maxwell, 2012)	
	5,3	7,3	SMNS 52036	Toarcian	Germany	Lias εI2	(Maxwell, 2012)	
	8	10,7	SMNS 53001	Toarcian	Germany	Lias εII10	(Maxwell, 2012)	
	6,3	7,9	SMNS 54062	Toarcian	Germany	Lias εII2	(Maxwell, 2012)	
	6,3	8,5	SMNS 54816	Toarcian	Germany	Lias εII3	(Maxwell, 2012)	
	8,2	9,9	SMNS 55748	Toarcian	Germany	Lias εII4	(Maxwell, 2012)	
	5,7	7,6	SMNS 56856	Toarcian	Germany	Lias εII2	(Maxwell, 2012)	
	5,8	8	SMNS 58881	Toarcian	Germany	Lias εII3	(Maxwell, 2012)	
	8,3	10,1	SMNS 80115	Toarcian	Germany	Lias εII4	(Maxwell, 2012)	

		7,4	9,6	GPIT 1491/1	Toarcian	Germany	Lias εII6	(Maxwell, 2012)
322		7,4	10,3	GPIT 1491/2	Toarcian	Holzmaden, Germany	Posidonia Shale, Lias εII10	(Maisch, 2008; Maxwell, 2012)
	67,24	7,4	9,9	GPIT 1491/8	Toarcian	Germany	Lias εII3	(Maxwell, 2012)
		8	10,7	GPIT 1491/9	Toarcian	Germany	Lias εII6	(Maxwell, 2012)
324	68,51		10,91	GPIT 1491/6	Early Toarcian	Germany, Baden- Wurttemberg, Holzmaden	Posidonia shale, Lias ε II 10	(Maisch, 2008)
<i>Stenopterygius</i> <i>triscissus</i>			6,1	SMNS 50815;	Toarcian	Germany	Posidonia Shale	(Maxwell, 2012)
270	68,78	4,88	7,81	BMK 813B	Early Toarcian	Germany, Baden- Wurttemberg, Holzmaden	Posidonia shale, Lias ε II 4	(Maisch, 2008)
287		7,78	10,56	GPIT 1491/7	Early Toarcian	Germany, Baden- Wurttemberg, Holzmaden	Posidonia shale, Lias ε II 4	(Maisch, 2008)
207		5	6,92	Private collection of Ward, Rochester, NY	Early Toarcian	Germany, Baden- Wurttemberg, Ohmden	Posidonia shale, Lias ε II 4	(Maisch, 2008; Maxwell, 2012)
285		8,89	9,45	Private collection of R. Leicht, Vaihingen, Germany;	Early Toarcian	Germany, Baden- Wurttemberg, Holzmaden	Posidonia shale, Lias ε II 4	(Maisch, 2008)
210		4,38	6,88	GPIT 12/0224-2	Early Toarcian	Germany, Baden- Wurttemberg, Ohmden	Posidonia shale, Lias ε II 6	(Maisch, 2008)
215		4,23	6,15	GPIT PV 24306	Early Toarcian	Germany, Baden- Wurttemberg, Holzmaden	Posidonia shale, Lias ε II 2	(Maisch, 2008)
		7,3	10,5	SMNS 50007	Toarcian	Germany	Lias εII3	(Maxwell, 2012)
		5,6	8,3	SMNS 54027	Toarcian	Germany	Lias εII1	(Maxwell, 2012)

		4,3	6,6	SMNS 80113	Toarcian	Germany	Lias εII4	(Maxwell, 2012)	
		5,1	7,6	GPIT RE/7297	Toarcian	Germany	Lias εII3	(Maxwell, 2012)	
<i>Stenopterygius uniter</i>			8,2	SMNS 57532	Toarcian	Germany	Posidonia Shale	(Maxwell, 2012)	
	313			SMNS 4865	Toarcian	Holzmaden, Germany	Posidonia Shale	(Maisch, 2008)	
	375	9	12,6	SMNS 17500	Toarcian	Germany	Lias εII8	(Maxwell, 2012)	
	340				Toarcian	Holzmaden Sammlung Rühle von Lilienstern	Posidonia Shale	(Maisch, 2008)	
	335			SMNS 14216	Toarcian	Holzmaden, Germany	Lias ε II,10	(Maisch, 2008)	
	234	52,73	6	9,1	GPIT 1491/10	Early Toarcian	Germany, Baden- Wurttemberg, Holzmaden	Posidonia shale, Lias ε II 10	(Maisch, 2008; Maxwell, 2012)
	230		5,58	8,37	Unknown, sold to Krantz, Bonn; lost (Plate 6,4)	Early Toarcian	Germany, Baden- Wurttemberg, Holzmaden	Posidonia shale, Lias ε II 11	(Maisch, 2008)
	308		6,7	11,6	GPIT 1491/12	Early Toarcian	Germany, Baden- Wurttemberg, Holzmaden	Posidonia shale, Lias ε II 6	(Maisch, 2008; Maxwell, 2012)
	340		10,35	17,24	Private collection of Baron von Lilienstern, Germany	Early Toarcian	Germany, Baden- Wurttemberg, Holzmaden	Posidonia shale, Lias ε II 10	(Maisch, 2008)
	328,5		10	15,46	PMUU R 167	Early Toarcian	Germany, Baden- Wurttemberg, Holzmaden	Posidonia shale, Lias ε II 10	(Maisch, 2008)
	313		8,49	12,12	SMNS 4865	Early Toarcian	Germany, Baden- Wurttemberg, Holzmaden	Posidonia shale, Lias ε II 6	(Maisch, 2008)
	335			12,67	SMNS 14216	Early Toarcian	Germany, Baden- Wurttemberg,	Posidonia shale, Lias ε II 10	(Maisch, 2008)

Holzmaden									
	350	9,68	13,55	NMC 8161	Early Toarcian	Germany, Baden-Wurttemberg, Holzmaden	Posidonia shale, Lias ε II 10	(Maisch, 2008)	
<i>Suevoleviathan integer</i>		8,5	11,8	MHH 1981/25	Toarcian	Germany	Lias εII8	(Maxwell, 2012)	
<i>Suevoleviathan integer</i>		32,13*	3,7	6,6 47409	Toarcian	Kingsthorpe, Northhamptonshire, England	Upper Lias	(Cleary <i>et al.</i> , 2015)	
<i>Suevoleviathan disinteger</i>		431	86	9,5	12,5	SMNS 15390	Early Toarcian	Holzmaden, Baden-Wurttemberg, Germany	Posidonia Shale, Lias II6
<i>Sveltonectes insolitus</i>		57,59		8,6*	IRSNB R269	Barremian	Ul'yanovsk Oblast, Russia		(Fischer <i>et al.</i> , 2011)
<i>Temnodontosaurus azerguensis</i>		208,66*	16,8*	20,51	MAMSPLP	Toarcian	Belmont d'Azergues, Rhône, France	Bifrons zone	(Martin <i>et al.</i> , 2012)
<i>Temnodontosaurus crassimanus</i>		95,59*	9,94*	11,6	NHMUK PV R 16080	Pliensbachian	England, Northamptonshire, Bugbrooke	Dyrham Fm.	(Cleary <i>et al.</i> , 2015)
<i>Temnodontosaurus eurycephalus</i>		102		12,10*	BMNH R1157	Simenurian	Broad Ledge, Church Cliffs	Lower Lias	(McGowan, 1974)
<i>Temnodontosaurus platyodon</i>		1200.	124		BMNH R1158	Late Sinemurian	Southwest coast of England	Lower Lias, Lyme Regis	(McGowan, 1995)
		139			BMNH (2003)	Late Sinemurian	Southwest coast of England	Lower Lias, Lyme Regis	(McGowan, 1996)
		10,5		Bristol City Museums	Late Sinemurian	Southwest coast of England	Lower Lias, Lyme Regis		(McGowan, 1996)
		189		BATGM M3577a	Late Sinemurian				(McGowan, 1996)
		124		BMNH R1 158	Late Sinemurian				(McGowan, 1996)
		108		BMNH 14564	Late Sinemurian				(McGowan, 1996)
		80		BMNH R311	Late Sinemurian				(McGowan, 1996)
		73,2		SMC J68446	Late Sinemurian				(McGowan, 1996)

	65,5			BMNH 43971	Late Sinemurian		(McGowan, 1996)
		17,3		SMNS 9445	Hettangian-Sinemurian		(McGowan, 1996)
	192			BMNH R 1155	Hettangian-Sinemurian		(McGowan, 1996)
<i>Thaisaurus chonglakmanii</i>	7,66*	3,15	1,84		Olenekian-Landinian	Phattalung, Southern Thailand	(Mazin et al., 1991)
<i>Toretocnemus zitteli</i>	24,55*	6,54*	6,1	M 8099	Carnian	Shasta County, California	Hosselkus Limestone Fm.
<i>Undorosaurus gorodischensis</i>	450	141,27*	10,5	15,2	UPM No. EIII-20(572)	Tithonian	Ul'yanovsk Oblast, Russia
				18,3	UPM No. EHII-24(785)	Tithonian	Ul'yanovsk Oblast, Russia
				16	UPM No. EIII-27(870)	Tithonian	Moscow region, Russia
<i>Utatsusaurus hataii</i>	300	18,49*	5,39*	4,57	IGPS 95941	Olenekian	Kitakami Massif, Japan
<i>Wahlisaurus massarae</i>		93,5*	7,8	11,43*	LEICT G454.1951.5	Lower Hettangian	Nottinghamshire, England, UK.
<i>Xinminosaurus catactes</i>	232	29	7	GMPKU-P-1071	Anisian	China, Guizhou Province, nr Yangjuan Village	Mb. II, Guanling
							(Jiang et al., 2009)

Supplementary Information. S1- Table of contents depicting total body size, skull, femur and humerus lengths, associated geologic unit, age interval, geographic localities, and identification of the material.

REFERENCES

- Adams, T.L. & Fiorillo A.R. 2011. *Platypterygius* Huene, 1922 (Ichthyosauria, Ophthalmosauridae) from the Late Cretaceous of Texas, USA, *Paleontol.Eletron.* 14: 1-12.
- Arkhangelsky, M.S., Averianov, A.O., Pervushov, E.M., Ratnikov, V.Y & Zozyrev, N.Y. 2008. On Ichthyosaur Remains from the Cretaceous of the Voronezh Region. *Paleontol. J.* 42: 287-291.
- Arkhangelsky, M.S. 2001. On a new ichthyosaur of the genus *Otschevia* from the Volgian stage of the Volga region near Ulyanovsk. *Paleontol. J.* 35: 629-634.
- Broili, F. 1907. Ein neuer Ichthyosaurus aus der norddeutschen Kreide, *Palaeontographica* 54: 139-162.
- Camp, C.L. 1981. Child of the rocks - The story of the Berlin-Ichthyosaur State Park. Nevada. Bureau of Mines and Geology, Special Publication 5: 1-36.
- Chen, X., Sander, P.M., Cheng, L. & Wang, X. 2013. A new Triassic Primitive Ichthyosaur from Yuanan, South China. *Acta Geol. Sin.* 87, 672-677.
- Chen, Z.Q. & Benton, M.J. 2012. The timing and pattern of biotic recovery following the end-Permian mass extinction. *Nat. Geosci.* 5: 375–383.
- Cleary, T.J., Moon, B.C., Dunhill, A.M. & Benton, M.J. 2015. The fossil record of ichthyosaurs, completeness metrics and sampling biases, *Palaeontology* 58: 1-16.
- Dal Sasso, C. & Pinna, G. 1996. *Besanosaurus leptorhynchus* n. gen. sp., a new Shastasaurid Ichthyosaur from the Middle Triassic of Besano (Lombardy, N. Italy). *Soc. Ital. Sci. Nat. Mus. CivicoStoria Nat. Milano.* 4: 3-21.
- Druckenmiller, P.S., Hurum, J.H., Knusten, E.M. & Nakrem, H.A. 2012. Two new Ophthalmosaurids (Reptilia: Ichthyosauria) from the Agardhfjellet Formation (Upper Jurassic: Volgian/Tithonian), Svalbard, Norway. *Nor. J. Geol.* 92: 311-339.
- Druckenmiller, P.S. & Maxwell, E.E. 2010. A new Lower Cretaceous (Lower Albian) ichthyosaur genus from the Clearwater Formation, Alberta, Canada. *Can. J. Earth Sci.* 47, 1037-1053.

Fernandez, M. & Aguirre-Urreta, M.B. 2005. Revision of *Platypterygius hauthali* von Huene, 1927 (Ichthyosauria: Ophthalmosauridae) from the Early Cretaceous of Patagonia, Argentina. J. Vert. Paleo. 25, 583-587.

Fernandez, M. & Aguirre-Urreta, M.B. 2010. Revision of *Platypterygius hauthali* von Huene, 1927 (Ichthyosauria: Ophthalmosauridae) from the Early Cretaceous of Patagonia, Argentina. J. Vertebr. Paleontol. 25: 583-587.

Fernández, M. 2007. Redescription and phylogenetic position of *Caypullisaurus* (Ichthyosauria: Ophthalmosauridae). J. Vert. Paleo. 81: 368-375.

Fernández, M.S. & Maxwell, E.E. 2012. The genus *Arthropterygius* Maxwell (Ichthyosauria: Ophthalmosauridae) in the Late Jurassic of the Neuquén Basin, Argentina. Geobios.45: 535-540.

Fischer, V., Appleby, R.M., Naish ,D., Liston, J., Riding, J.B., Brindley S. et al. 2013. A basal Thunnosaurian from Iraq reveals disparate phylogenetic origins for Cretaceous ichthyosaurs. Biol. Lett. 9: 1-6.

Fischer, V., Bardet, N., Benson, R.B.J., Arkhangelsky, M.S. & Friedman, M. 2016. Extinction of fish-shaped marine reptiles associated with reduced evolutionary rates and global environmental volatility. Nat. Commun. 7: 1-11.

Fischer, V., Cappetta, H., Vincent, P., Garcia, G., Goolaerts, S., Martin, J.E. et al. 2014. Ichthyosaurs from the French Rhaetian indicate a severe turnover across the Triassic–Jurassic boundary. Naturwissenschaften 101: 1027-1040.

Fischer, V., Masure, E., Arkhangelsky, M.S. & Godefroit, P. 2011. A new Barremian (Early Cretaceous) ichthyosaur from western Russia.J. Vert. Paleontol. 31: 1010-1025.

Huene, F.V. 1922. Die Ichthyosaurier des Lias undihre Zusammenhige. Monographienzur Geologie und Paliontologie. Verlag von GebriiderBorntraeger, Berlin, 1-114.

Jiang, D., Motani, R., Hao, W., Rieppel, O., Sun, Y., Tintori, A. et al. 2009. Biodiversity and sequence of the Middle Triassic Panxian Marine Reptile Fauna, Guizhou Province, China. Acta Geol. Sin. 83: 451-459.

Jiang, D.Y., Hao, W.C., Maisch, M.W., Matzke, A.T. & Sun, Y.L. 2005. A basal mixosaurid ichthyosaur from the Middle Triassic of China. Paleontology 28: 869–882.

- Jiang, D.Y., Motani, R., Tintori, A., Rieppel, O., Chen, G.B., Huang, J.D. et al. 2014. The Early Triassic Eosauropterygian Majiashanosaurus discocoracoidis, gen. et sp. nov.(Reptilia, Sauropterygia), from Chaohu, Anhui Province, People's Republic of China. *J. Vert. Pal.* 34: 1044-1052.
- Jiang, D.Y., Schmitz, L., Hao, W.C. & Sun, Y.L. 2006. A new mixosaurid ichthyosaur from the Middle Triassic of China. *J. Vert. Paleo.* 26: 60-69.
- Kolb, C. & Sander, P.M. 2009. Redescription of the ichthyosaur *Platyptegygiushercynicus* (Kuhn 1946) from the Lower Cretaceous of Salzgitter (Lower Saxony, Germany). *Palaeontographica* 228: 151-192.
- Maisch, M.W. & Matzke, A.T. 2000. The Ichthyosauria. *StuttgarterBeitr.Naturk.* 298: 1-154.
- Maisch, M.W. & Reisdorf, A.G. 2006. Evidence for the longest stratigraphic range of a post-Triassic Ichthyosaur: a Leptonectestenuirostris from the Pliensbachian (Lower Jurassic) of Switzerland. *Geobios* 39: 491–505.
- Maisch, M.W. 2008. Revision der Gattung *Stenopterygius* Jaekel, 1904 emend. Von Huene, 1922 (Reptilia: Ichthyosauria) aus dem unteren Jura Westeuropas. *Palaeodiversity* 1: 227-271.
- Maisch, M.W. 1998. A new ichthyosaur genus from the Posidonia Shale (Lower Toarcian, Jurassic) of Holzmaden, SW-Germany with comments on the phylogeny of post-Triassic ichthyosaurs. *N. Jb. Geol. Palaont. Abh.* 209: 47-78.
- Massare, J.A., Buchholtz, E.A., Kenney, J.M. & Chomat, A.M. 2006. Vertebral morphology of *Ophthalmosaurus natans* (Reptilia: Ichthyosauria) from the Jurassic Sundance Formation of Wyoming. *Paludicola* 5: 242-254.
- Maxwell, E.E. & Caldwell, M.W. 2006. A new genus of Ichthyosaur from the Lower Cretaceous of Western Canada. *Palaeontology* 49: 1043-1052.
- Maxwell, E.E. & Kear, B.P. 2010. Postcranial Anatomy of *Platypterygius americanus* (Reptilia: Ichthyosauria) from the Cretaceous of Wyoming, *J. Vertebr. Paleontol.* 30: 1059–1068.
- Maxwell, E.E. 2012. New Metrics to Differentiate Species of *Stenopterygius* (Reptilia: Ichthyosauria) from the Lower Jurassic of Southwestern Germany. *J. Paleontol.* 86: 105–115.

- Mazin, J. M., Suteethorn, V., Buffetaut, E., Jaeger, J. J. & Helmcke-Ingavat, R. 1991. Preliminary description of *Thaisaurus chonglakmanii* n. g. n. sp. a new ichthyopterygian (Reptilia) from the Early Triassic of Thailand.- C.-R. Seanc. Acad. Sci. Paris. 313: 1207–1212.
- McGowan, C. 2003. A new specimen of *Excalibosaurus* from the English Lower Jurassic. *J. Vert. Paleo* 23: 950-956.
- McGowan, C. & Motani, R. 2003. Handbook of Paleoherpetology. In: Part 8 Ichthyopterygia (V.F. Pfeil, ed), pp. 1-175, München, Germany.
- McGowan, C. 1972. The systematics of Cretaceous ichthyosaurs with particular reference to the material from North America, Contributions to Geology 11: 9-29.
- McGowan, C. 1974. A Revision of the Latipinnate Ichthyosaurs of the Lower Jurassic of England (Reptilia: Ichthyosauria). Life Sciences Contribution Royal Ontario Museum 100: 1-30.
- McGowan, C. 1994. A new species of *Shastasaurus* (Reptilia: Ichthyosauria) from the Triassic of British Columbia: the most complete exemplar of genus. *J. Vert. Pal.* 14:168–179.
- McGowan, C. 1978. Further Evidence for the Wide Geographical Distribution of Ichthyosaur Taxa (Reptilia: Ichthyosauria). *J. Pal.* 53: 1155-1162.
- McGowan, C. 1993. A new species of large, long-snouted ichthyosaur from the English lower Lias. *Can. J. Earth Sci.* 30: 1197-1204.
- McGowan, C. 1995. A remarkable small ichthyosaur from the Upper Triassic of British Columbia, representing a new genus and species. *Can. J. Earth Sci.* 32: 292-303.
- McGowan, C. 1996. Giant ichthyosaurs of the Early Jurassic. *Can. J. Earth. Sci.* 33: 1011-1021.
- Merriam, J.C. 1902. Triassic Ichthyopterygia from California and Nevada. University of California Publications - Bulletin of the Department of Geology 3: 63–108.
- Merriam, J.C. 1908. Triassic Ichthyosauria, with special reference to the American forms. Memoirs of the University of California 1: 1-252.
- Motani, R. & You, H. 2008. Taxonomy and limb ontogeny of *Chaohusaurus geishanensis* (Ichthyosauria), with a note on the allometric equation. *J. Vert. Pal.* 18: 533-540.

- Motani, R. 1997. New information on the forefin of *Utatsusaurushataii* (Ichthyosauria). *J. Paleontol.* 71: 475-479.
- Motani, R. 1998. First complete forefin of the ichthyosaur *Grippia longirostris* from the Triassic of Spitsbergen. *Palaeontology* 41: 591-599.
- Motani, R. 2005. True skull roof configuration of *Ichthyosaurus* and *Stenopterygius* and its implications. *J. Vert. Paleo.* 25: 338-342.
- Nace, R.L. A new ichthyosaur from the Upper Cretaceous Mowry Formation of Wyoming. *Am. J. Sci.* 237: 673-686.
- Nicholls, E., Wei, C. & Manabe, M. 2002. New material of *Qianichthyosaurus* Li, 1999 (Reptilia, Ichthyosauria) from the late Triassic of southern China, and implications for the distribution of Triassic ichthyosaurs. *J. Vert. Pal.* 22: 759-765.
- Nicholls, E.L. & Manabe, M. 2004. Giant ichthyosaurs of the Triassic-A new species of *Shonisaurus* from the Pardonet Formation (Norian: Late Triassic) of British Columbia. *J. Vert. Paleontol.* 24: 838-849.
- Quenstedt, FA., 1856. *Der Jura.* 1-842, Laupp, Tübingen.
- Rieppel, O., Jinling, L. & Jun, L. 2003. *Lariosaurus xingyiensis* (Reptilia: Sauropterygia) from the Triassic of China. *Can. J. Earth Sci.* 40: 621–634.
- Roberts, A.J., Druckenmiller, P.S., Saetre, G.P. & Hurum, J.H. 2014. A New Upper Jurassic Ophthalmosaurid Ichthyosaur from the Slottsmøya Member, Agardhfjellet Formation of Central Spitsbergen. *PLoS ONE* 9: 1-24.
- Sander, P.M., Chen, X., Cheng, L. & Wang, X. 2011. Short-Snouted Toothless Ichthyosaur from China Suggests Late Triassic Diversification of Suction Feeding Ichthyosaurs. *PLoS ONE* 6: 1-10.
- Sander, P.M. 1989. The large ichthyosaur *Cymbospondylusbuchseri*, sp. nov., from the Middle Triassic of Monte San Giorgio (Switzerland), with a survey of the genus in Europe. *J. Vert. Paleo* 9: 163-173.
- Schmitz, L., Sander, P.M., Stoors, G.W. & Rieppel, O. 2004. New Mixosauridae (Ichthyosauria) from the Middle Triassic of the Augusta Mountains (Nevada, USA) and their implications for mixosaur taxonomy. *Palaeontographica Abt. A.* 270: 133-162.
- Shang, Q.H. & Chun, Li. 2009. On the occurrence of the ichthyosaur *Shastasaurus* in the Guanling biota (Late Triassic), Guizhou, China. *Vertebrata PalAsiatica* 47: 178-193.

Stoors, G.W., Arkhangelsky, M.S. & Efimov ,V.M. 2003. Mesozoic marine reptiles of Russia and other former Soviet republics. In: The age of dinosaurs in Russia and Mongolia, vol. 1 (M.J. Benton, M.A. Shishkin, D.M. Unwin, E.N. Kurochkin, eds), pp.187-209. Cambridge University Press.

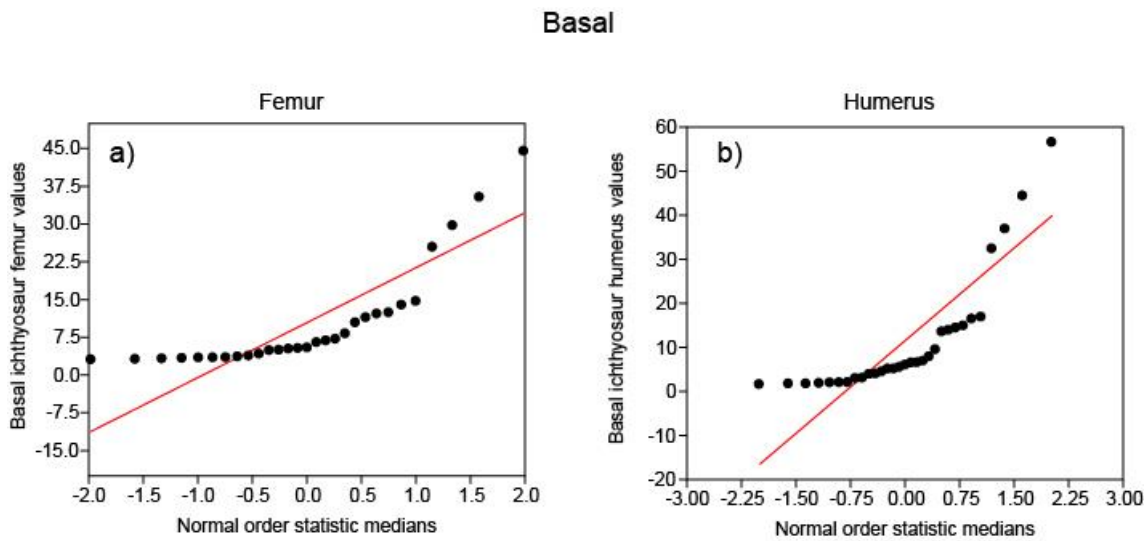
Xiaofeng, W., Bachmann, G.H., Hagdorn, H., Sander, P.M., Cuny, G., Xiaohong, C. et al. 2008. The Late Triassic black shales of the Guanling area, Guizhou province, south-west China: a unique marine reptile and pelagic crinoid fossil Lagerstatte. *Palaeontology* 51: 27-61.

Yang, P., Ji, C., Jiang, D., Motani, R., Tintori, A., Sun, Y. et al. 2013. A New Species of *Qianichthyosaurus* (Reptilia: Ichthyosauria) from Xingyi Fauna (Ladinian, Middle Triassic) of Guizhou. *Acta Sci. Natur. Univ. Pekinensis* 49: 1002-1008.

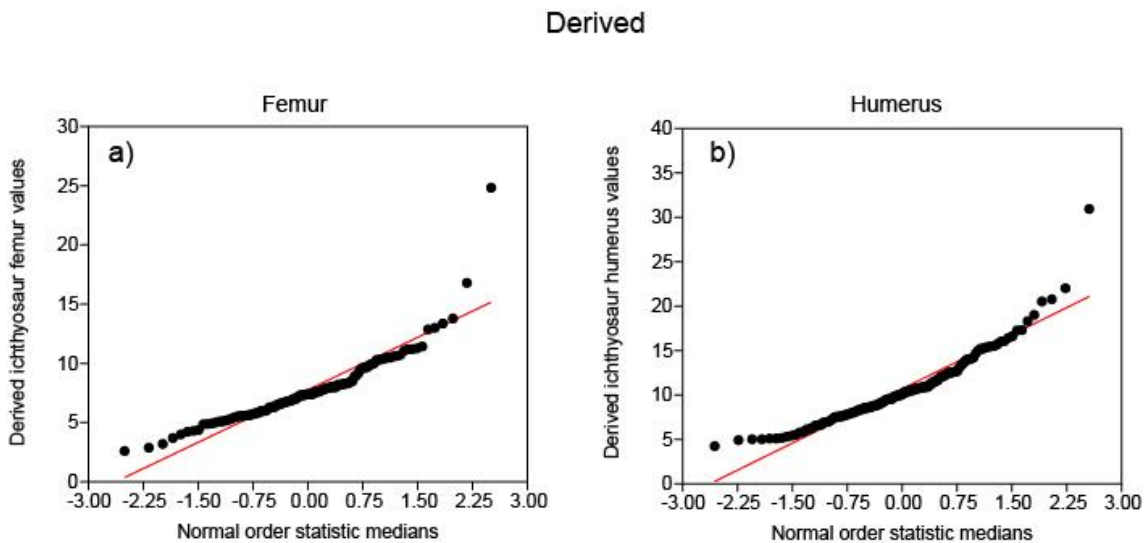
Zammit, M., Norris, R.M. & Kear, B.P. 2010. The Australian Cretaceous Ichthyosaur *Platypterygius australis*: A Description and Review of Postcranial Remains. *J. Vert. Paleo.* 30: 1726-1735.

Zammit, M. 2010. A review of Australasian ichthyosaurs. *Alcheringa* 34: 281-292.

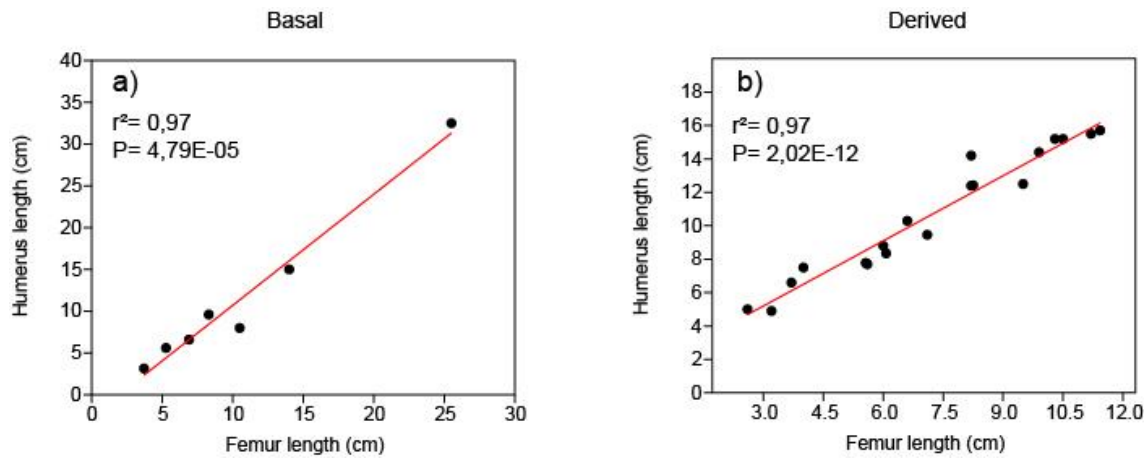
Supplementary Information S2



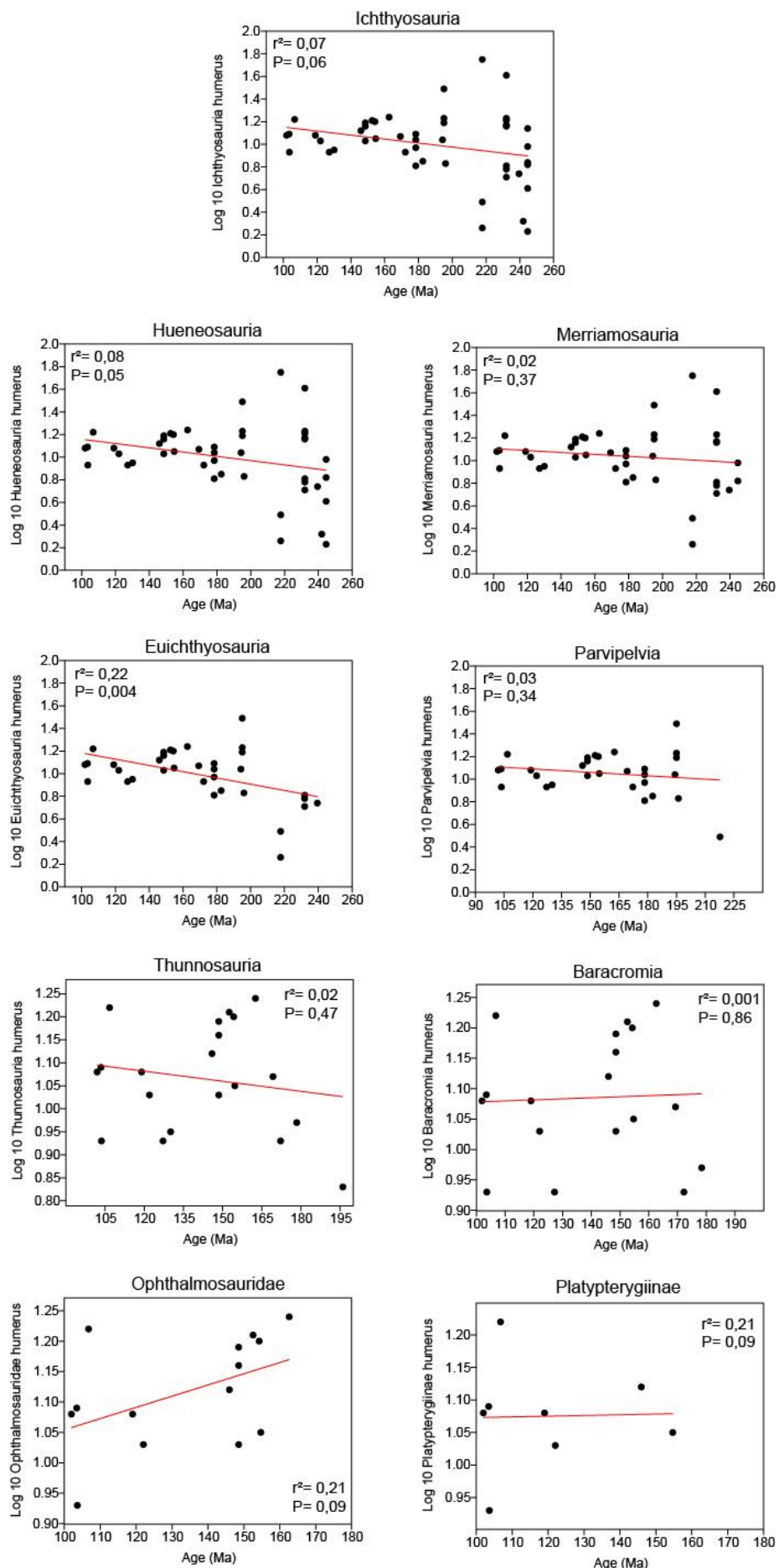
A-Normal probability plot (Shapiro-Wilk test) using: a) femur, b) humerus lengths for basal clades Ichthyosuria, Hueneosuria, Merriamosuria, Euichthyosuria and Parvipelvia considered in this study.



A.1-Normal probability plot (Shapiro-Wilk test) using: a) humerus, b) femur lengths for derived clades Thunnosauria, Baracromia, Ophtalmosauridae, and Platypterygiinae considered in this study.

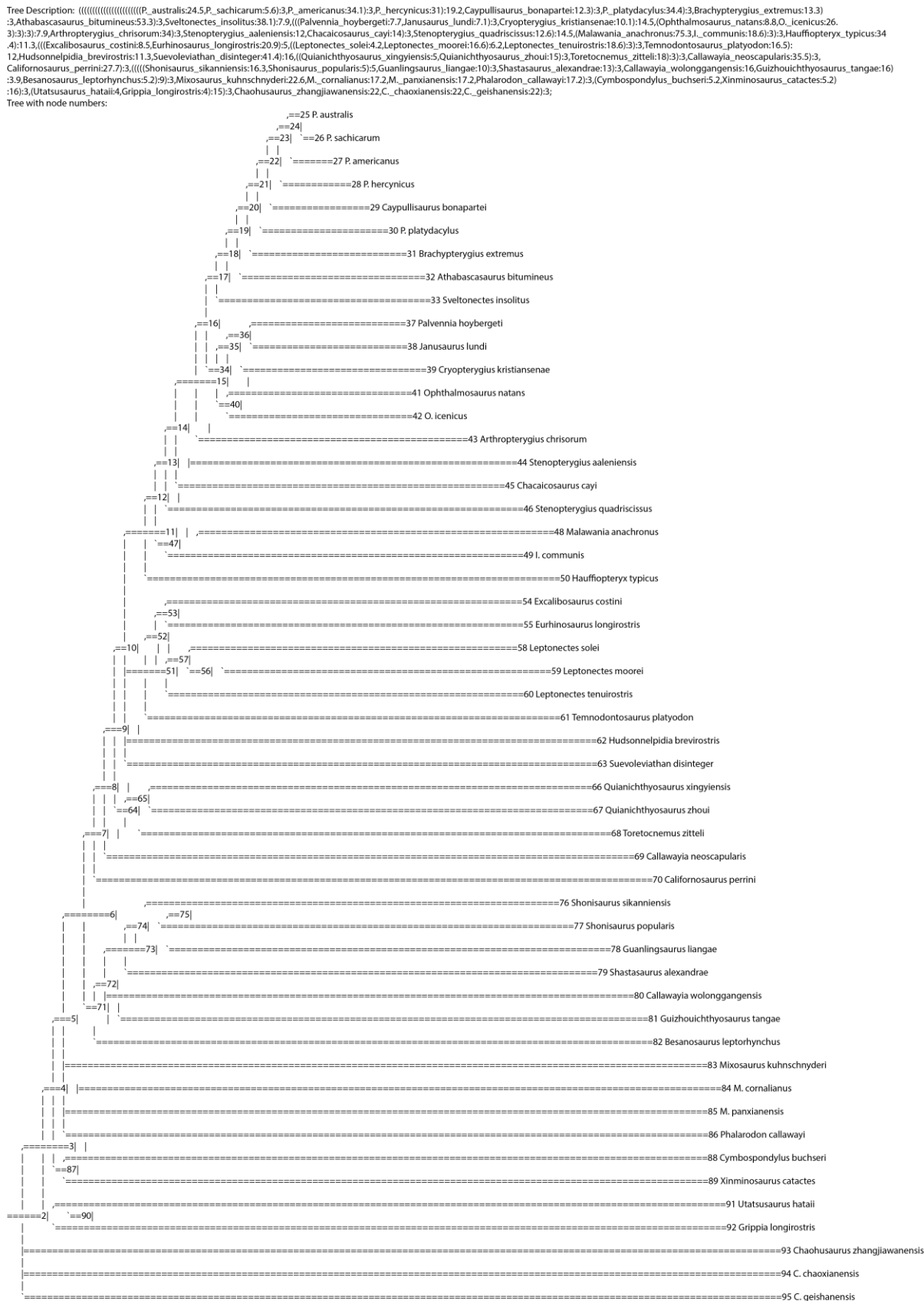


B- Linear regression of humeral length (y-axis, in centimeters) against femoral length (x-axis, in centimeters) for a) basal ichthyosaurs (regression line is $y = 0,2523x - 0,0951$) and b) derived ichthyosaurs (regression line is $y = 0,0788x + 4,0674$). Each pair of humerus and femur values refers to the same ichthyosaurs specimens being that in some species the average of the sizes was used (see Table 1 Supplementary material).



C- Scatter plot comparing log10 humerus length (y-axis, proxy for body mass) against age (x-axis, Ma) for some ichthyosaurs subclades. The age assigned to each taxon was calculated as the mid-point of its total stratigraphic range.

Supplementary Information S3-Ichthyosauria



Supertree with the values of each taxon of Ichthyosauria and the ancestor values of each internal point constructed in the program Mesquite version 3.40.

----- Trace Character History -----

Character 1: Character 1

Parsimony reconstruction (Squared) [Squared length: 0.13869678]

node 2: 0.5358694
node 3: 0.58599779
node 4: 0.63983167
node 5: 0.63718679
node 6: 0.72052317
node 7: 0.71126889
node 8: 0.70215203
node 9: 0.73040014
node 10: 0.81382019
node 11: 0.86251213
node 12: 0.88001875
node 13: 0.98587844
node 14: 1.01156102
node 15: 1.04511123
node 16: 1.09747124
node 17: 1.06374803
node 18: 1.0614731
node 19: 1.06659814
node 20: 1.07546713
node 21: 1.08306872
node 22: 1.07407006
node 23: 1.07209016
node 24: 1.06941437
node 25: 1.22
node 26: 1.03
node 27: 1.08
node 28: 1.08
node 29: 1.12
node 30: 1.09
node 31: 1.05
node 32: 0.93
node 33: 0.93
node 34: 1.13016107
node 35: 1.13351878
node 36: 1.11743688
node 37: 1.03
node 38: 1.16
node 39: 1.19
node 40: 1.1621562
node 41: 1.24
node 42: 1.21
node 43: 1.2
node 44: 0.93
node 45: 1.07
node 46: 0.97
node 47: 0.87562335
node 48: 0.95
node 49: 0.83

node 50: 0.81
node 51: 1.08850469
node 52: 1.13144939
node 53: 1.1383243
node 54: 1.19
node 55: 1.04
node 56: 1.17026915
node 57: 1.29391969
node 58: 1.49
node 59: 0.85
node 60: 1.04
node 61: 1.23
node 62: 0.49
node 63: 1.09
node 64: 0.74300698
node 65: 0.74944832
node 66: 0.74
node 67: 0.81
node 68: 0.78
node 69: 0.26
node 70: 0.71
node 71: 0.99829512
node 72: 1.13238431
node 73: 1.21579896
node 74: 1.29593644
node 75: 1.49246713
node 76: 1.75
node 77: 1.61
node 78: 1.17
node 79: 1.23
node 80: 1.21
node 81: 1.16
node 82: 0.98
node 83: 0.32
node 84: 0.23
node 85: 0.61
node 86: 0.82
node 87: 0.94105174
node 88: 1.14
node 89: 0.84
node 90: 0.56747033
node 91: 0.65
node 92: 0.48
node 93: 0.6
node 94: 0.31
node 95: 0.33

#NEXUS

[written Tue Feb 27 09:58:44 BRT 2018 by Mesquite version 3.40 (build 877) at DESKTOP-M9K2NNB/192.168.0.10]

BEGIN TAXA;

TITLE Untitled_Block_of_Taxa;

DIMENSIONS NTAX=52;

TAXLABELS

P._australis P._sachicarum P._americanus P._hercynicus Caypullisaurus._bonapartei
P._platydacus Brachypterygius._extremus Athabascasaurus._bitumineus Sveltonectes._insolitus
Palvennia._hoyergeti Janusaurus._lundi Cryopterygius._kristiansenae Ophthalmosaurus._natans O._icenicus
Arthropterygius._chrisorum Stenopterygius._aaleniensis Chacaicosaurus._cayi Stenopterygius._quadriscissus
Malawania._anachronus I._communis Hauffiopteryx._typicus Excalibosaurus._costini Eurhinosaurus._longirostris
Leptonectes._solei Leptonectes._moorei Leptonectes._tenuirostris Temnodontosaurus._platyodon
Hudsonnelpidia._brevirostris Suevoleviathan._disinteger Quianichthyosaurus._xingyiensis Quianichthyosaurus._zhoui
Toretocnemus._zitteli Callawayia._neoscapularis Californosaurus._perrini Shonisaurus._sikanniensis
Shonisaurus._popularis Guanlingsaurus._liangae Shastasaurus._alexandrae Callawayia._wolonggangensis
Guizhouichthyosaurus._tangae Besanosaurus._leptorhynchus Mixosaurus._kuhnschnyderi M._cornalianus
M._panxianensis Phalarodon._callawayi Cymbospondylus._buchseri Xinminosaurus._catactes Utatsusaurus._hataii
Grippia._longirostris Chaohusaurus._zhangjiawanensis C._chaoxianensis C._geishanensis
;

END;

BEGIN CHARACTERS;

TITLE Character_Matrix;

DIMENSIONS NCHAR=1;

FORMAT DATATYPE = CONTINUOUS GAP = - MISSING = ?;

MATRIX

P._australis	1.22
P._sachicarum	1.03
P._americanus	1.08
P._hercynicus	1.08
Caypullisaurus._bonapartei	1.12
P._platydacus	1.09
Brachypterygius._extremus	1.05
Athabascasaurus._bitumineus	0.93
Sveltonectes._insolitus	0.93
Palvennia._hoyergeti	1.03
Janusaurus._lundi	1.16
Cryopterygius._kristiansenae	1.19
Ophthalmosaurus._natans	1.24
O._icenicus	1.21
Arthropterygius._chrisorum	1.2
Stenopterygius._aaleniensis	0.93
Chacaicosaurus._cayi	1.07
Stenopterygius._quadriscissus	0.97
Malawania._anachronus	0.95
I._communis	0.83
Hauffiopteryx._typicus	0.81
Excalibosaurus._costini	1.19
Eurhinosaurus._longirostris	1.04
Leptonectes._solei	1.49
Leptonectes._moorei	0.85
Leptonectes._tenuirostris	1.04
Temnodontosaurus._platyodon	1.23
Hudsonnelpidia._brevirostris	0.49
Suevoleviathan._disinteger	1.09
Quianichthyosaurus._xingyiensis	0.74
Quianichthyosaurus._zhoui	0.81
Toretocnemus._zitteli	0.78
Callawayia._neoscapularis	0.26
Californosaurus._perrini	0.71
Shonisaurus._sikanniensis	1.75
Shonisaurus._popularis	1.61
Guanlingsaurus._liangae	1.17

Shastasaurus_alexandrae	1.23
Callawayia_wolonggangensis	1.21
Guizhouichthysaurus_tangae	1.16
Besanosaurus_leptorhynchus	0.98
Mixosaurus_kuhnschnyderi	0.32
M._cornalianus	0.23
M._panxianensis	0.61
Phalarodon_callawayi	0.82
Cymbospondylus_buchseri	1.14
Xinminosaurus_catactes	0.84
Utatsusaurus_hataii	0.65
Grippia_longirostris	0.48
Chaohusaurus_zhangjiawanensis	0.6
C._chaoxianensis	0.31
C._geishanensis	0.33

;

END;

BEGIN TREES;

Title Trees from "matrixfinalrevisada.tree";

ID 0161d74331681;

LINK Taxa = Untitled_Block_of_Taxa;

TRANSLATE

- [0] 1 P._australis,
- [1] 2 P._sachicarum,
- [2] 3 P._americanus,
- [3] 4 P._hercynicus,
- [4] 5 Caypullisaurus_bonapartei,
- [5] 6 P._platydacylus,
- [6] 7 Brachypterygius_extremus,
- [7] 8 Athabascasaurus_bitumineus,
- [8] 9 Sveltonectes_insolitus,
- [9] 10 Palvennia_hoyergeti,
- [10] 11 Janusaurus_lundi,
- [11] 12 Cryopterygius_kristiansenae,
- [12] 13 Ophthalmosaurus_natans,
- [13] 14 O._icenicus,
- [14] 15 Arthropterygius_chrisorum,
- [15] 16 Stenopterygius_aalenensis,
- [16] 17 Chacaicosaurus_cayi,
- [17] 18 Stenopterygius_quadriscissus,
- [18] 19 Malawania_anachronus,
- [19] 20 I._communis,
- [20] 21 Hauffiopteryx_typicus,
- [21] 22 Excalibosaurus_costini,
- [22] 23 Eurhinosaurus_longirostris,
- [23] 24 Leptonectes_solei,
- [24] 25 Leptonectes_moorei,
- [25] 26 Leptonectes_tenuirostris,
- [26] 27 Temnodontosaurus_platyodon,
- [27] 28 Hudsonelpidia_brevirostris,
- [28] 29 Suevoleviathan_disinteger,
- [29] 30 Quianichthysaurus_xingyiensis,
- [30] 31 Quianichthysaurus_zhoui,
- [31] 32 Toretocnemus_zitteli,
- [32] 33 Callawayia_neoscapularis,
- [33] 34 Californosaurus_perrini,
- [34] 35 Shonisaurus_sikanniensis,
- [35] 36 Shonisaurus_popularis,
- [36] 37 Guanlingsaurus_liangae,
- [37] 38 Shastasaurus_alexandrae,
- [38] 39 Callawayia_wolonggangensis,
- [39] 40 Guizhouichthysaurus_tangae,
- [40] 41 Besanosaurus_leptorhynchus,
- [41] 42 Mixosaurus_kuhnschnyderi,
- [42] 43 M._cornalianus,

```

[43]        44 M._panxianensis,
[44]        45 Phalarodon_callawayi,
[45]        46 Cymbospondylus_buchseri,
[46]        47 Xinminosaurus_catactes,
[47]        48 Utatsusaurus_hataii,
[48]        49 Grippia_longirostris,
[49]        50 Chaohusaurus_zhangjiawanensis,
[50]        51 C._chaoxianensis,
[51]        52 C._geishanensis;
TREE 'PAUP_1'=
(((((((((((((((((1,2),3),4),5),6),7),8),9),(((10,11),12),(13,14))),15),16,17),18),(19,20)),21),(((22,23),((24,25),26)),2
7),28,29),((30,31),32)),33),34),((((35,36),37),38),39,40,41)),42,43,44,45),(46,47),(48,49)),50,51,52);

END;

BEGIN ASSUMPTIONS;
    TYPESET * UNTITLED = Squared: 1;
END;

BEGIN MESQUITECHARMODELS;
    ProbModelSet * UNTITLED = Brownian_default: 1;
END;

Begin MESQUITE;
    MESQUITESCRIPTVERSION 2;
    TITLE AUTO;
    tell ProjectCoordinator;
    timeSaved 1519736324247;
    getEmployee #mesquite.minimal.ManageTaxa.ManageTaxa;
    tell It;
        setID 0 4946644881309471289;
    endTell;
    getEmployee #mesquite.charMatrices.ManageCharacters.ManageCharacters;
    tell It;
        setID 0 7149772231604281569;
        mqVersion 340;
        checksumv 0 3 30522680 null numChars 1 numItems 1 min 0.23 max 1.75
sumSquares 52.19560000000001 NumFiles 1 NumMatrices 1;
        mqVersion;
    endTell;
    getWindow;
    tell It;
        suppress;
        setResourcesState false false 19;
        setPopoutState 400;
        setExplanationSize 0;
        setAnnotationSize 0;
        setFontIncAnnot 0;
        setFontIncExp 0;
        setSize 1366 649;
        setLocation -8 -8;
        setFont SanSerif;
        setFontSize 10;
        getToolPalette;
        tell It;
        endTell;
        desuppress;
    endTell;
    getEmployee #mesquite.trees.BasicTreeWindowCoord.BasicTreeWindowCoord;
    tell It;
        makeTreeWindow #4946644881309471289
#mesquite.trees.BasicTreeWindowMaker.BasicTreeWindowMaker;
    tell It;
        suppressEPCResponse;
        setTreeSource #mesquite.trees.StoredTrees.StoredTrees;

```

```

tell It;
    setTreeBlock 1;
    setTreeBlockID 0161d74331681;
    toggleUseWeights off;
endTell;
setAssignedID 831.1472817970082.8563898523809976213;
getTreeWindow;
tell It;
    setExplanationSize 30;
    setAnnotationSize 20;
    setFontIncAnnot 0;
    setFontIncExp 0;
    setSize 1347 577;
    setLocation -8 -8;
    setFont SanSerif;
    setFontSize 10;
    getToolPalette;
    tell It;
        setTool
mesquite.trees.BranchLengthsAdjust.AdjustToolExtra.adjustor;
    endTell;
    showPage 1;
    setActive;
    getTreeDrawCoordinator
#mesquite.trees.BasicTreeDrawCoordinator.BasicTreeDrawCoordinator;
    tell It;
        suppress;
        setTreeDrawer #mesquite.trees.SquareTree.SquareTree;
        tell It;
            setNodeLocs
#mesquite.trees.NodeLocsStandard.NodeLocsStandard;
        tell It;
            branchLengthsToggle off;
            toggleScale on;
            toggleBroadScale off;
            toggleCenter on;
            toggleEven on;
            setFixedTaxonDistance 0;
        endTell;
        setEdgeWidth 6;
        orientUp;
        setCornerMode Right_Angle 50;
    endTell;
    setBackground White;
    setBranchColor Black;
    showNodeNumbers off;
    showBranchColors on;
    labelBranchLengths off;
    centerBrLenLabels on;
    showBrLensUnspecified on;
    showBrLenLabelsOnTerminals on;
    setBrLenLabelColor 0 0 255;
    setNumBrLenDecimals 6;
    desuppress;
    getEmployee
#mesquite.trees.BasicDrawTaxonNames.BasicDrawTaxonNames;
    tell It;
        setColor Black;
        toggleColorPartition on;
        toggleColorAssigned off;
        toggleShadePartition off;
        toggleShowFootnotes on;
        toggleNodeLabels on;
        toggleCenterNodeNames off;
        toggleShowNames on;
        namesAngle ?>;
    endTell;

```

```

        endTell;
        setTreeNumber 1;
        setTree
'((((((((((((((1:24.5,2:5.6):3,3:34.1):3,4:31):19.2,5:12.3):3,6:34.4):3,7:13.3):3,8:53.3):3,9:38.1):7.9,(((10:7.7,1
1:7.1):3,12:10.1):14.5,(13:8.8,14:26.3):3):3):7.9,15:34):3,16:12,17:14):3,18:12.6):14.5,(19:75.3,20:18.6):3):3,21:34.4
):11.3,(((22:8.5,23:20.9):5,((24:4.2,25:16.6):6,2,26:18.6):3):3,27:16.5):12,28:11.3,29:41.4):16,((30:5.31:15):3,32:18):
3):3,33:35.5):3,34:27.7):3,((((35:16.3,36:5):5,37:10):3,38:13):3,39:16,40:16):3,9,41:5.2):9):3,42:22.6,43:17.2,44:17.
2,45:17.2):3,(46:5.2,47:5.2):16):3,(48:4,49:4):15):3,50:22,51:22,52:22):3:';
        setDrawingSizeMode 0;
        toggleLegendFloat on;
        scale 0;
        toggleTextOnTree off;
        togglePrintName on;
        showWindow;
        newAssistant
#mesquite.ancstates.TraceCharacterHistory.TraceCharacterHistory;
        tell It;
        suspend ;
        setDisplayMode
#mesquite.ancstates.ShadeStatesOnTree.ShadeStatesOnTree;
        tell It;
        toggleLabels off;
        togglePredictions off;
        toggleGray off;
        endTell;
        setHistorySource
#mesquite.ancstates.RecAncestralStates.RecAncestralStates;
        tell It;
        getCharacterSource
#mesquite.charMatrices.CharSrcCoordObed.CharSrcCoordObed;
        tell It;
        setCharacterSource
#mesquite.charMatrices.StoredCharacters.StoredCharacters;
        tell It;
        setDataSet #7149772231604281569;
        endTell;
        endTell;
        setMethod
#mesquite.parsimony.ParsAncestralStates.ParsAncestralStates;
        tell It;
        setModelSource
#mesquite.parsimony.CurrentParsModels.CurrentParsModels;
        tell It;
        toggleMPRsMode off;
        getEmployee
#mesquite.parsimony.ParsimonySquared.ParsimonySquared;
        tell It;
        toggleWeight on;
        endTell;
        endTell;
        toggleShowSelectedOnly off;
        endTell;
        setCharacter 1;
        setMapping 1;
        toggleShowLegend on;
        setColorMode 0;
        toggleWeights on;
        setInitialOffsetX 4;
        setInitialOffsetY -309;
        setLegendWidth 142;
        setLegendHeight 132;
        resume ;
        endTell;
        endTell;
        desuppressEPCResponse;
        getEmployee #mesquite.trees.ColorBranches.ColorBranches;
        tell It;
        setColor Red;

```

```

removeColor off;
endTell;
getEmployee #mesquite.ornamental.BranchNotes.BranchNotes;
tell It;
    setAlwaysOn off;
endTell;
getEmployee
#mesquite.ornamental.ColorTreeByPartition.ColorTreeByPartition;
tell It;
    colorByPartition off;
endTell;
getEmployee
#mesquite.ornamental.DrawTreeAssocDoubles.DrawTreeAssocDoubles;
tell It;
    setOn on;
    toggleShow consensusFrequency;
    toggleShow bootstrapFrequency;
    toggleShow posteriorProbability;
    toggleShow consensusFrequency;
    toggleShow posteriorProbability;
    toggleShow bootstrapFrequency;
    setDigits 4;
    setThreshold ?>;
    writeAsPercentage off;
    toggleCentred on;
    toggleHorizontal on;
    toggleWhiteEdges on;
    toggleShowOnTerminals on;
    setFontSize 10;
    setOffset 0 0;
endTell;
getEmployee
#mesquite.ornamental.DrawTreeAssocStrings.DrawTreeAssocStrings;
tell It;
    setOn on;
    toggleCentred on;
    toggleHorizontal on;
    setFontSize 10;
    setOffset 0 0;
    toggleShowOnTerminals on;
endTell;
getEmployee #mesquite.trees.TreeInfoValues.TreeInfoValues;
tell It;
    panelOpen false;
endTell;
endTell;
endTell;
getEmployee #mesquite.charMatrices.BasicDataWindowCoord.BasicDataWindowCoord;
tell It;
    showDataWindow #7149772231604281569
#mesquite.charMatrices.BasicDataWindowMaker.BasicDataWindowMaker;
tell It;
    getWindow;
tell It;
    getTable;
tell It;
    rowNamesWidth 110;
endTell;
setExplanationSize 30;
setAnnotationSize 20;
setFontIncAnnot 0;
setFontIncExp 0;
setSize 1347 577;
 setLocation -8 -8;
setFont SanSerif;
setFontSize 10;
getToolPalette;

```

```

        tell It;
            setTool
mesquite.charMatrices.BasicDataWindowMaker.BasicDataWindow.ibeam;
            endTell;
            setTool
mesquite.charMatrices.BasicDataWindowMaker.BasicDataWindow.ibeam;
            colorCells #mesquite.charMatrices.NoColor.NoColor;
            colorRowNames
#mesquite.charMatrices.TaxonGroupColor.TaxonGroupColor;
            colorColumnNames
#mesquite.charMatrices.CharGroupColor.CharGroupColor;
            colorText #mesquite.charMatrices.NoColor.NoColor;
            setBackground White;
            toggleShowNames on;
            toggleShowTaxonNames on;
            toggleTight off;
            toggleThinRows off;
            toggleShowChanges on;
            toggleSeparateLines off;
            toggleShowStates on;
            toggleAutoWCharNames on;
            toggleAutoTaxonNames off;
            toggleShowDefaultCharNames off;
            toggleConstrainCW on;
            toggleBirdsEye off;
            toggleShowPaleGrid off;
            toggleShowPaleCellColors off;
            toggleShowPaleExcluded off;
            togglePaleInapplicable on;
            toggleShowBoldCellText off;
            toggleAllowAutosize on;
            toggleColorsPanel off;
            toggleLinkedScrolling on;
            toggleScrollLinkedTables off;
        endTell;
        showWindow;
        getWindow;
        tell It;
            forceAutosize;
        endTell;
        getEmployee #mesquite.charMatrices.AlterData.AlterData;
        tell It;
            toggleBySubmenus off;
        endTell;
        getEmployee #mesquite.charMatrices.ColorByState.ColorByState;
        tell It;
            setStateLimit 9;
            toggleUniformMaximum on;
        endTell;
        getEmployee #mesquite.charMatrices.ColorCells.ColorCells;
        tell It;
            setColor Red;
            removeColor off;
        endTell;
        getEmployee #mesquite.charMatrices.AnnotPanel.AnnotPanel;
        tell It;
            togglePanel off;
        endTell;
        getEmployee
#mesquite.charMatrices.CharReferenceStrip.CharReferenceStrip;
        tell It;
            showStrip off;
        endTell;
        getEmployee #mesquite.charMatrices.SelSummaryStrip.SelSummaryStrip;
        tell It;
            showStrip off;
        endTell;

```

```
        getEmployee  
#mesquite.cont.ItemsEditorForInfoPanel.ItemsEditorForInfoPanel;  
        tell It;  
                panelOpen false;  
        endTell;  
    endTell;  
endTell;  
endTell;  
end;
```

Capítulo 2

Variação do tamanho corporal em répteis marinhos e sua relação com as extinções do Mesozoico

RESUMO

Os répteis predadores marinhos desenvolveram-se na Era Mesozoica, período conhecido como “Idade dos Répteis”, tornando-se componentes dominantes dos ecossistemas marinhos mundiais daquele intervalo de tempo. Esses tetrápodos carnívoros são representados por distintas linhagens de tamanhos geralmente grandes que se originaram de ancestrais terrestres e reconfiguraram sua estrutura física, morfológica e fisiológica para adaptar-se a ambientes aquáticos. O tamanho corporal é uma das propriedades biológicas mais básicas e significantes para a compreensão de um grupo. Esta característica influencia a forma como as espécies interagem com o meio abiótico e biótico e atua nos princípios fisiológicos, anatômicos, ecológicos e evolutivos que são limitantes para a distribuição em escalas temporais e espaciais. Estas modificações podem esclarecer as influências que a disparidade de tamanhos de um grupo pode causar dentro e fora das linhagens. As variações corporais dos répteis marinhos foram pouco debatidas e ainda não são completamente compreendidas, sendo que a busca por padrões de diversificação de um clado em um amplo espaço de tempo fundamenta múltiplos estudos como: biogeografia, ecologia, comportamento, paleobiologia e fisiologia. Nós realizamos análises filogenéticas e não filogenéticas para a análise de padrões de tamanho corporal em notossauros, mosassauros e plesiossauros. Foram obtidos dados de corporais de tamanho corporal total, crânio, fêmur e úmero para 251 materiais bem preservados de indivíduos adultos de 119 espécies publicadas, além das informações de unidade geológica, intervalo de tempo, localidade geográfica e número de identificação do material através da literatura. Os resultados mostraram que estes grupos de répteis marinhos não seguem nenhuma variação de aumento/diminuição dos tamanhos corporais ao longo do tempo. Ao contrário, os plesiossauros apresentam uma seleção os tamanhos médios sendo estes os sobreviventes do evento de extinção Jurássico-Cretáceo.

Palavras-chave: répteis marinhos, tamanho corporal, extinção em massa, hábitos alimentares.

1- Introdução

Os répteis predadores marinhos desenvolveram-se na Era Mesozoica, período conhecido como “Idade dos Répteis”, tornando-se componentes dominantes dos ecossistemas marinhos mundiais (Motani, 2009). Esses tetrápodos carnívoros são representados por distintas linhagens de tamanhos geralmente grandes que surgiram a partir de ancestrais terrestres e reconfiguraram sua estrutura física, morfológica e fisiológica para adaptar-se a ambientes aquáticos (Pyenson et al., 2014). Ao longo de 190 milhões de anos este grupo apresentou sucesso evolutivo como predadores de topo, sendo expostos a flutuações ambientais, stress climático e extinções em massa (Pyenson et al., 2014; Scheyer et al., 2014).

Diversos grupos de répteis marinhos são conhecidos, porém alguns destacam-se mais que outros pelo sucesso evolutivo, apresentando variados padrões morfológicos corporais como: pescoço longo (notossauros e plesiossauros), formato semelhante aos golfinhos (ictiossauros) e os que lembram lagartos monitores (mosassauros) (Everhart, 2005; Motani, 2009; Thorne et al., 2011). Os répteis marinhos são resultado de invasões independentes do ambiente marinho, os ictiossauros, plesiossauros e notossauros originaram-se após a extinção Permiano-Triássico. As linhagens sobreviventes se diversificaram no Jurássico e persistiram ao longo do Mesozoico. No Cenomaniano os ictiossauros extinguiram-se e no Turoniano os plesiossauros foram restritos aos elasmourideos e polycotylideos e, neste mesmo período, os mosassauros se diversificaram rapidamente, tornando-se um dos principais predadores de topo no Neocretáceo (Benson et al., 2013; Everhart, 2005; Stubbs and Benton, 2016).

Os répteis marinhos têm sido estudados com foco na descrição de novas espécies, revisão taxonômica e análises cladísticas. A busca por padrões paleoecológicos em larga escala tem sido de interesse recente entre os biólogos/paleontólogos e este tema ainda é pouco

estudado (Benson et al., 2010; Pyenson et al., 2014; Stubbs and Benton, 2016) . Estes podem desvendar processos em escalas macro- e microevolutivas que são essenciais para o entendimento da estrutura das comunidades biológicas. O tamanho corporal é uma das propriedades biológicas mais básicas e significantes para a compreensão da história evolutiva de um grupo. Esta característica influencia a forma como as espécies interagem com o meio abiótico e biótico e atua nos princípios fisiológicos, anatômicos, ecológicos e evolutivos que são limitantes para a distribuição em escalas temporais e espaciais (Smith et al., 2016). Os tamanhos corporais revelam informações tanto sobre os indivíduos, como também sobre as comunidades ecológicas como, por exemplo, disponibilidade dos recursos alimentares, preferência de presas, predação e competição (Ferrón et al., 2017; Hone and Benton, 2005).

As transições de vários grupos de vertebrados da terra para o mar resultaram em mudanças dos ecossistemas marinhos, extinções em massa e alterações corporais, tornando estas linhagens únicas para analisar padrões de tamanho (Mazin, 2001; Pyenson et al., 2014). As mudanças nas oportunidades ecológicas permitem impulsos para a inovações fenotípicas, gerando novas e importantes morfologias (Benton, 2015; Stubbs and Benton, 2016). As variações corporais dos répteis marinhos foram pouco debatidas e ainda não são completamente compreendidas e a busca por padrões de diversificação de um clado em um amplo intervalo de tempo fundamenta múltiplos estudos como: biogeografia, ecologia, comportamento, paleobiologia e fisiologia (Benton, 2015).

As variações de tamanhos corporais das espécies podem revelar grandes mudanças evolutivas nas comunidades, como: competição por recursos, amplitude da área de vida e diversidade fenotípica (Pincheira-Donoso et al., 2015). Estas modificações podem esclarecer as influências que a disparidade de tamanhos de um grupo pode causar dentro e fora das linhagens. Vertebrados de grande porte têm a importante função de estruturar os ecossistemas marinhos recentes, do mesmo modo os répteis marinhos conquistaram os níveis tróficos mais

altos ao longo de 250 milhões de anos de evolução dos tetrápodos marinhos até a extinção K-Pg (Kelley et al., 2014).

Identificar padrões de tamanho corporal em grupos extintos, como nos répteis predadores marinhos, pode ampliar a interpretação acerca da estruturação dos ecossistemas marinhos atuais, auxiliando na diferenciação entre perturbações antropológicas e padrões resultantes de processos ecológicos e evolutivos em um grande intervalo de tempo (Kelley and Pyenson, 2015; Smith et al., 2016). Além disso, este trabalho integra pela primeira vez dados de tamanhos corporais de plesiossauros, mosassauros e notossauros juntamente com os ictiossauros Souza and Santucci (no prelo), sob a óptica tanto de fatores biológicos, como: variação do tamanho corporal, morfologia dentária e preferências alimentares, e fatores abióticos relacionados aos eventos de extinção (nível do mar, carbono, oxigênio e temperatura), bem como a distribuição geográfica das espécies de cada grupo.

Considerando os répteis marinhos como importantes componentes dos ecossistemas marinhos Mesozóicos, nós testamos para Nothosauria, Mosasauroidea e Plesiosauria mudanças direcionais do tamanho corporal usando análises filogenéticas e não filogenéticas, para verificar se estes grupos possuem variação na mudança evolutiva do tamanho corporal ao longo do tempo (aumento ou diminuição) e como os tamanhos variaram (ou foram afetados) através das extinções em massa. Também foi analisada a diversidade de tamanhos corporais para Nothosauria, Mosasauroidea e Plesiosauria com o objetivo de verificar se os eventos de extinção em massa selecionam as espécies maiores, médias ou menores de cada clado ou, ao contrário, se não há padrão nenhum na seleção de tamanhos corporais dos répteis marinhos.

2- Materiais e Métodos

Nós realizamos análises filogenéticas e não filogenéticas para o estudo de padrões de tamanho corporal em notossauros, mosassauros e plesiosauros. As análises filogenéticas têm a finalidade de calcular os aumentos e diminuições corporais das espécies considerando as relações de parentesco entre os grupos baseando-se em uma árvore filogenética calibrada com o tempo. Já as análises não filogenéticas possuem o propósito de verificar os aumentos e diminuições corporais das espécies ao longo do tempo através de regressões lineares e cálculos de desvio padrão (Hone & Benton, 2007; Hone *et al.*, 2008).

Foram obtidos dados de tamanho corporal total, crânio, fêmur e úmero para 251 materiais bem preservados de indivíduos adultos de 119 espécies publicadas, além das informações sobre unidade geológica, intervalo de tempo, localidade geográfica e número de identificação do material através da literatura. Os indivíduos adultos são identificados nos respectivos artigos de descrição de cada espécie (Informação Suplementares S1), táxons e/ou espécies juvenis ou com ausência de fêmur/úmero e crânio ou com materiais incompletos que comprometam a medição mais precisa não foram considerados.

Estimativa do tamanho corporal

O tamanho corporal é um parâmetro difícil de ser estimado em espécies fósseis, porém os répteis marinhos possuem ocorrência global (Bardet *et al.*, 2014), materiais bem amostrados e, em muitos casos, preservação excepcional (Tutin and Butler, 2017). O comprimento total nem sempre se encontra disponível para todas as espécies, portanto é necessário o uso de algum osso ou estrutura, mais comumente encontrado no registro fóssil,

como parâmetro para o tamanho total. Foram escolhidos ossos longos (úmero e fêmur) como parâmetro de tamanho corporal para os plesiossauros e tamanhos de crânio para os mosassauros e notossauros em função da alta preservação de crânios nestes dois últimos grupos.

Os ossos longos possuem correlações positivas com o tamanho do corpo em aves extintas (Butler and Goswami, 2008; Field et al., 2013), mamíferos (Christiansen, 1999; Egi, 2001), crocodilomorfos (Young et al., 2011), tetrápodes terrestres (Campione and Evans, 2012) e dinossauros (Carrano, 2006; de Souza and Santucci, 2014; Therrien et al., 2007). O tamanho de crânio também possui correlação positiva com tamanho corporal em mamíferos Mesozoicos (Hu et al., 2005), arcosauromorfos (Hurlburt et al., 2003), crocodilomorfos (Farlow et al., 2005; Young et al., 2011), ictiossauros (Scheyer et al., 2014), baleias rorqual e os répteis marinhos Hupehsuchia (Motani et al., 2015).

Correlações entre úmero e fêmur foram feitas para plesiossauros com o objetivo de estimar tamanhos de úmeros não preservados a partir dos tamanhos de fêmures preservados e entre crânio e úmero para notossauros, com o objetivo de estimar tamanhos de crânios não preservados a partir dos tamanhos de úmeros preservados, maximizando o uso de táxons nas análises. Não foram estimados tamanhos de crânios para mosassauros em decorrência da ausência de preservação de materiais de crânio e úmero em um mesmo espécime, impossibilitando a construção de uma curva de correlação confiável.

Após checar a normalidade dos dados (Informação Suplementar S2A), foram geradas duas equações da reta a partir da correlação úmero e fêmur com espécies que possuíam ambos os materiais da mesma espécie para plesiossauros. As equações foram usadas para estimar os úmeros de espécies que só possuíam fêmur preservados. Da mesma forma, a equação da reta gerada a partir da correlação úmero e crânio foi usada para estimar os crânios de notossauros que só possuíam úmero preservados. Os crânios de mosassauros não foram estimados devido à pouca quantidade de espécimes com ambos úmero e crânio para gerar a

equação da reta. Os úmeros estimados foram usados como proxy para tamanho em plesiossauros e os crânios estimados foram usados como proxy para tamanho em notossauros, enquanto que as análises de mosassauros utilizaram tamanhos de crânio obtidas diretamente da literatura. As estimativas foram necessárias para maximizar o número de táxons nas análises.

A história evolutiva dos grupos deve ser considerada para obter resultados confiáveis de estimativa corporal, os plesiossauros são o grupo com a maior amplitude temporal desta análise e estão mais sujeitos a mudanças morfológicas. Os plesiossauros adaptaram-se inicialmente ao ambiente aquático na radiação dos Plesiosauroidea, linhagem basal que apresenta espécies de pescoço muito comprido, até 1,9 vezes maior que o tronco. A ramificação do clado supostamente ocorrida no Triássico originou os Pliosauroidea, linhagem derivada que possui espécies de pescoço curto (Benson et al., 2012). Portanto, nós dividimos os plesiossauros em dois grupos Plesiosauroidea e Pliosauroidea, de acordo com as diferenças morfológicas resultantes da história evolutiva.

Mudanças direcionais para o tamanho corporal

O tempo foi calculado a partir da média da amplitude total do táxon disponível na literatura e de acordo com carta cronoestratigráfica internacional (Cohen et al., 2017). As estatísticas paramétricas necessárias para realizar as análises não filogenéticas foram executadas no programa PAST (Hammer et al., 2001). As mudanças de aumento/diminuição do tamanho corporal, segundo as análises não filogenéticas, foram realizadas ajustando os tamanhos de crânio e idade estratigráfica para cada táxon de Nothosauria e Mosasauroidea e seus subclados (Russellosaurina e Mosasaurinae) e também entre úmero e idade estratigráfica para cada táxon de Plesosauria e seus subclados (Pliosauroidea, Pliosauridae, Leptocleidida,

Plesiosauroidea e Elasmosauridae) para verificar a existência de algum padrão de mudança de tamanho corporal (aumento ou diminuição) em diferentes níveis taxonômicos.

Também foram calculados a média e o desvio padrão dos tamanhos de crânio para os mosassauros e notossauros e tamanhos de úmero para plesiossauros em diferentes intervalos de tempo afim de testar se as espécies inclusas na análise não filogenética apresentaram aumento ou diminuição na variação corporal. Os intervalos de tempo foram estabelecidos considerando a duração de cada um dos três grupos no registro geológico, visto que os notossauros possuem curta duração (cerca de 29,5 Ma no Triássico), mossasauros com duração de 31 Ma no Cretáceo e plesiossauros com a maior extensão temporal (aproximadamente 143,5 Ma desde o Triássico até o final Cretáceo). Para os plesiossauros foram considerados os intervalos de tempo Meso/Neotriássico (241,5 Ma-201,3 Ma), Eojurássico (201,3-174,1 Ma), Meso/Neojurássico (174,1-145), Eocretáceo (145 Ma-100,5) e Neocretáceo (100,5 Ma-66 Ma). Para os mosassauros foram considerados os intervalos Cenomaniano-Santoniano (100,5 Ma-83,6 Ma) e Campaniano-Maastrichiano (83,6 Ma-66 Ma) e para os notossauros foi usado o intervalo de tempo total da espécie Meso/Neotriássico (247,1 Ma-201,3 Ma). Optou-se por não fragmentar o Triássico Médio do Triássico Superior devido a distribuição desigual das espécies em cada intervalo.

As análises filogenéticas foram realizadas através da comparação par a par entre ancestrais e descendentes e os valores dos nós ancestrais e dos táxons terminais determinam as variações nas mudanças de tamanho corporal. Três árvores bem resolvidas que abrangem a maior quantidade possível de táxons foram escolhidas, uma para cada grupo. A filogenia presente em Druckenmiller and Knutson (2012) foi escolhida para os plesiossauros, Simões et al. (2017) para os mosassauros e Liu et al. (2014) para os notossauros. As árvores foram usadas para calcular os valores ancestrais de tamanho corporal através da comparação par a par usando o método *weighted squared-change parsimony* (SCP) no programa Mesquite 3.4 (Maddison &

Maddison, 2018). Este método consistiu no cálculo de valores ancestrais de tamanho corporal para 35 espécies de plesiossauros, 19 de notossauros e 22 de mosassauros através da comparação dos traços dentro das linhagens em cada ramo.

Os valores ancestrais foram dados em função do tamanho do crânio em notossauros e mosassauros, já para plesiossauros os valores foram dados em função dos tamanhos de úmero. Em todos os casos considerou-se a distância em milhões de anos entre os tamanhos dos táxons apicais e dos seus descendentes através de uma árvore calibrada com o tempo em Ma, com um intervalo de tempo de 3 Ma entre os nós. As variações de aumento/diminuição foram calculadas comparando os valores dos táxons terminais, os nós ancestrais e os valores dos nós internos para os clados Nothosauria, Mosasauroidea e seus subclados (Russellosaurina e Mosasaurinae) e Plesiosauria e seus subclados (Pliosauroidea, Pliosauridae, Leptocleidida, Plesiosauroidea e Elasmosauridae). Foi usado o teste de Qui Quadrado para testar se as mudanças de aumento/diminuição em cada grupo ocorrem em taxas iguais (hipótese nula) ou se eles seguem alguma mudança direcional (Informação Suplementar S3).

3- Resultados

Os tamanhos de úmero usados para as estimativas de tamanho corporal dos Plesiosauria (Pliosauroidea, Pliosauridae, Leptocleidida, Plesiosauroidea e Elasmosauridae) e Mosasauroidea (Russellosaurina e Mosasaurinae) foram realizadas através da equação da reta resultante da correlação entre fêmur e úmero. As espécies de plesiossauros que possuíam ambos fêmur e úmero foram testadas em regressão linear afim de verificar a correlação dos materiais, 18 espécies de Pliosauroidea com fêmur e úmero pertencentes ao mesmo espécime foram testadas em regressão linear resultando na equação $y = 0,7936x + 6,576$ (Pearson's $r^2 = 0,91855$ e $P < 0,05$) usada para estimar tamanhos de úmero para as espécies que possuíam

apenas tamanho de fêmur (Supplementary Information S2B-a). Da mesma forma, 14 espécies de Plesiosauroidea com fêmur e úmero pertencentes ao mesmo espécime foram testadas em regressão linear resultando a regressão $y = 1,0723x + 0,0282$ (Pearson's $r^2 = 0,92207$ e $P < 0,05$) com a finalidade de estimar tamanhos de úmero para as espécies que possuíam apenas tamanho de fêmur (Supplementary Information S2B-b).

Para os Nothosauria a preservação de ossos longos é escassa, dessa forma decidimos usar o tamanho do crânio como proxy para o tamanho corporal total. Para estimar os materiais de crânio ausentes através do úmero, foram correlacionadas 6 espécies que possuíam ambos materiais em regressão linear resultando na equação $y = 1,3347x + 3,6032$ (Pearson's $r^2 = 0,85209$ e $P < 0,05$) (Supplementary Information S2B-c). As análises não filogenéticas consistiram em correlacionar os proxys para tamanho corporal e o tempo médio para cada grupo em regressão linear.

Dentre as 60 espécies de Plesiosauria, 9 foram estimadas através da equação do ajuste de reta, os tamanhos de úmero logaritimizados foram correlacionados com a média da amplitude temporal em uma regressão linear para cada espécie, resultando na equação $y = -0,0001x + 1,5746$ (Pearson's $r^2 = 0,0015039$ e $P = 0,76667$). A linha de tendência mostra que o eixo x (tempo) não explica nenhuma variação do eixo y (Log 10 cm tamanho do úmero) sugerindo uma fraca correlação entre tamanho corporal e tempo. Os subclados Pliosauroidea, Pliosauridae, Leptocleidida, Plesiosauroidea e Elasmosauroidae também mostram correlações muito fracas, apenas Plesiosauroidea apresenta resultados significativos $P = 0,02$ com $r^2 = 0,166$.

Para as 23 espécies de Mosasauroidea a correlação entre tamanhos de crânio logaritimizados e média da amplitude temporal resultou na seguinte equação $y = -0,0167x + 3,1527$ (Pearson's $r^2 = 0,33183$ e $P < 0,05$). O eixo x (tempo) explica 33,1% da variação do eixo y (Log 10 cm tamanho do crânio). O tempo é estatisticamente insuficiente

para explicar o aumento do tamanho corporal nos Mosasauroidea e seus subclados com correlação fraca e não significativa.

O grupo dos Nothosauria foi representado por 30 espécies, sendo que duas espécies tiveram os tamanhos de crânio estimados através da equação do ajuste de reta. Os tamanhos de crânio logaritimizados foram correlacionados com a média da amplitude temporal em uma regressão linear para cada espécie, resultando na equação $y = 0,0014x + 0,9192$ (Pearson's $r^2 = 0,00052582$ e $P = 0,9$). O eixo x (tempo) não explica nenhuma variação corporal em Nothosauria.

Na segunda análise não filogenética usou-se a média dos tamanhos de úmero para 60 espécies de plesiossauros para testar a variação de aumento/diminuição do tamanho corporal (Tabela 1) nos intervalos de tempo Meso/Neotriássico (241,5 Ma-201,3 Ma) Eojurássico (201,3-174,1 Ma), Meso/Neojurássico (174,1-145), Eocretáceo (145 Ma-100,5) e Neocretáceo (100,5 Ma-66 Ma). As médias dos tamanhos para plesiossauros são menores no início (Triássico) e no final (Cretáceo) da história evolutiva do grupo. Esta disposição dos dados também é observada no desvio padrão, que possui valores menores no início (Triássico), gradativamente os valores aumentam no Jurássico com espécies que variam de *Pliosaurus funkei* (13 m) (Knutsen et al., 2012) a *Pirocleidus beloclis* (5 a 6 m) (Seeley, 1874). Porém, no Cretáceo estes valores diminuem severamente mostrando que a transição Jurássico-Cretáceo foi crítica para o grupo (Benson and Druckenmiller, 2014).

Intervalo de Tempo Plesiosauroidea	n	Úmero mínimo (cm)	Úmero máximo (cm)	Média (cm)	Desvio padrão
Meso/Neotriássico (241,5 Ma-201,3 Ma)	2	23,3	23,4	23,3	0,04
Eojurássico (201,3 Ma-174,1 Ma)	13	19,4	71	36,4	13,6
Meso/Neojurássico (174,1 Ma-145 Ma)	19	18,3	90	45,1	21,1
Eocretáceo (145 Ma-100,5)	3	20	36	29,4	8,3
Neocretáceo (100,5 Ma-66 Ma)	23	20,1	45,7	36,3	6,3

Tabela 1. Análise da variação corporal para Plesiosauria para cinco intervalos de tempo (Meso/Neotriássico, 241,5 Ma-201,3 Ma; Eojurássico, 201,3-174,1 Ma; Meso/Neojurássico, 174,1-145; Eocretáceo, 145 Ma-100,5 e Neocretáceo, 100,5 Ma-66 Ma).

Para as 23 espécies de mosassauros foram usados os tamanhos médios de crânios para os intervalos de tempo Cenomaniano-Santoniano (100,5 Ma-83,6 Ma) e Campaniano-Maastrichiano (83,6 Ma-66 Ma) (Tabela 2). O primeiro intervalo de tempo mostrou um valor menor para a média e o desvio padrão, enquanto que no segundo intervalo esses valores aumentaram consideravelmente. O aumento da disparidade no Neocretáceo ilustra a permanência de espécies de tamanho pequeno e médios ao longo da ascensão das espécies de tamanho grande (Pyenson et al., 2014). Os tamanhos variam de *Tylosaurus bernardi* (15 m) (Bullard and Caldwell, 2010) a *Dolichosaurus longicollis* (1m) (Caldwell, 2000).

Intervalo de Tempo Mosasauroidea	n	Crânio mínimo (cm)	Crânio máximo (cm)	Média (cm)	Desvio padrão
Cenomaniano-Santoniano (100,5 Ma-83,6 Ma)	9	12	79,5	52,89	23,01
Campaniano-Maastrichiano (83,6 Ma-66 Ma)	14	37,56	145,00	85,04	31,93

Tabela 2. Análise da variação corporal para Mosasauria para dois intervalos de tempo (Cenomaniano-Santoniano, 100,5 Ma-83,6 Ma e Campaniano-Maastrichiano, 83,6 Ma-66 Ma).

Para as 30 espécies de notossauros usou-se os tamanhos médios de crânio para o intervalo de tempo Meso/Neotriássico (247,1 Ma-201,3 Ma), os valores de média e desvio padrão são altos em relação aos plesiossauros e mosassauros evidenciando uma alta variação

corporal ao longo de toda a história evolutiva do grupo (Tabela 3). Os tamanhos variam de *Nothosaurus giganteus* (crânio 70 cm) (Rieppel and Wild, 1996) a *Nothosaurus winkeihorsti* (crânio 4,6 m) (Klein and Albers, 2009).

Intervalo de Tempo Nothosauria	n	Crânio mínimo (cm)	Crânio máximo (cm)	Média (cm)	Desvio padrão
Meso/Neotriássico (247,1 Ma-201,3 Ma)	30	4,6	70,4	21,9	16

Tabela 3. Análise da variação corporal para Nothosauria para o intervalos de tempo Meso/Neotriássico, 247,1 Ma-201,3 Ma.

A abordagem filogenética engloba o total 76 espécies, 35 espécies de plesiossauros, 22 espécies de mosassauros e 19 de notossauros (tabela 4, figura 1) inclusas nas respectivas filogenias escolhidas (Druckenmiller and Knutsen, 2012; Liu et al., 2014; Simões et al., 2017). As 45 espécies não usadas nesta análise foram excluídas por não possuírem relações filogenéticas bem estabelecidas. Três árvores calibradas com o tempo foram usadas para calcular as mudanças entre ancestrais e descendentes (veja informação suplementar S3) para os Plesiosauria e seus subclados (Pliosauroidea, Pliosauridae, Leptocleidida, Plesiosauroidea e Elasmosauroidae), Mosasauroidea e seus subclados (Mosasaurinae e Russellosaurina) e Nothosauria.

Subclados	Soma	Média	Mediana	Desvio	n	Mudanças	Mudanças	χ^2	P
						positivas	negativas		
Plesiosauria	-1,48	-0,02	-0,02	0,07	65	26	39	1,3	0,25
Pliosauroidea	-1,23	-0,03	-0,02	0,08	40	16	24	0,8	0,36
Pliosauridae	-0,57	-0,04	-0,02	0,09	14	5	9	0,58	0,44
Leptocleidida	-0,27	-0,02	-0,02	0,11	12	6	6	0	1
Plesiosauroidea	-0,29	-0,01	-0,01	0,06	25	10	15	0,49	0,48
Elasmosauridae	-0,14	-0,02	-0,01	0,04	6	2	4	0,45	0,5
Mosasauroidea	-0,83	-0,01	-0,03	0,11	42	10	32	6,18	0,01
Russellosaurina	-0,49	-0,03	-0,03	0,08	16	5	11	1,16	0,28
Mosasaurinae	-0,74	-0,03	-0,04	0,09	21	3	18	6,03	0,01
Nothosauria	0,27	0,008	0	0,16	33	19	14	0,37	0,54

Tabela 4. Resultado da análise ancestral-descendente comparada para Plesiosauros, mosassauros e notossauros e seus subclados baseada em dados filogenéticos avaliada para árvore filogenética compilada de cada grupo. Os valores de soma, média, mediana, desvio, mudanças positivas, mudanças negativas foram calculadas através das subtrações entre o tamanho (\log_{10}) dos táxons terminais e os estados ancestrais (nos internos) e entre cada nó para cada subclado. O qui-quadrado testa a hipótese nula de que as mudanças positivas e negativas ocorrem em mesmo número.

Para os Plesiosauria a variação corporal entre ancestrais e descendentes possui mais mudanças negativas do que positivas em todos os subclados. Porém, em nenhum deles o resultado é significativo. A soma, média, mediana são negativas e o desvio padrão são positivos para todos os subclados de Plesiosauria. As mudanças neste clado (valores dos nós comparados com as mudanças ao logo dos ramos) variam de -0,26 até 0,18 (Informação Suplementar S2-Fa e Tabela 4). Para os mosassauros as mudanças negativas são mais comuns que as positivas e significativas para Mosasauroidea e Mosasaurinae. A soma, média e a mediana são negativas e o desvio padrão é positivo. As mudanças para Mosasauroidea variaram de 0,45 até -0,31 (Informação Suplementar S2-Fb e Tabela 4).

Os Nothosauria apresentaram mudanças positivas superiores as negativas e não significativas. A soma, média e mediana resultaram em valores positivos com mudanças que variaram de 0,31 até -0,52 (Informação Suplementar S2 Fc e Tabela 4). Para Plesiosauria e

Nothosauria o teste Qui Quadrado mostra que a hipótese nula de que as mudanças positivas e negativas ocorram em proporções iguais não pode ser rejeitada, pois estes resultados não estão fora do padrão de 50% de aumentos ou diminuições. Porém, para Mosasauroidea o teste Qui Quadrado mostra que a hipótese nula pode ser rejeitada, já que há mais mudanças negativas do que positivas. Dessa forma, plesiosauros e notossauros não parecem apresentar variação de aumento ou diminuição do tamanho corporal ao longo do tempo, enquanto que mosassauros apresentam uma tendência de diminuição no tamanho corporal ao longo do tempo.

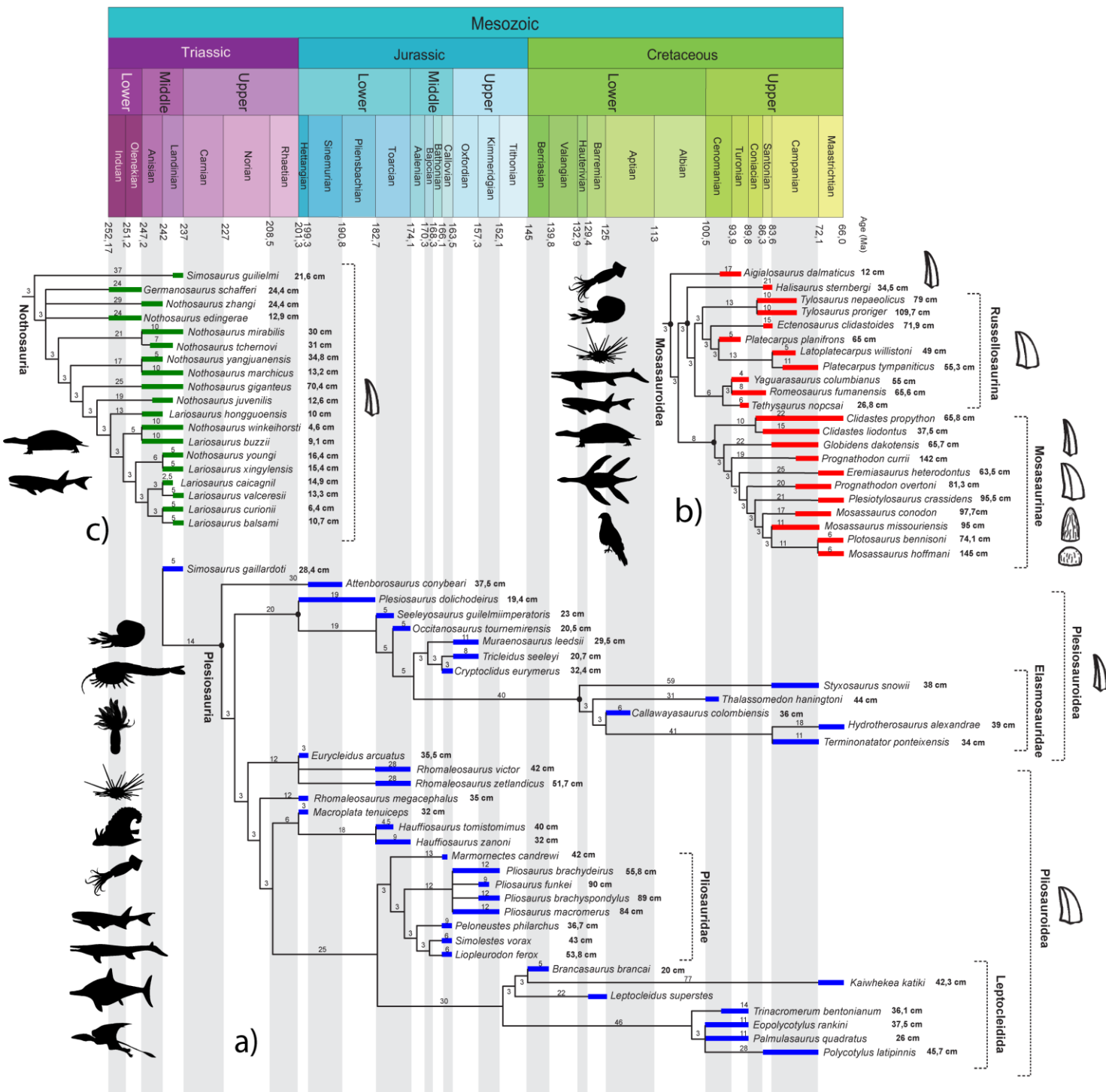


Fig. 1. Supertree calibrada com o tempo retratando as relações filogenéticas de: A) Plesiosauria (cor azul), B) Mosasauroidea (cor vermelha) e C) Nothosauria (cor verde). O número ao lado de cada táxon indica sua amplitude temporal e os números no topo de cada táxon indicam o tamanho (em cm) do material usado para cada grupo: A) Plesiosauria (úmero), B) Mosasauroidea (crânio) e C) Nothosauria (crânio). As imagens das morfologias dentárias foram retiradas de Ross (2009) e a disposição destas nos clados foi sugerida por Massare (1987). As silhuetas foram retiradas do site “phylopic.org” e foram arranjadas segundo revisão bibliográfica presente no texto.

4- Discussão

A variação do tamanho corporal ao longo do tempo foi testada para três grupos de répteis marinhos através de abordagens filogenéticas e não filogenéticas. As análises não filogenéticas não indicaram nenhuma correlação forte entre aumento ou diminuição de tamanho e tempo para Plesiosauria, Nothosauria, e Mosasauroidea. As análises filogenéticas de comparações par a par mostraram mais mudanças positivas do que negativas para Plesiosauria e seus subclados, de modo que as mudanças corporais positivas (aumento) são mais frequentes do que as negativas (diminuição) porém, estatisticamente não significantes. Para Nothosauria as mudanças negativas foram mais frequentes do que as positivas e não significantes. Para Mosasauroidea, assim como para Nothosauria as mudanças negativas foram mais frequentes do que as positivas, porém estatisticamente significativas apenas em Mosasauroidea. Dessa forma, os resultados mostraram que estes grupos de répteis marinhos não seguem a Regra de Cope (Tabela 4, Informação Suplementar S2 C, D, E).

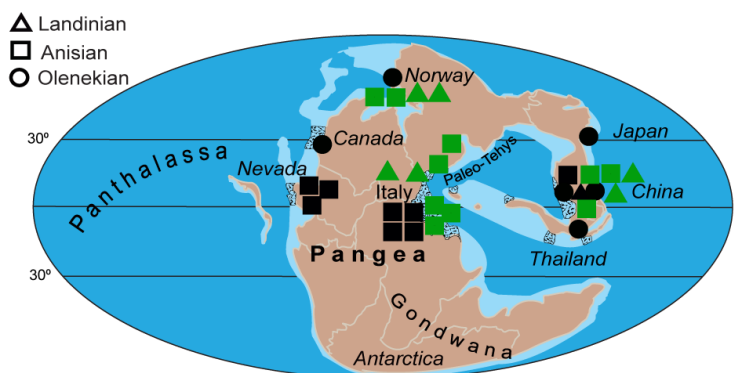
Após a extinção do Permiano os primeiros répteis marinhos predadores se originaram no Eotriássico ocupando nichos vagos (Scheyer et al., 2014; Thorne et al., 2011). A Figura 3a mostra que os tamanhos corporais de notossauros seguem este padrão, apresentando grande amplitude de diversificação logo no início da história evolutiva do grupo, como também é observado nos ictiossauros. Nota-se na Figura 1c que há um único formato de dente predominante em toda a história evolutiva dos notossauros, a morfologia “dentes de agulha” que é descrita como a guilda “*pierce*” por Massare (1987). Pequenos pachypleurosauros e peixes são encontrados em conteúdos estomacais de notossauros. Porém, o formato de dente pinça indica uma alimentação preferencial por presas de corpo mole logo, toda a fauna de bivalves, gastrópodos, equinodermos e braquiópodos, estaria descartada da dieta desses animais

(Diedrich, 2009; Sander, 1989). A baixa variação morfológica dos dentes de notossauros indica uma baixa diversidade alimentar do grupo, que contrasta com uma maior variação morfológica dentária (refletindo numa alimentação variada) dos ictiossauros para este intervalo de tempo (Souza and Santucci, no prelo). A Figura 3 indica também que não há predominante sobreposição geográfica entre as ocorrências de ictiossauros e notossauros, descartando-se assim a possibilidade de competição intensa.

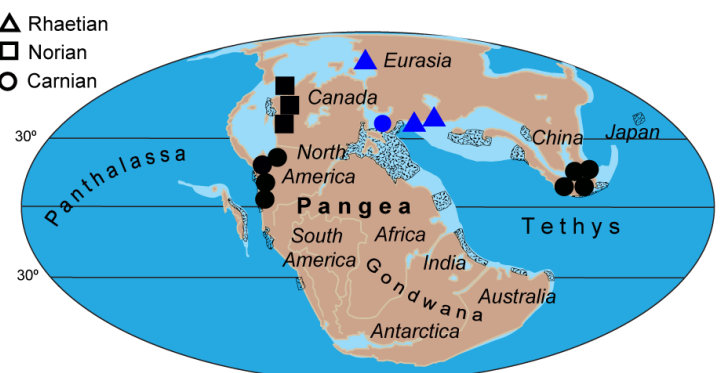
Os plesiossauros, ao contrário dos notossauros, apresentam amplitude de tamanhos reduzida (Figura 3a) logo no início da história evolutiva do grupo, e se diversificaram logo após a extinção Triássico-Jurássico (Benson et al., 2012; Ketchum and Benson, 2010; Wintrich et al., 2017). As figuras 1, 2 e 3 mostram que quando os primeiros plesiossauros surgem, os notossauros já estavam extintos, entretanto já havia uma relativa diversidade de tamanhos e hábitos alimentares dos ictiossauros. Ao menos no final do Triássico não há sobreposição de ocorrência entre estes dois grupos (Figura 2). Após a extinção Triássico-Jurássico (que afetou mais severamente os ictiossauros (Fischer et al., 2014) é possível notar na Figura 3a o início da diversificação dos plesiossauros (pontos azuis) paralelamente à perda de diversidade dos ictiossauros (pontos pretos). Nossos dados sugerem que os plesiossauros diversificaram seus tamanhos em relação à perda de diversidade de tamanhos dos ictiossauros. Neste período de tempo parece haver competição entre estes dois grupos, visto que a Figura 2 mostra que as principais ocorrências destes grupos estão restritas às porções mais interiores do Mar de Tethys e visto que apresentam conteúdo estomacal muito semelhantes, inclusive apresentando evidências de que um predasse o outro (Cicimurri and Everhart, 2001; Neumann and Hampe, 2018; Russell, 1967). Fatores biológicos, químicos e físicos como por exemplo: ambientes deposicionais de preservação excepcional com alta concentração de componentes inorgânicos como os *fóssil-lagerstätten* e a melhor preservação de ictiossauros em amplitudes temporais cujas áreas apresentam níveis menores de inundações continentais (Cleary et al., 2015) podem

ter influenciado a grande concentração de ictiossauros e plesiossauros na porção mais interior do Mar de Tethys, logo os vieses temporais, geográficos e taxonômicos devem ser considerados neste caso.

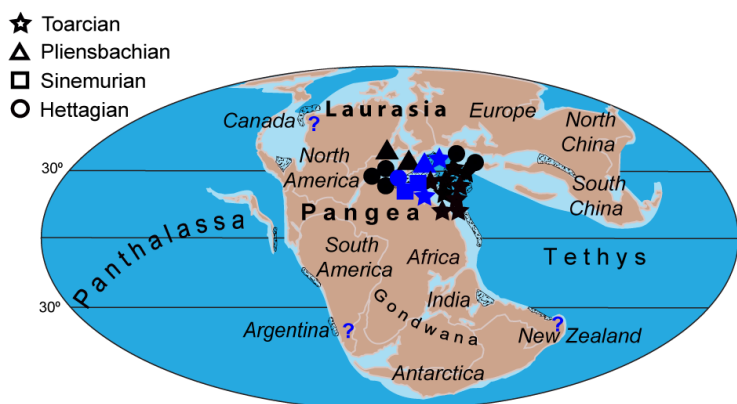
Early/Middle Triassic



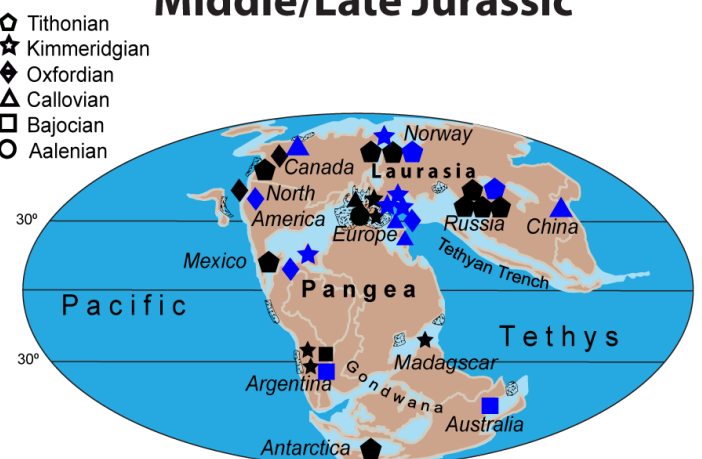
Late Triassic



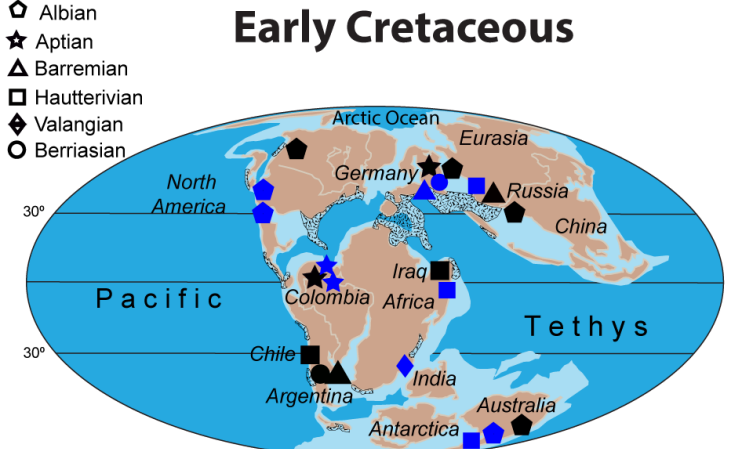
Early Jurassic



Middle/Late Jurassic



Early Cretaceous



Late Cretaceous

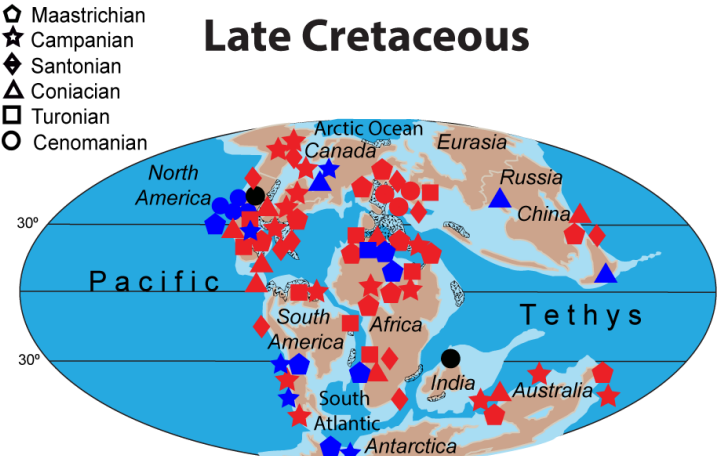


Fig. 2. Distribuição paleogeográfica de: Ichthyosuria (cor preta), Plesiosauria (cor azul), Mosasauroidea (cor vermelha) e Nothosuria (cor verde) (veja detalhes no material suplementar S1). Os mapas paleogeográficos foram modificados de Scotese (2014a,b)

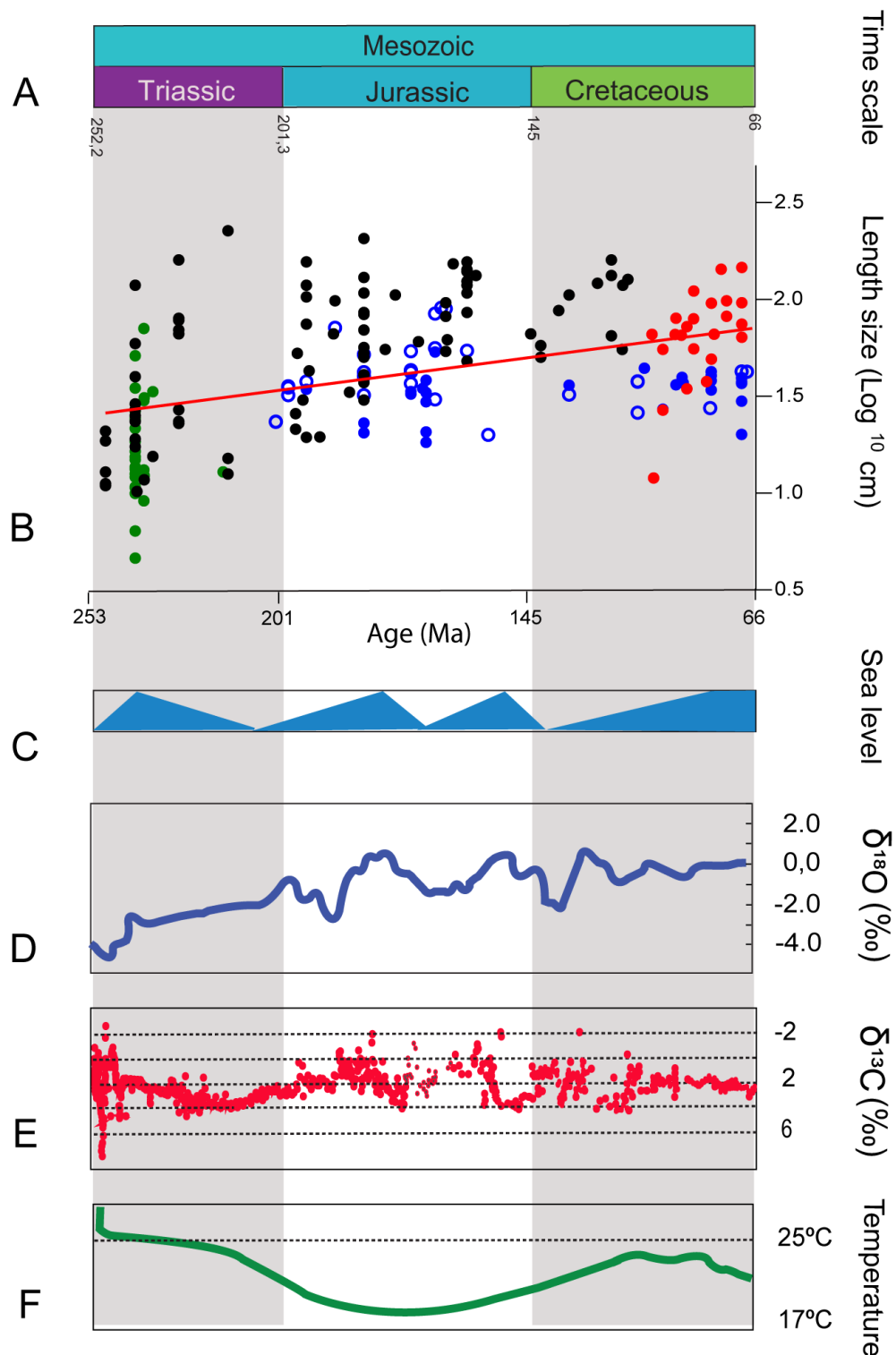


Fig. 3. A e B) Carta Estratigráfica (Cohen et al., 2013) e plotagem dos tamanhos (\log_{10}) e idade de espécies de Ichthyopterygia, Plesiosauria, Mosasauroidea e Nothosauria (incluindo 189 táxons) correlacionados com, C) nível eustático do mar (Gradstein et al., 2012), D) Variação de Oxigênio ($\delta^{18}\text{O}$) (Price et al., 2013), E) Variação de carbono (Saltzman & Thomas, 2012) e F) Variação climática global através do Mesozoico (Scotesse, 2015).

Os hábitos alimentares *pierce* e *cut guilds* estão presentes em ambos os grupos, bem como a preferência destes pelas mesmas presas, como: peixes, belemnitas, moluscos bivalves, amonóides e cefalópodos (Cicimurri and Everhart, 2001; Davenport, 2012; Massare, 1987). A hipótese de competição foi abordada por Kear (2003) entre linhagens de Polycotilídeos e ictiossauros que ocorrem simpatricamente nos depósitos Aptiano-Albiano e que exibem características morfológicas típicas de caçadores oportunistas “*pursuit-style*”, o que poderiam levá-los a competir diretamente. O’Keefe et al. (2009) descreve um ictiossauro juvenil como conteúdo estomacal de um plesiosauro articulado no Oxfordiano da América do Norte, sugerindo uma disputa entre dois grupos de predadores por recursos variados em uma mesma área geográfica. O cenário de competição entre estes dois grupos tem seu registro mais antigo no Oxfordiano., Porém, o cenário competitivo entre répteis marinhos é intensificado pelo confinamento dos registros em uma bacia restrita e não em mar aberto (Jouve et al., 2008). A sobreposição geográfica de espécies no Eojurássico observada no mapa da Figura 2, revela grande potencial competitivo entre ictiossauros e plesiosauros após o evento de extinção Triássico-Jurássico.

Similarmente aos plesiosauros, os mosassauros apresentaram o mesmo padrão de baixa amplitude de variação dos tamanhos corporais no início da diversificação do grupo (Figura 3a). Este grupo iniciou-se no Cenomaniano com indivíduos pequenos, apresentando um aumento da diversidade dos tamanhos corporais a partir do Turoniano (Bardet et al., 2008) e intensificada diversidade de tamanho a partir do Campaniano (Tabela 2). Os mosassauros foram os últimos grandes répteis terrestres a retornar ao ambiente marinho (Everhart, 2005) e a esta altura outros predadores marinhos de grande porte como plesiosauros, crocodilos e ictiossauros eram bem diversificados e já ocupavam o topo das cadeias alimentares (Benson et al., 2010). Os ictiossauros do Cretáceo possuíam hábitos alimentares generalistas e tinham por preferência uma grande diversidade de tipos e tamanhos de presas. As estratégias alimentares e

a preferência por presas similares àquelas dos mosassauros tornariam os ictiossauros potenciais competidores. Porém, o hiato de 3 Ma entre a última ocorrência de ictiossauros e a primeira de mosassauros no registro geológico inviabiliza a hipótese de competição. Mesmo não havendo competição direta, a similaridade de preferências alimentares sugere que alguns nichos antes ocupados pelos ictiossauros podem ter sido preenchidos pelos mosassauros (Fischer et al., 2016).

Ross (2009) descreve a predominância da morfologia “cut” em espécies basais de mosassauros predadoras de ambientes costeiros rasos e que novidades morfológicas dentárias surgiram a partir do Campaniano se estendendo até o Maastrichiano (Figura 1b). A variação da morfologia dentária observada por Ross (2009) parece estar correlacionada com o aumento do valor da variação do tamanho corporal a partir do Campaniano observada na Tabela 2. Neste caso, novas estratégias alimentares podem ter influenciado o aumento do tamanho corporal do grupo, permitido a competição com grupos já estabelecidos e alcançando muitos nichos deixados por outros répteis marinhos (Everhart, 2005). Essa diversificação dos mosassauros logo após a extinção dos ictiossauros também poderia explicar a ausência de uma diversificação dos plesiossauros no final do Cretáceo, visto que estes dois grupos remanescentes apresentam hábitos alimentares similares e sobreposição de ocorrência de áreas geográficas em uma mesma unidade geológica (Everhart, 2016; Jacobs et al., 2006; Spielmann and Lucas, 2006).

Com relação à seleção do tamanho corporal pelos eventos de extinção em massa, nota-se que em ictiossauros a ampla variedade de tamanhos corporais no Triássico apresenta uma variação de diminuição da diversificação dos tamanhos após o evento de extinção Triássico-Jurássico (Figura 3a). Houve persistência das espécies de tamanhos médios em detrimento do desaparecimento das espécies de tamanhos extremos (pequenos e grandes). Provavelmente porque ictiossauros de tamanhos extremos possuíam dietas mais especializadas.

Os gêneros de tamanhos menores, como *Grippia* e *Utatsusaurus*, bem como os tamanhos grandes, *Shonisaurus*, possuem hábitos alimentares especializados como prováveis sugadores (Motani, 1997; Nicholls and Manabe, 2004). Dick & Maxwell (2015a) também verificam que há uma diminuição grave de diversidade dos ecoespaços resultando na extinção de grupos de alimentação especializada no Eojurássico com a contínua ocupação de hábitos alimentares generalistas ao longo do Cretáceo. Um padrão similar é visto nos plesiossauros porém, a predominância das espécies de tamanho médio é marcada após a extinção Jurássico-Cretáceo. Entretanto, devido à falta de informações alimentares para este grupo neste período, não é possível afirmar com segurança que os tamanhos extremos correspondam a hábitos alimentares mais especializados.

5- Conclusões

1-A tendência ao tamanho grande ou pequeno não foi um direcionador evolutivo na história dos grupos estudados.

2-Os notossauros e ictiossauros apresentam ampla diversidade de tamanhos corporais no Neotriássico imediatamente após ao seu aparecimento no registro fóssil. Apesar da ampla diversificação dos tamanhos corporais dos notossauros, as morfologias dentárias apresentaram pouca variação, o que indicaria também uma baixa variação na dieta. Em contrapartida, os ictiossauros apresentam maior variação dentária e alimentar.

3-Os mosassauros e plesiossauros basais apresentam uma amplitude de diversificação do tamanho corporal baixa quando comparados com os notossauros e ictiossauros.

4-Nossos dados sugerem um cenário de competição entre plesiossauros e ictiossauros quando sobrepostas as informações de distribuição geográfica, morfologia dentária e conteúdo estomacal.

5-Houve um aumento na variação de tamanho dos plesiossauros após a extinção Triássico-Jurássico, juntamente com a diminuição na variação dos tamanhos dos ictiossauros. A extinção Triássico-Jurássico extinguiu muitas espécies de ictiossauros. Em contrapartida, a partir deste evento, houve um aumento na diversidade dos tamanhos dos plesiossauros. Após o evento de extinção Triássico-Jurássico a diversidade de plesiossauros aumentou como consequência da perda de diversidade dos ictiossauros.

6-Após a extinção dos ictiossauros seria esperado um aumento na variação corporal dos plesiossauros. Isto não ocorreu provavelmente pelo surgimento e diversificação dos mosassauros, que também apresentavam hábitos alimentares semelhantes aos dos plesiossauros.

7-Com relação a seleção dos tamanhos ao longo dos eventos de extinção em massa, ictiossauros predominantemente de tamanho médio sobreviveram ao evento Triássico-Jurássico. O mesmo padrão ocorreu com os plesiossauros no evento Jurássico-Cretáceo, mostrando que táxons distintos vivendo no mesmo ambiente apresentam padrões semelhantes ao longo de eventos de extinção em massa.

6- Referências

- Bardet, N., Falconnet, J., Fischer, V., Houssaye, A., Jouve, S., Pereda Suberbiola, X., Pérez-García, A., Rage, J.C., Vincent, P., 2014. Mesozoic marine reptile palaeobiogeography in response to drifting plates. *Gondwana Res.* 26, 869–887. <https://doi.org/10.1016/j.gr.2014.05.005>
- Bardet, N., Houssaye, A., Rage, J.C., Pereda Suberbiola, X., 2008. The Cenomanian-Turonian (Late Cretaceous) radiation of marine squamates (Reptilia): The role of the Mediterranean Tethys. *Bull. la Soc. Geol. Fr.* 179, 605–622. <https://doi.org/10.2113/gssgbull.179.6.605>
- Benson, R.B.J., Butler, R.J., Lindgren, J., Smith, A.S., 2010. Mesozoic marine tetrapod diversity: mass extinctions and temporal heterogeneity in geological megabiases affecting vertebrates. *Proc. R. Soc. B Biol. Sci.* 277, 829–834. <https://doi.org/10.1098/rspb.2009.1845>
- Benson, R.B.J., Druckenmiller, P.S., 2014. Faunal turnover of marine tetrapods during the Jurassic-Cretaceous transition. *Biol. Rev.* 89, 1–23. <https://doi.org/10.1111/brv.12038>
- Benson, R.B.J., Evans, M., Druckenmiller, P.S., 2012. High diversity, low disparity and small body size in plesiosaurs (Reptilia, Sauropterygia) from the Triassic-Jurassic boundary. *PLoS One* 7. <https://doi.org/10.1371/journal.pone.0031838>
- Benson, R.B.J., Evans, M., Smith, A.S., Sasoon, J., Moore-Faye, S., Ketchum, H.F., Forrest, R., 2013. A giant pliosaurid skull from the Late Jurassic of England. *PLoS One* 8. <https://doi.org/10.1371/journal.pone.0065989>
- Benton, M.J., 2015. Exploring macroevolution using modern and fossil data. *Proc. R. Soc. Biol.* 282, 1–10. <https://doi.org/10.1098/rspb.2015.0569>
- Bullard, T.S., Caldwell, M.W., 2010. Redescription and rediagnosis of the tylosaurine mosasaur *Hainosaurus pembedensis* Nicholls, 1988, as *Tylosaurus pembedensis* (Nicholls, 1988). *J. Vertebr. Paleontol.* 30, 416–426. <https://doi.org/10.1080/02724631003621870>
- Butler, R.J., Goswami, A., 2008. Body size evolution in Mesozoic birds: Little evidence for Cope's rule. *J. Evol. Biol.* 21, 1673–1682. <https://doi.org/10.1111/j.1420-9101.2008.01594.x>
- Caldwell, M.W., 2000. On the aquatic squamate *Dolichosaurus longicollis* (Cenomanian, Cretaceous), and the evolution of elongate necks in squamates. *J. Vertebr. Paleontol.* 20, 720–735. [https://doi.org/10.1671/0272-4634\(2000\)020\[0720:OTASDL\]2.0.CO;2](https://doi.org/10.1671/0272-4634(2000)020[0720:OTASDL]2.0.CO;2)
- Campione, N.E., Evans, D.C., 2012. A universal scaling relationship between body mass and proximal limb bone dimensions in quadrupedal terrestrial tetrapods. *BMC Biol.* 10, 60. <https://doi.org/10.1186/1741-7007-10-60>
- Carrano, M.T., 2006. Body-size evolution in the Dinosauria. *Amniote Paleobiol. Perspect. Evol. mammals, birds, Reptil.* 225–268.

- Christiansen, P., 1999. Scaling of mammalian long bones: small and large mammals compared. *J. Zool.* 247, 333–348. <https://doi.org/10.1017/S0952836999003052>
- Cicimurri, D.D.J., Everhart, M.M.J., 2001. An elasmosaur with stomach contents and gastroliths from the Pierre Shale (Late Cretaceous) of Kansas. *Trans. Kansas Acad. Sci.* 104, 129–143. [https://doi.org/10.1660/0022-8443\(2001\)104\[0129:AEWSCA\]2.0.CO;2](https://doi.org/10.1660/0022-8443(2001)104[0129:AEWSCA]2.0.CO;2)
- Cleary, T. J., Moon, B. C., Dunhill, A. M., Benton, M. J. 2015. The fossil record of ichthyosaurs, completeness metrics and sampling biases. *Palaeontology* 58: 3 521-536.
- Cohen, K.M., Finney, S.C., Gibbard, P.L. & Fan, J.-X. (2017; updated) The ICS International Chronostratigraphic Chart. *Episodes* 36: 199-204.
- Davenport, J., 2012. High-trophic-level consumers: Trophic relationships of reptiles and Amphibians of coastal and estuarine ecosystems. *Treatise Estuar. Coast. Sci.* 6, 227–249. <https://doi.org/10.1016/B978-0-12-374711-2.00618-5>
- De Souza, L.M., Santucci, R.M., 2014. Body size evolution in Titanosauriformes (Sauropoda, Macronaria). *J. Evol. Biol.* 27, 2001–2012. <https://doi.org/10.1111/jeb.12456>
- Dick, D.G. & Maxwell, E.E. 2015a. Ontogenetic tooth reduction in *Stenopterygius quadriscissus* (Reptilia: Ichthyosauria): Negative allometry, changes in growth rate, and early senescence of the dental lamina. *PLoS One* 10: 1–14.
- Dick, D.G. & Maxwell, E.E. 2015b. The evolution and extinction of the ichthyosaurs from the perspective of quantitative ecospace modelling. *Biol. Lett.* 11: 1–5.
- Diedrich, C., 2009. The vertebrates of the Anisian/Ladinian boundary (Middle Triassic) from Bissendorf (NW Germany) and their contribution to the anatomy, palaeoecology, and palaeobiogeography of the Germanic Basin reptiles. *Palaeogeogr. Palaeoclimatol. Palaeoecol.* 273, 1–16. <https://doi.org/10.1016/j.palaeo.2008.10.026>
- Druckenmiller, P.S., Knutsen, E.M., 2012. Phylogenetic relationships of Upper Jurassic (Middle Volgian) plesiosaurians (Reptilia: Sauropterygia) from the Agardhfjellet Formation of central Norway. *Geological Magazine* 149, 277–284.
- Egi, N., 2001. Body mass estimates in extinct mammals from limb bone dimensions: the case of North American hyaenodontids. *Palaeontology* 44, 497–528. <https://doi.org/10.1111/1475-4983.00189>

Everhart, M.J., 2016. Rare Occurrence of mosasaur (Squamata: Mosasauroidea) remains in the Blue Hill Shale (Middle Turonian) of Mitchell County, Kansas. 1. Trans. Kansas Acad. Sci. 119, 375–380. <https://doi.org/10.1660/062.119.0410>

Everhart, M.J., 2005. Rapid evolution, diversification and distribution of mosasaurs (Reptilia; Squamata) prior to the K-T Boundary, in: Tate 2005 11th Annual Symposium in Paleontology and Geology, Casper, WY. pp. 16–27.

Farlow, J.O., Hurlburt, G.R., Elsey, R.M., Britton, A.R.C., Langston, W., 2005. Femoral dimensions and body size of *Alligator mississippiensis*: estimating the size of extinct mesoeucrocodylians. *J. Vertebr. Paleontol.* 25, 354–369. [https://doi.org/10.1671/0272-4634\(2005\)025\[0354:FDABSO\]2.0.CO;2](https://doi.org/10.1671/0272-4634(2005)025[0354:FDABSO]2.0.CO;2)

Ferrón, H.G., Martínez-Pérez, C., Botella, H., 2017. The evolution of gigantism in active marine predators. *Hist. Biol.* 2963, 0–5. <https://doi.org/10.1080/08912963.2017.1319829>

Field, D.J., Lynner, C., Brown, C., Darroch, S.A.F., 2013. Skeletal correlates for body mass estimation in modern and fossil flying birds. *PLoS One* 8, 1–13. <https://doi.org/10.1371/journal.pone.0082000>

Fischer, V., Bardet, N., Benson, R.B.J., Arkhangelsky, M.S., Friedman, M., 2016. Extinction of fish-shaped marine reptiles associated with reduced evolutionary rates and global environmental volatility. *Nat. Commun.* 7, 1–11. <https://doi.org/10.1038/ncomms10825>

Fischer, V., Cappetta, H., Vincent, P., Garcia, G., Goolaerts, S., Martin, J.E., Roggero, D., Valentin, X., 2014. Ichthyosaurs from the French Rhaetian indicate a severe turnover across the Triassic Jurassic boundary. *Naturwissenschaften* 101, 1027–1040. <https://doi.org/10.1007/s00114-014-1242-7>

Hammer, O., Harper, D.A.T. & Ryan, P.D. 2001. PAST: paleontological statistics software package for education and data analysis. *Paleontol. Electron.* 4: 4–9.

Hone, D.W.E., Benton, M.J., 2005. The evolution of large size : how does Cope's Rule work ? *Trends Ecol. Evol.* 20, 4–6. <https://doi.org/10.1016/j.tree.2004.10.012>

Hone, D.W.E. & Benton, M.J. 2007. Cope0s Rule in the Pterosauria, and differing perceptions of Cope's Rule at different taxonomic levels. *Eur. Soc. Evol. Biol. J.* 21: 618–624.

Hone, D.W., Dyke, G.J., Haden, M. & Benton, M.J. 2008. Body size evolution on Mesozoic birds. *J. Evol. Biol.* 21: 618–624.

Hu, Y., Meng, J., Wang, Y., Li, C., 2005. Large Mesozoic mammals fed on young dinosaurs. *Nature* 433, 149–152. <https://doi.org/10.1038/nature03102>

Hurlburt, G.R., Heckert, A.B., Farlow, J.O., 2003. Body mass estimates of phytosaurs (Archosauria : Parasuchidae) from the Petrified Forest Formation (Chinle Group : Revueltian)

based on skull and limb bone measurements, in: Zeigler, K.E., Heckert, A.B., Lucas, S.G. (Eds.), Paleontology and Geology of the Snyder Quarry, New Mexico Museum of Natural History and Science Bulletin No. 24, pp. 105–114.

Jacobs, L.L., Mateus, O., Polcyn, M.J., Schulp, A.S., Antunes, M.T., Morais, M.L., Tavares, T. da T., 2006. The occurrence and geological setting of Cretaceous dinosaurs, mosasaurs, plesiosaurs, and turtles from Angola. *J. Palaeontological Soc. Korea* 22, 91–110. <https://doi.org/10.1017/CBO9781107415324.004>

Jouve, S., Bardet, N., Jalil, N.-E., Pereda Suberbiola, X., Bouya, B., Amaghzaz, M., 2008. The oldest African crocodylian: phylogeny, paleobiogeography, and differential survivorship of marine reptiles through the Cretaceous-Tertiary boundary. *J. Vertebr. Paleontol.* 28, 409–421. [https://doi.org/10.1671/0272-4634\(2008\)28](https://doi.org/10.1671/0272-4634(2008)28)

Kear, B.P., 2003. Cretaceous marine reptiles of Australia: A review of taxonomy and distribution. *Cretac. Res.* 24, 277–303. [https://doi.org/10.1016/S0195-6671\(03\)00046-6](https://doi.org/10.1016/S0195-6671(03)00046-6)

Kelley, N.P., Motani, R., Jiang, D. yong, Rieppel, O., Schmitz, L., 2014. Selective extinction of Triassic marine reptiles during long-term sea-level changes illuminated by seawater strontium isotopes. *Palaeogeogr. Palaeoclimatol. Palaeoecol.* 400, 9–16. <https://doi.org/10.1016/j.palaeo.2012.07.026>

Kelley, N.P., Pyenson, N.D., 2015. Evolutionary innovation and ecology in marine tetrapods from the Triassic to the Anthropocene. *Science* (80). 348. <https://doi.org/10.1126/science.aaa3716>

Ketchum, H.F., Benson, R.B.J., 2010. Global interrelationships of Plesiosauria (Reptilia, Sauropterygia) and the pivotal role of taxon sampling in determining the outcome of phylogenetic analyses. *Biol. Rev.* 85, 361–392. <https://doi.org/10.1111/j.1469-185X.2009.00107.x>

Klein, N., Albers, P.C.H., 2009. A New Species of the Sauropsid Reptile *Nothosaurus* from the Lower Muschelkalk of the Western Germanic Basin, Winterswijk, the Netherlands. *Acta Palaeontol. Pol.* 54, 589–598. <https://doi.org/10.4202/app.2008.0083>

Knutsen, E.M., Druckenmiller, P.S., Hurum, J.H., 2012. A new species of *Pliosaurus* (Sauropterygia: Plesiosauria) from the Middle Volgian of central Spitsbergen, Norway. *Norwegian J. Geol.* 92, 235–258.

Liu, J., Hu, S.X., Rieppel, O., Jiang, D.Y., Benton, M.J., Kelley, N.P., Aitchison, J.C., Zhou, C.Y., Wen, W., Huang, J.Y., Xie, T., Lv, T., 2014. A gigantic nothosaur (Reptilia: Sauropterygia) from the Middle Triassic of SW China and its implication for the Triassic biotic recovery. *Sci. Rep.* 4, 1–9. <https://doi.org/10.1038/srep07142>

Maddison, W.P. & Maddison, D.R. 2017. Mesquite: a modular system for evolutionary analysis. Version 3.2. <http://mesquiteproject.org>.

- Massare, J.A., 1987. Tooth Morphology and Prey Preference of Mesozoic Marine Reptiles Author (s): Judy A . Massare Published by : Taylor & Francis , Ltd . on behalf of The Society of Vertebrate Paleontology Stable URL : <http://www.jstor.org/stable/4523132> . 7, 121–137.
- Mazin, J.-M., 2001. Mesozoic Marine Reptiles: An Overview. Second. Adapt. Tetrapods to Life Water - Proc. Int. Meet. Poitiers, 1996 95–117.
- Motani, R., 2009. The Evolution of Marine Reptiles. Evol. Educ. Outreach 2, 224–235. <https://doi.org/10.1007/s12052-009-0139-y>
- Motani, R., 1997. New information on the forefin of *Utatsusaurus hataii* (Ichthyosauria). J. Paleontol. 71, 475–479. <https://doi.org/10.1007/s12052-009-0139-y>
- Motani, R., Chen, X.H., Jiang, D.Y., Cheng, L., Tintori, A., Rieppel, O., 2015. Lunge feeding in early marine reptiles and fast evolution of marine tetrapod feeding guilds. Sci. Rep. 5, 1–8. <https://doi.org/10.1038/srep08900>
- Neumann, C., Hampe, O., 2018. Eggs for breakfast? Analysis of a probable mosasaur biting trace on the Cretaceous echinoid *Echinocorys ovata* Leske, 1778. Foss. Rec. 21, 55–66. <https://doi.org/10.5194/fr-21-55-2018>
- Nicholls, E.L., Manabe, M., 2004. Giant ichthyosaurs of the Triassic—a new species of *Shonisaurus* from the Pardonet Formation (Norian: Late Triassic) of British Columbia. J. Vertebr. Paleontol. 24, 838–849. [https://doi.org/10.1671/0272-4634\(2004\)024\[0838:GIOTTN\]2.0.CO;2](https://doi.org/10.1671/0272-4634(2004)024[0838:GIOTTN]2.0.CO;2)
- O’Keefe, F.R., Street, H.P., Cavigelli, J.P., Socha, J.J., O’Keefe, R.D., 2009. A plesiosaur containing an ichthyosaur embryo as stomach contents from the Sundance Formation of the Bighorn Basin, Wyoming. J. Vertebr. Paleontol. 29, 1306–1310. <https://doi.org/10.1671/039.029.0403>
- Pincheira-Donoso, D., Harvey, L.P., Ruta, M., 2015. What defines an adaptive radiation? Macroevolutionary diversification dynamics of an exceptionally species-rich continental lizard radiation. BMC Evol. Biol. 15, 1–13. <https://doi.org/10.1186/s12862-015-0435-9>
- Pyenson, N.D., Kelley, N.P., Parham, J.F., 2014. Marine tetrapod macroevolution: Physical and biological drivers on 250Ma of invasions and evolution in ocean ecosystems. Palaeogeogr. Palaeoclimatol. Palaeoecol. 400, 1–8. <https://doi.org/10.1016/j.palaeo.2014.02.018>
- Rieppel, O., Wild, R., 1996. A Revision of the Genus *Nothosaurus* (Reptilia: Sauropterygia) from the Germanic Triassic, with Comments on the Status of *Conchiosaurus clavatus*. Fieldiana Geol. 2–98.
- Ross, M.R., 2009. Charting the Late Cretaceous seas: mosasaur richness and morphological diversification. J. Vertebr. Paleontol. 29, 409–416. <https://doi.org/10.1671/039.029.0212>

Russell, D.A., 1967. Systematics and Morphology of American Mosasaurs. Bull. Peabody Museum Nat. Hist. Yale Univ. 23, 1–240.

Sander, P.M., 1989. The large ichthyosaur *Cymbospondylus buchseri*, sp. nov., from the Middle Triassic of Monte San Giorgio (Switzerland), with a survey of the genus in Europe. J. Vertebr. Paleontol. 9, 163–173. <https://doi.org/10.1080/02724634.1989.10011750>

Scheyer, T.M., Romano, C., Jenks, J., Bucher, H., 2014. Early triassic marine biotic recovery: The predators' perspective. PLoS One 9. <https://doi.org/10.1371/journal.pone.0088987>

Scotese, C.R. 2014a. The PALEOMAP Project PaleoAtlas for ArcGIS, version 2, Volume 2, Cretaceous Plate Tectonic, Paleogeographic, and Paleoclimatic Reconstructions, Maps 16-32, Mollweide projection. PALEOMAP Project, Evanston, IL.

Scotese, C.R. 2014b. The PALEOMAP Project PaleoAtlas for ArcGIS, version 2, Volume 3, Triassic and Jurassic Plate Tectonic, Paleogeographic, and Paleoclimatic Reconstructions, Map 33-48, Mollweide projection. PALEOMAP Project, Evanston, IL.

Seeley, H.G., 1874. On *Muraenosaurus leedsii*, a Plesiosaurian from the Oxford Clay, Part 1. Q. J. Geol. Soc. 30, 197–208. <https://doi.org/10.1144/GSL.JGS.1874.030.01-04.35>

Simões, T.R., Vernygora, O., Paparella, I., Jimenez-Huidobro, P., Caldwell, M.W., 2017. Mosasauroid phylogeny under multiple phylogenetic methods provides new insights on the evolution of aquatic adaptations in the group. PLoS One 12, 1–20. <https://doi.org/10.1371/journal.pone.0176773>

Smith, F.A., Payne, J.L., Heim, N.A., Balk, M.A., Finnegan, S., Kowalewski, M., Lyons, S.K., McClain, C.R., McShea, D.W., Novack-Gottshall, P.M., Anich, P.S., Wang, S.C., 2016. Body Size Evolution Across the Geozoic. Annu. Rev. Earth Planet. Sci. 44, 523–553. <https://doi.org/10.1146/annurev-earth-060115-012147>

Spielmann, J.A., Lucas, S.G., 2006. Late Cretaceous marine reptiles (Mosasauridae and Plesiosauria) from New Mexico and their biostratigraphic distribution. Bull. New Mex. Museum Nat. Hist. Sci. 35, 217–221.

Stubbs, T.L., Benton, M.J., 2016. Ecomorphological diversifications of Mesozoic marine reptiles: The roles of ecological opportunity and extinction. Paleobiology 42, 547–573. <https://doi.org/10.1017/pab.2016.15>

Therrien, F., Henderson, D.M., Journal, S., Mar, N., Therrien, F.O.I.S., Henderson, D.M., 2007. My theropod is bigger than yours ... Or not: Estimating body size from skull length in theropods. J. Vertebr. Paleontol. 27, 108–115.

Thorne, P.M., Ruta, M., Benton, M.J., 2011. Resetting the evolution of marine reptiles at the Triassic-Jurassic boundary. *Proc. Natl. Acad. Sci. U. S. A.* 108, 8339–44. <https://doi.org/10.1073/pnas.1018959108>

Tutin, S.L., Butler, R.J., 2017. The completeness of the fossil record of plesiosaurs, marine reptiles from the Mesozoic. 1. *Acta Palaeontol. Pol.* 62, 563–573.

Winrich, T., Hayashi, S., Houssaye, A., Nakajima, Y., Sander, P.M., 2017. A Triassic plesiosaurian skeleton and bone histology inform on evolution of a unique body plan. *Sci. Adv.* 3. <https://doi.org/10.1126/sciadv.1701144>

Young, M.T., Bell, M.A., de Andrade, M.B., Brusatte, S.L., 2011. Body size estimation and evolution in metriorhynchid crocodylomorphs: Implications for species diversification and niche partitioning. *Zool. J. Linn. Soc.* 163, 1199–1216. <https://doi.org/10.1111/j.1096-3642.2011.00734.x>

Supplementary Information S1- Plesiosauria

Taxa	Total (cm)	Skull (cm)	Femur	Humerus (cm)	Material	Time interval	Localization	Geologic Unit	Reference
<i>Albertonectes vanderveldei</i>		38,7	40,32		TMP 2007.011.0001	Upper Campanian	Alberta, Canada	Bearpaw Fm.	(Kubo et al., 2012)
<i>Aphrosaurus furlongi</i>		37,3	39,4		CIT 2748	Maastrichian	Panoche Hills, USA	Moreno Fm.	(Welles, 1943)
<i>Aristonectes parvidens</i>	73,5				MLP 40-XI-14-6	Maastrichian	Chubut Province, Argentina	Lefipán Fm.	(Gasparini et al., 2003)
<i>Aristonectes quiriquinensis</i>				42,22	SGO.PV.957	Upper Maastrichian	Biobío Region, Chile	Quiriquina Fm.	(Otero et al., 2014)
<i>Archaeonectrus rostratus</i>	340				NHMUK 39514	Sinemurian			(Ketchum and Smith, 2010)
<i>Attenborosaurus conybeari</i>	50,16	37,59	37,59		BRSMG Cb 2479	Sinemurian	Northwest corner of Black Ven Water, United Kingdom	Charmouth Mudstone Fm.	(Sollas, 1881)
<i>Augustasaurus hagdorni</i>	184				FMNH PR 1974	Late Anisian	County, Nevada, U.S.A	Fossil Hill Member, Favret Fm., Star Peak Group.	(Sander et al., 1997)
<i>Avalonnectes arturi</i>		21,73	23,39*		NHMUK 14550	Rhaetian–Hettangian	Street, Somerset, UK	Blue Lias Fm., Lower Lias Group	(Benson et al., 2012)
<i>Borealonectes russelli</i>	45,5		33,4		NMC 40729	Callovian	Melville Island,	Hicles Cove Fm.	(Sato and Wu,

						Canada		2008)
<i>Brancasaurus brancai</i>		20	20	GWWU A3.B4	Berriasian	Gronau, Germany	Bückeberg Fm.	(Wegner, 1914)
<i>Brachauchenius lucasi</i>	152,5			FHSM VP-321	Middle Turonian	Fairport, USA	Fairport Chalk	(Schumacher and Everhart, 2005)
				USNM 4989	Turonian	Ottawa County, Kansas	Greenhorn Limestone	(Schumacher, 2008)
<i>Callawayasaurus colombiensis</i>	35	33	41	UCMP 38349	Lower Aptian	Loma de la Catalina, Leiva, Boyacá, Colombia	Machique Member-Apón Fm.	(Wiffen and Moisley, 2012)
<i>Colymbosaurus trochanterius</i>		60,96		Oxfordian-Kimmeridgian	Foxcombe, Wheatley			(Phillips, 1871)
					Foxcombe, Wheatley			(Phillips, 1871)
					Downham Market	Kimmeridge clay		(Brown, 1981)
<i>Cryptoclidus eurymerus</i>	400	25,92	32,4	H.M.G.V-1104	Callovian	Peterborough, England	Lower Oxford Clay Fm.	(Brown, 1981)
<i>Dolichorhynchops herschelensis</i>	49			RSM P2310.1	Campanian-Maastrichtian	Saskatchewan, Canada	Bearpaw Fm.	(Sato, 2005)
<i>Dolichorhynchops osborni</i>	98			KUVP 40001	Campanian	South Dakota	Sharon Springs Member, Pierre Shale	(Carpenter, 1996)
<i>Dolichorhynchops tropicensis</i>		57,96	37,69	MNA V10046	Cenomanian-Turonian	Utah, USA	Tropic Shale	(McKean et al., 2015)
<i>Edgarosaurus muddi</i>	350	47,5		MOR 751	Late Albian	Montana, USA	Thermopolis Shale	
<i>Elasmosaurus morgani</i>		46		SMU	Turonian			(Wiffen & Moisley, 2012)
<i>Elasmosaurus platyurus</i>		60,96		ANSP 10081	Lower Campanian	Western Kansas, USA	Sharon Springs Fm.	(Cope, 1869)
<i>Eoplesiosaurus antiquior</i>		23,33	23,33	TTNCM 8348	Rhaetian–Hettangian	Street, Somerset, UK	Blue Lias Fm., Lower Lias Group	(Benson et al., 2012)

<i>Eopolycotylus rankini</i>		37,5	MNA V9449	Cenomanian-Turonian	Utah, USA	Tropic Shale	(Titus & Loewen, 2013)	
<i>Elasmosaurus marshii</i>	37	39,49*	1645	Upper Coniacian-Lower Campanian	County, Kansas	Smoky Hill Chalk Member	(Williston, 1906)	
<i>Eurycleidus arcuatus</i>	30,48	35,56	BMNH 2030	Hettangian	Street, UK	Blue Lias Fm.	(Owen, 1840)	
<i>Futabasaurus suzukii</i>	28,6	37	NSM PV15025	Lower Santonian	fukushima, japan	Irimazawa Member,Tamayama Fm.	(Sato et al., 2006)	
<i>Georgiasaurus penzensis</i>	80		POKM 11658	Santonian	Penza, Russia	Building stone quarry	(Stoors, 2000)	
<i>Hauffiosaurus tomistomimus</i>	423	37	40	MANCH LL 8004	Lower Toarcian	The bay between Old Peak and Blea Wyke Point, UK	Whitby Mudstone Fm. (Benson et al., 2011)	
<i>Hauffiosaurus zanoni</i>	250	43	35	32	holotype	Toarcian	Holzmaden, Germany	Posidonien-Schiefer (O'Keefe, 2001)
<i>Hydrotherosaurus alexandrae</i>	33	36	39	UCMP, 33912	Maastrichian	Panoche Hills, USA	Moreno Fm. (Wiffen & Moisley, 2012)	
<i>Hydrorion brachypterygius</i>	280		UMH	Toarcian	Holzmaden, Germany	Holzmaden Shale	(Selden & Nudds, 2012)	
<i>Hydralmosaurus serpentinus</i>	40		46	AMNH 5835	Campanian	South Dakota, USA	Sharon Springs Shale Member, Pierre Shale (Wiffen & Moisley, 2012)	
<i>Kaiwhekea katiki</i>	62	45,33	42,35*	OU 12649	Maastrichian	South Island, New Zealand	Kaitiki Fm. (Cruickshank and Fordyce, 2002)	
<i>Kronosaurus boyacensis</i>		32,2		Upper Aptian	Villa de Leyva, Provinz Boyaca/Colombia	Formacion Paja	(Hampe, 1992)	
<i>Leptocleidus capensis</i>	38,1		SAM-K5822	Upper Valangian-Early Hauterivian	Swartkops River, South Africa	Sundays River Fm.	(Andrews, 1910)	
<i>Leptocleidus superstes</i>		28		Barremian	Sussex, England	Weald Clay Fm.	(Andrews, 1922)	

<i>Libonectes atlasense</i>	40	26,25	27,08	SMNK-PAL 3978	Turonian	Goulmima region, Morroco	Limestone bar, north of Goulmima	(Marie-Céline, 2010)	
<i>Liopleurodon ferox</i>	112		R 2680		Callovian	Peterborough, UK	Peterborough Member, Oxford Clay Fm.	(Andrews, 1910)	
	154	53,8	R 3536		Callovian	Peterborough, UK	Peterborough Member, Oxford Clay Fm.	(Andrews, 1910)	
<i>Liopleurodon macromerus</i>		86,36		OUMNHJ.12498	Oxfordian-Kimmeridgian	Swindon	Kimmeridge clay	Phillips, 1871	
<i>Luskhan itilensis</i>	650	96	84	YKM 68344/1_262	Kimmeridgian Upper Hauterivian	Stretham, UK Slantsevy Rudnik village, western Russia	Kimmeridge Clay Speetoniceras versicolor Zone	(Tarlo, 1959) (Fischer et al., 2017)	
<i>Macroplata tenuiceps</i>	465	56	35	32	BMNH R5488	Hettangian	Harbury, Warwickshire, U.K	Blue Lias Fm.	(Ketchum and Smith, 2010)
<i>Maresaurus coccaei</i>		111,81		MOZ 4386 V	Lower Bajocian	Neuquén Province, Argentina	Los Molles Fm.	(Gasparini, 1997)	
<i>Marmornectes candrewi</i>			42	BEDFM 1999.201	Lower Callovian	Bedfordshire, UK	Oxford Clay Fm.	(Ketchum and Benson, 2011)	
<i>Mauiasaurus haasti</i>		34,3	36,77*	DMR 1529	Maastrichtian			(Wiffen & Moisley, 2012)	
<i>Meyerasaurus victor</i>	335	40	38,5	42	SMNS 12478	Toarcian	Holzmaden, Germany	Posidonien-Schiefer, Upper Lias	(Smith and Vincent, 2010)
<i>Megacephalosaurus eulerti</i>		152,25		FHSM VP-321	Middle Turonian	Kansas, USA	Fairport Chalk Member, Carlile Shale	(Schumacher et al., 2013)	
<i>Microcleidus homalospondylus</i>		28		NHMUK 36184	Toarcian	Yorkshire, UK	Upper Lias of Whitby	(Brown et al., 2013)	
<i>Morenosaurus stocki</i>		36	37,4	CIT 2802	Maastrichtian	Panoche Hills, USA	Moreno Fm.	(Wiffen & Moisley, 2012)	

<i>Muraenosaurus durobrivensis</i>	35,7	38,28*	R2861	Middle Orxfordian	Peterborough, England	Lower Oxford Clay Fm.	(Andrews, 1906)
<i>Muraenosaurus leedsii</i>		31,42	R2426	Middle Orxfordian	Peterborough, England	Lower Oxford Clay Fm.	(Brown, 1981)
	30,4	33,2	R2422	Middle Orxfordian	Peterborough, England	Lower Oxford Clay Fm.	(Andrews, 1906)
	17,7	25,4		Oxfordian	Huntingdonshire, England	Lower Oxford Clay	(Seeley, 1874)
	39	26,3	28,3	R2421	Oxfordian	Peterborough, England	Oxford Clay
<i>Muraenosaurus platyclylus</i>	31,4	33,7	R2678	Middle Orxfordian	Peterborough, England	Lower Oxford Clay Fm.	(Andrews, 1906)
	34,9	36,7	R2425	Middle Orxfordian	Peterborough, England	Lower Oxford Clay Fm.	(Andrews, 1906)
<i>Occitanosaurus tournemirensis</i>	29,5	20	20,5	MMM J. T. 86-100	Upper Toarcian	Tournemire, Aveyron Department	Des Causses Basin
<i>Pahasapasaurus haasi</i>	600	49	45	AMM 98.1.1	Cenomanian	South Dakota, USA	Greenhorn Limestone
<i>Palmulasaurus quadratus</i>		27	29	MNA V9442	Cenomanian-Turonian	Utah, USA	Tropic Shale
<i>Peloneustes philarchus</i>	83			NHMUK R4058	Callovian	Peterborough, UK	Peterborough Member, Oxford Clay Fm.
	78,5			UNIL 9865	Callovian	Peterborough, UK	Peterborough Member, Oxford Clay Fm.
	60	39	33	NHMUK R3318	Callovian	Peterborough, UK	Peterborough Member, Oxford Clay Fm.
	76,6			NHMUK R8574	Callovian	Bedfordshire, UK	Peterborough Member, Oxford Clay Fm.
	71,5			NHMUK R3803	Callovian	Peterborough, UK	Peterborough Member, Oxford Clay Fm.

	43,4		R.2439	Callovian	Peterborough, UK	Peterborough Member, Oxford Clay Fm.	(Andrews, 1910)
<i>Picrocleidus beloclis</i>		18,3	R1965	Middle Orxfordian	Peterborough, England	Lower Oxford Clay Fm.	(Andrews, 1906)
	16		R3698	Middle Orxfordian	Peterborough, England	Lower Oxford Clay Fm.	(Andrews, 1906)
<i>Plesiosaurus australis</i>	17,78	20,1*		Maastrichtian	Waipara river, New Zealand		(Hector, 1874)
<i>Plesiosaurus dolichodeirus</i>	17,43	18,52	BMNH 22656	Sinemurian	Lyme Regis, UK	Charmouth Mudstone Fm.	(Conybeare, 1824)
	17,78	20,32	OUMNH J.28587/1-57	Hettangian- Pliensbachian	Lyme Regis, UK	Lias marl	(Owen, 1840)
<i>Plesiosaurus laticeps</i>	31,75	34,29	BMNH 40140,	Sinemurian	Charmouth	Charmouth Mudstone Fm.	(Sollas, 1881)
<i>Plesiosaurus oxoniensis</i>	335	27	28,5	R2860	Middle Orxfordian	Peterborough, England	Lower Oxford Clay Fm.
		33,1	34,1	R2862	Middle Orxfordian	Peterborough, England	Lower Oxford Clay Fm.
		33,7	36,2	R2412	Middle Orxfordian	Peterborough, England	Lower Oxford Clay Fm.
		30,2	33,2	R2420	Middle Orxfordian	Peterborough, England	Lower Oxford Clay Fm.
		30,2		R3703	Middle Orxfordian	Peterborough, England	Lower Oxford Clay Fm.
<i>Plesiopleurodon wellesi</i>	71,2		CM 2815	Lower Cenomanian	Wyoming, UK	Belle Fourche Shale	(Carpenter, 1996)
<i>Plesiopterys wildi</i>	220	14,8	15,5	15,4	SMNS 16812	Lower Toarcian	Baden- Württemberg, Germany
<i>Pliosaurus funkei</i>		90	PMO 214.135	Lower Kimmeridgian	Svalbard, Norway	Agardhfjellet Fm.	(Knutson et al., 2012)
<i>Pliosaurus irgisensis</i>	60	54,14*	PIN 426	Tithonian	Saratov, Russia	Savel'evsk oil shales	(Stoors, 2000)
<i>Pliosaurus kevani</i>	199,5		DORCM G.13.675	Lower	Dorset, UK	Kimmeridge Clay Fm.	(Benson et al.

					Kimmeridgian		2013)	
<i>Pliosaurus brachyspondylus</i>	180		BRSMG Cc332	Kimmeridgian	Westbury, Wiltshire	Lower Kimmeridge Clay	(Grange et al., 1996)	
	105	89	J.35991	Kimmeridgian	Cambridgeshire	Kimmeridge clay	(Tarlo, 1959)	
<i>Pliosaurus grandis</i>	30,48	30,42*		Oxfordian-Kimmeridgian	Peterborough, England		(Phillips, 1871)	
<i>Pliosaurus brachydeirus</i>	66,8	55,8		Oxfordian-Kimmeridgian	Great Western Railway, Swindon	Kimmeridge clay	(Phillips, 1871)	
	68,07			Oxfordian-Kimmeridgian	Swindon		(Phillips, 1871)	
	46,99			Oxfordian-Kimmeridgian	Shotover, England		(Phillips, 1871)	
	49,53			Oxfordian-Kimmeridgian	Shotover, England		(Phillips, 1871)	
<i>Polycotylus latipinnis</i>		45,71	PR 187	Santonian-Campanian	Kansas, USA	Niobrara Fm.	(O'Keefe, 2004)	
<i>Rhomaleosaurus cramptoni</i>	700	106	NMING F8785	Toarcian	Yorkshire, UK	Upper Lias	(Smith and Dyke, 2008)	
<i>Rhomaleosaurus megacephalus</i>	460	81,3	34	35	BRSMG Cb2335	Hettangian	Somerset, UK	Blue Lias Fm. (Cruickshank, 1994)
	83,8				LEICS G221.1851	Hettangian	County of Leicestershire	Botton flor limestone (Cruickshank, 1994)
	90				TCD.47762	Hettangian		(Jackson, 2004)
	83		35	BGS GSM 118410	Hettangian	Somerset, UK	Blue Lias Fm. (Smith, 2015)	
<i>Rhomaleosaurus thorntoni</i>		67,8	71	R. 4853	Pliensbachian	Northamptonshire, UK	Upper Liassic beds (Andrews, 1922)	
<i>Rhomaleosaurus zetlandicus</i>	98,21	50	51,78	YORYM G503	Toarcian	Yorkshire, England	Mudstone Fm. (Taylor, 1992)	
<i>Stratesaurus taylori</i>	18		OUMNH J.10337	Hettangian	Somerset, UK	Blue Lias Fm. (Benson et al., 2012)		
<i>Styxosaurus snowii</i>	48		KUMNH, 1301	Lower Campanian	Hell Creek, Logan	Smoky Hill Chalk	(Wiffen &	

					County	Member	Moisley, 2012)	
	37,5	38	SDSMT 451	Campanian	Pierre Shale of South Dakota	Smoky Hill Chalk Member	(Wiffen & Moisley, 2012)	
<i>Seeleyosaurus guilelmiiimperatoris</i>	21,5	23	MB.R.1992	Lower Toarcian	Holzmaden, Germany	Posidonia shale, Lias e II4	(Dames, 1845)	
<i>Simolestes vorax</i>	73	50	R 3319	Callovian	Peterborough, UK	Peterborough Member, Oxford Clay Fm.	(Andrews, 1910)	
<i>Terminonatator ponteixensis</i>	28,5	35,9	34	RSM P2414.1	Upper Campanian	Saskatchewan, Canada	Berpaw Fm.	(Sato, 2003)
<i>Thalassomedon haningtoni</i>		44	44	CMNH 1508	Lower Cenomanian	Baca County, Colorado, USA	Graneros Shale	(Wiffen & Moisley, 2012)
	55			UNSM 50132	Lower Cenomanian	Baca County, Colorado, USA	Graneros Shale	(Wiffen & Moisley, 2012)
<i>Thalassiodracon hawkinsii</i>	18		OUM J.10337	Rhaetian-Hettangian				(O'Keefe, 2001)
	17		CAMSM J.46986	Rhaetian	Somerset, England	Lias quarries	(Storrs and Taylor, 1996)	
	180		BMNH.2018	Rhaetian			(Storrs and Taylor, 1996)	
<i>Thalassonomosaurus nobilis</i>	33,7	36,16*	YPM 1640	Coniacian	Jewell County, Kansas	Fort Hays limestone	(Welles 1943)	
<i>Thililua longicollis</i>	66		MNHGr.PA.11710	Cenomanian- Turonian	Rachidia Province, southern Morocco	Limestone bar	(Bardet et al., 2003)	
<i>Trinacromerum bentonianum</i>		36,11	ESU 5000	Early Turonian	Russell County	Pfeifer Member, Greenhorn Limestone	(Schumacher and Everhart, 2005)	
	68		KUVP 5070	Lower Turonian	Cloud County, Kansas	Hartland Shale Member, Greenhorn	(Carpenter, 1996)	

						Fm.	
	90		SM 3025	Upper Cenomanian		The Lake Waco Fm.	(Carpenter, 1996)
<i>Trinacromerum bonneri</i>	94		KUVP 40001	Lower Campanian	South Dakota, USA	Pierre Shale	(O'Keefe, 2008)
<i>Tricleidus seeleyi</i>	21,6	20,7	R3539	Middle Oxfordian	Peterborough, England	Lower Oxford Clay Fm.	(Andrews, 1906)
<i>Vegasaurus molyi</i>	28	29,8	MLP 93-I-5-1	Lower Maastrichtian	Ross Archipelago, Antarctic Peninsula	Cape Lamb Member, Snow Hill Island Fm.	(Gorman, 2015)
<i>Zarafasaura oceanis</i>	36,6		OCP DEK/GE 315	Upper Maastrichtian	Abdoun Basin, Morocco	Upper CIII level	(Vincent et al., 2011)
	42,14		OCP DEK/GE 456	Upper Maastrichtian	Abdoun Basin, Morocco	Upper CIII level	(Vincent et al., 2011)
<i>Westphaliasaurus simonsensii</i>	27,5	27	SMNS 16812. 1	Pliensbachian	Stuttgart, Germany	Jura Fm.	(Schwermann and Sander, 2011)

Supplementary Information. S1- Table of contents depicting total body size, skull, femur and humerus lengths, associated geologic unit, age interval, geographic localities, and identification of the material.

REFERENCES

- Andrews, C.W., 1922. Note on the Skeleton of a large Plesiosaur (*Rhomaleosaurus thorntoni*, sp n.) from the Upper Lias of Northamptonshire. 1. Ann. Mag. Nat. Hist. 10, 407–415. <https://doi.org/10.1080/00222932208632790>
- Andrews, C.W., 1910. A descriptive catalogue of the marine reptiles of The Oxford Clay. Based on the Leeds Collection in the British Museum (Natural History), London. Part 1. 205.
- Bardet, N., Godefroit, P., Sciau, J., 1999. A new Elasmosaurid plesiosaur from the Lower Jurassic of southern France. Palaeontology 42, 927–952. <https://doi.org/10.1111/1475-4983.00103>
- Bardet, N., Suberbiola, X.P., Jalil, N.E., 2003. Un nouveau plésiosaure polycotylidé du Crétacé supérieur (Turonien) du Maroc. Comptes Rendus - Palevol 2, 307–315. [https://doi.org/10.1016/S1631-0683\(03\)00063-0](https://doi.org/10.1016/S1631-0683(03)00063-0)
- Benson, R.B.J., Evans, M., Druckenmiller, P.S., 2012. High diversity, low disparity and small body size in plesiosaurs (Reptilia, Sauropterygia) from the Triassic-Jurassic boundary. PLoS One 7. <https://doi.org/10.1371/journal.pone.0031838>
- Benson, R.B.J., Ketchum, H.F., Noè, L.F., Gómez-Pérez, M., 2011. New information on Hauffiosaurus (Reptilia, Plesosauria) based on a new species from the Alum Shale Member (Lower Toarcian: Lower Jurassic) of Yorkshire, UK. Palaeontology 54, 547–571. <https://doi.org/10.1111/j.1475-4983.2011.01044.x>
- Brown, D.S., Vincent, P., Bardet, N., 2013. Osteological Redescription of the Skull of *Microcleidus homalospondylus* (Sauropterygia, Plesosauria) from the Lower Jurassic of England. J. Paleontol. 87, 537–549. <https://doi.org/10.1666/11-104>
- Carpenter, K., 1996. Carpenter, 1996, A review of short-necked plesiosaurs from the Cretaceous of the Western Interior, North America. N.Jb.Geol.Palaont. Abh 201, 259–287.

- Cope, E., 1869. Synopsis of the extinct Batrachia and Reptilia of North America. *Transactions of the American Philosophical Society*. 14-1.
- Cruickshank, A.R.I., Fordyce, R.E., 2002. A new marine reptile (Sauropterygia) from New Zealand: Further evidence for a Late Cretaceous austral radiation of cryptoclidid plesiosaurs. *Palaeontology* 45, 557–575. <https://doi.org/10.1111/1475-4983.00249>
- Fischer, V., Benson, R.B.J., Zverkov, N.G., Soul, L.C., Arkhangelsky, M.S., Lambert, O., Stenshin, I.M., Uspensky, G.N., Druckenmiller, P.S., 2017. Plasticity and Convergence in the Evolution of Short-Necked Plesiosaurs. *Curr. Biol.* 27, 1667–1676.e3. <https://doi.org/10.1016/j.cub.2017.04.052>
- Gasparini, Z., 1997. A new pliosaur from the Bajocian of the Neuquen Basin, Argentina. *Palaeontology*. 40, 135–147.
- Gasparini, Z., Bardet, N., Martin, J.E., Fernandez, M., 2003. The Elasmosaurid Plesiosaur *Aristonectes Cabrera* from the Latest Cretaceous of South America and Antarctica. *J. Vertebr. Paleontol.* 23, 104–115.
- Gorman, J.P.O., 2015. New insights on the (Plesiosauria , Elasmosauridae) specimen. *Ameghiniana*. 53, 397–417.
- Grange, D.R., Storrs, G.W., Carpenter, S., Etches, S., 1996. An important marine vertebrate-bearing locality from the Lower Kimmeridge Clay (Upper Jurassic) of Westbury, Wiltshire. *Proc. Geol. Assoc.* 107, 107–116. [https://doi.org/10.1016/S0016-7878\(96\)80004-6](https://doi.org/10.1016/S0016-7878(96)80004-6)
- Hampe, O., 1992. Ein großwüchsiger Pliosauride (Reptilia: Plesiosauria) aus der Unterkreide (oberes Aptium) von Kolumbien. *Cour. Forschungsinstitut Senckenb.* 145, 1–32.
- Hector, J., 1874. On the fossil reptilia of New Zealand. *Trans. New Zeal. Inst.* 6, 333–358. <https://doi.org/10.1017/CBO9781107415324.004>
- Jackson, P., 2004. Thomas Hawkins, Lord Cole, William Sollas and all: casts of Lower Jurassic marine reptiles in the Geological Museum, Trinity College, Dublin, Ireland 1831, 11–18.
- Ketchum, H.F., Benson, R.B.J., 2011. A new pliosaurid (Sauropterygia, Plesiosauria) from the Oxford Clay Formation (Middle Jurassic, Callovian) of England: Evidence for a gracile, longirostrine grade of Early-Middle Jurassic pliosaurids. *Spec. Pap. Palaeontol.* 109–129. <https://doi.org/10.1111/j.1475-4983.2011.01083.x>
- Ketchum, H.F., Smith, A.S., 2010. The anatomy and taxonomy of *Macroplata tenuiceps* (Sauropterygia, Plesiosauria) from the Hettangian (Lower Jurassic) of Warwickshire, United Kingdom. *J. Vertebr. Paleontol.* 30, 1069–1081. <https://doi.org/10.1080/02724634.2010.483604>
- Knutsen, E.M., Druckenmiller, P.S., Hurum, J.H., 2012. A new species of *Pliosaurus* (Sauropterygia: Plesiosauria) from the Middle Volgian of

centram Spitsbergen, Norway. Norwegian J. Geol. 92, 235–258.

Kubo, T., Mitchell, M.T., Henderson, D.M., 2012. Albertonectes vanderveldei, a new elasmosaur (Reptilia, Sauropterygia) from the Upper Cretaceous of Alberta. J. Vertebr. Paleontol. 32, 557–572. <https://doi.org/10.1080/02724634.2012.658124>

Marie-Céline, B., 2010. First Record of Ophthalmosaurus (Reptilia: Ichthyosauria) from the Tithonian (Upper Jurassic) of Mexico. J. Paleontol. 84, 149–155. <https://doi.org/10.1666/08-122.1>

McKean, S., L., R., Gillette, D.D., 2015. Taphonomy of large marine vertebrates in the Upper Cretaceous (Cenomanian-Turonian) Tropic Shale of southern Utah. Cretac. Res. 56, 278–292. <https://doi.org/10.1016/j.cretres.2015.05.009>

O'Keefe, F.R., 2008. Cranial Anatomy and Taxonomy of *Dolichorhynchops bonneri* New Combination, a Polycotylid (Sauropterygia : Plesiosauria) from the Pierre Shale of Wyoming and South Dakota Author (s): F . Robin O ' Keefe Published by : Taylor & Francis , Ltd . on behalf. J. Vertebr. Paleontol. 28, 664–676.

O'Keefe, F.R., 2004. On the cranial anatomy of the polycotylid plesiosaurs, including new material of *Polycotylus latipinnis*, Cope, from Alabama. J. Vertebr. Paleontol. 24, 326–340. <https://doi.org/10.1671/1944>

O'Keefe, F.R., 2001. A cladistic analysis and taxonomic revision of the Plesiosauria (Reptilia:Sauropterygia). Acta Zool. Fennica 213: 1–63.

Otero, R.A., Soto-Acuña, S., O'Keefe, F.R., O'Gorman, J.P., Stinnesbeck, W., Suárez, M.E., Rubilar-Rogers, D., Salazar, C., Quinzio-Sinn, L.A., 2014. *Aristonectes quiriquinensis* , sp. nov., a new highly derived elasmosaurid from the upper Maastrichtian of central Chile. J. Vertebr. Paleontol. 34, 100–125. <https://doi.org/10.1080/02724634.2013.780953>

Owen, R. 1840. A description of a specimen of the *Plesiosaurus macrocephalus*, Conybeare, in the collection of Viscount Cole. Transactions of the Geological Society of London, Second series, 5, 515-535.

Sander, P.M., Rieppel, O.C., Bucher, H., 1997. A new pistosaurid (Reptilia: Sauropterygia) from the middle Triassic of Nevada and its implications for the origin of the plesiosaurs. J. Vertebr. Paleontol. 17, 526–533. <https://doi.org/10.1080/02724634.1997.10010999>

Sato, T., 2005. new polycotylid plesiosaur (Reptilia, Sauropterygia) from the Upper Cretaceous Bearpaw Formation in Saskatchewan, Canada. Journal of Paleontology, 79(5):969-980.

Sato, T., Hasegawa, Y., Manabe, M., 2006. A new elasmosaurid plesiosaur from the upper cretaceous of Fukushima, Japan. Palaeontology 49, 467–484. <https://doi.org/10.1111/j.1475-4983.2006.00554.x>

Sato, T., Wu, X., 2008. A new Jurassic pliosaur from Melville Island, Canadian Arctic Archipelago. Can. J. Earth Sci. 45, 303–320. <https://doi.org/10.1139/E08-003>

Schumacher, B.A., 2008. On the skull of a pliosaur (Plesiosauria; Pliosauridae) from the Upper Cretaceous (Early Turonian) of the North American Western Interior. Trans. Kansas Acad. Sci. 111, 203–218. <https://doi.org/10.1660/0022-8443-111.3.203>

Schumacher, B.A., 2007. A new polycotylid plesiosaur (Reptilia; Sauropterygia) from the Greenhorn Limestone (Upper Cretaceous; Lower Upper Cenomanian), Black Hills, South Dakota. Geol. Soc. Am. Spec. Pap. 427, 133–146. [https://doi.org/10.1130/2007.2427\(09\)](https://doi.org/10.1130/2007.2427(09)).

Schumacher, B.A., Carpenter, K., Everhart, M.J., 2013. A new Cretaceous Pliosaurid (Reptilia, Plesiosauria) from the Carlile Shale (Middle Turonian) of Russell County, Kansas. J. Vertebr. Paleontol. 33, 613–628. <https://doi.org/10.1080/02724634.2013.722576>

Schumacher, B.A., Everhart, M.J., 2005. A stratigraphic and taxonomic review of plesiosaurs from the old “Fort Benton Group” of central Kansas: A new assessment of old records. Paludicola 5, 33–54.

Schwarzmann, L., Sander, P.M., 2011. Osteology and phylogeny of *Westphaliasaurus simonsensis*: A new plesosaurid (Sauropterygia) from the Lower Jurassic (Pliensbachian) of Sommersell (Höxter District), North Rhine-Westphalia, Germany. Geol. und Palaeontol. 79, 5–60.

Seeley, H.G., 1874. On *Muraenosaurus leedsii*, a Plesiosaurian from the Oxford Clay, Part 1. Q. J. Geol. Soc. 30, 197–208. <https://doi.org/10.1144/GSL.JGS.1874.030.01-04.35>

Smith, A.S., 2015. Reassessment of 'Plesiosaurus' megacephalus (Sauropterygia: Plesiosauria) from the Triassic-Jurassic boundary. Palaeo. Eletron. 18.1.20A: 1-19.

Smith, A.S., Dyke, G.J., 2008. The skull of the giant predatory pliosaur *Rhomaleosaurus cramptoni*: Implications for plesiosaur phylogenetics. Naturwissenschaften 95, 975–980. <https://doi.org/10.1007/s00114-008-0402-z>

Smith, A.S., Vincent, P., 2010. A new genus of pliosaur (Reptilia: Sauropterygia) from the Lower Jurassic of Holzmaden, Germany. Palaeontology 53, 1049–1063. <https://doi.org/10.1111/j.1475-4983.2010.00975.x>

Sollas, W.J., 1881. On a new species of plesiosaurus from the Lower Lias of Charmouth; with observations on *P. megacephalus*, Stutchbury and *P. brachycephalus*, Owen. Quarterly J. Geol. Soc. 37, 440–480. <https://doi.org/10.1144/GSL.JGS.1881.037.01-04.42>

Storrs, G.W., Taylor, M.A., 1996. Cranial anatomy of a new plesiosaur genus from the Lowermost Lias (Rhaetian/Hettangian) of Street, Somerset, England. J. Vertebr. Paleontol. 16, 403–420. <https://doi.org/10.1080/02724634.1996.10011330>

- Tarlo, L.B., 1959. *Pliosaurus brachyspondylus* (Owen) from the Kimeridge Clay. *Palaeontology* 1, 91–283.
- Taylor, M.A., 1992. Taxonomy and taphonomy of *Rhomaleosaurus zetlandicus* (Plesiosauria, Reptilia) from the Toarcian (Lower Jurassic) of the Yorkshire coast. *Proc. Yorksh. Geol. Soc.* 49, 49–55. <https://doi.org/10.1144/pygs.49.1.49>
- Titus, A.L., and Loewen, M.A. (Eds). 2013. At the top of the Grand Staircase—the Late Cretaceous of southern Utah: Bloomington, Indiana University Press, 656 p.
- Vincent, P., Bardet, N., Pereda Suberbiola, X., Bouya, B., Amaghzaz, M., Meslouh, S., 2011. *Zarafasaura oceanis*, a new elasmosaurid (Reptilia: Sauropterygia) from the Maastrichtian Phosphates of Morocco and the palaeobiogeography of latest Cretaceous plesiosaurs. *Gondwana Res.* 19, 1062–1073. <https://doi.org/10.1016/j.gr.2010.10.005>
- Wegner, T. 1914. *Brancasaurus brancai* n.g.n.sp., ein Elasmosauride aus dem Wealden Westfalens. *Palaeontogr. Abteilung A Paläozoologie—Stratigraphie* 8, 235–305.
- Welles, S.P., 1943. Elasmosaurid plesiosaurs with description of new material from California and Colorado. *Mem. Univ. Calif.* 13, 125–254.
- Wiffen, J., Moisley, W.L., 2012. Late Cretaceous reptiles (families elasmosauridae and pliosauridae) from the mangahouanga stream, North Island, New Zealand. *New Zeal. J. Geol. Geophys.* 29, 205–252. <https://doi.org/10.1080/00288306.1986.10427535>
- Williston, S.W., 1906. North American Plesiosaurs. *Am. J. Sci.* 21, 221–236.

Supplementary Information S1- Mosasauroidea

Taxa	Total (cm)	Skull (cm)	Femur (cm)	Humerus (cm)	Material	Time interval	Localization	Geologic Unit	Reference
<i>Aigialosaurus dalmaticus</i>			4,5	3,75	BSP 1902II501	Upper Cenomanian-Lower Turonian	Hvar, Croatia	Limestone quarry of Stratigrad and Vrboska	(Dutchak and Caldwell, 2006)
<i>Clidastes liodontus</i>	400			7,5		Santonian-Campanian			Nicholls & Callaway, 1997
		37,56			USNM 11719	Santonian-Campanian	Kansas, USA	Smoky Hill Chalk Member, Niobrara Fm.	Merriam, 1894
<i>Clidastes propyton</i>	500	65,8			KUVP 1000	Santonian/Maastrichtian	Alabama, USA	Mooreville Chalk Fm., Selma Group	(Everhart, 2015)
		9,5	9,2			Upper Coniacian-Lower Santonian	Kansas, USA	Mc Allaster, Fort Pierre	(Williston, 1898)
<i>Ectenosaurus clidastoides</i>		71,95		10,33	FHSM VP-401	Santonian	Trego County, Kansas, USA	Smoky Hill Chalk member, Niobrara Chalk Fm.,	(Lindgren et al., 2011)
<i>Eremiasaurus heterodontus</i>		63,5			UALVP 51744	Maastrichtian	Oulad Abdoun Basin, Morocco	Upper Couche III	(Leblanc et al., 2012)
<i>Eonatator coellensis</i>		41,5			IGM p881237	Campanian	Tolima, Colombia	Nivel de Lutitas y Arenas	(Páramo Fonseca, 2014)
<i>Globidens dakotensis</i>	500	65,7			PR 846	Campanian	South Dakota, USA	Sharon Spring Member of Pierre Shale	(Russel, 1975)
<i>Globidens schurmanni</i>	600			14,8	SDSM 74764	Late Campanian	South Dakota, USA	DeGrey Fm. of the Pierre Shale Group	(Martin, 2007)
<i>Halisaurus</i>	300		10,4	10,26	OCP DEK/GE	Late Maastrichtian	Grand	Oulad Abdoun Basin,	(Bardet et al.,

<i>arambourgii</i>				100		Daoui, Morroco	upper Couche III,	2005)
<i>Haasiasaurus gittelmani</i>		5,1	4,73714	EJ700	Cenomanian	Ein Yabrud, Israel	Bet Meir Forrnation	(Polcyni et al., 1999)
<i>Halisaurus sternbergi</i>	260	34,5	5,5	6	UPI R 163	Santonian	Kansas, USA	Smoky Hill Chalk member, Niobrara Chalk Fm.
<i>Kourisodon putledgensis</i>	400		5,9	6,6	CDM 022	Upper Santonian	Courtenay, British Columbia	Pender Fm., Nanaimo Group
<i>Latoplatecarpus willistoni</i>		49		TMP 84.162.01	Lower-Middle Campanian	Manitoba, Canada	Pierre Shale Fm.	(Konishi and Caldwell, 2016)
<i>Mosassaurus conodon</i>	1000		16,56	AMNH 1380	Upper Campanian- Lower Maastrichtian	New Jersey, USA	Navesink Fm.	(Ikejiri and Lucas, 2014)
		97,7		MOR 006	Upper Campanian- Lower Maastrichtian	Montana, USA	Bearpaw Shale	(Ikejiri & Lucas, 2014)
<i>Mosassaurus hoffmanni</i>		145		IRSNB R26	Maastrichian	Maastricht, Netherlands		(Lingham- Soliar, 1995)
			7,5	IRSNB R12	Maastrichian	Maastricht, Netherlands		(Lingham- Soliar, 1995)
<i>Mosassaurus missouriensis</i>	900	95		KUVP 1034	Campanian	South Dakota, USA	Pierre Shale Fm.	(Lindgren et al., 2008)
		13		TMP 2008.036.0001	Upper Campanian	Alberta, Canada		(Konishi et al., 2014)
<i>Platecarpus planifrons</i>	500	65		UALVP 24240	Upper Coniacian- Lower Santonian	Kansas, USA	Smoky Hill Chalk member, Niobrara Chalk Fm.	(Konishi and Caldwell, 2007)
<i>Platecarpus tympaniticus</i>	540	59	15,4	LACM 128319	Upper Coniacian- Lower Santonian	Grahan county, Kansas, USA		(Williston, 1898)
	550	51,7	12,9	12,7	Upper Santonian-	Logan	Smoky Hill Niobrara	(Konishi et al.,

					Lowermost Campanian	county, Kansas, U.S.A	Chalk Fm.	2012)
		11,6	14,1		Upper Coniacian or Lower Santonian			(Williston, 1898)
<i>Plesiotylosaurus</i> <i>crassidens</i>	700	95,5		LACM/CIT- 328	Maaschichian	Panoche Hills of Fesno County	Moreno Fm.	Camp, 1942
<i>Plioplatecarpus</i> <i>nichollsae</i>			11,53	83.10.18	Campanian	Miami Manitoba, Canada	Pierre Shale Fm.	(Konishi and Caldwell, 2009)
<i>Plotosaurus</i> <i>bennisoni</i>	900		11,11		Maastichian			(Nicholls & Callaway, 1997)
		74,15		UCPM 2750	Maastichian	California, USA	Moreno Fm.	(Camp, 1942)
			12	UCMP 126284	Maastichian	California, USA	Moreno Fm.	(Lindgren et al., 2008)
<i>Prognathodon currii</i>	10000	142		HUJ.OR 100	Late Campanian	Negev desert, Israel	"Main Phosphate-Bed IV"	(Christiansen and Bonde, 2002)
<i>Prognathodon</i> <i>overtoni</i>	600	92,5		MP 2007.034.0001	Upper Campanian	Alberta, Canada	lower Bearpaw Fm.	(Konishi et al., 2011)
			14	13,66	Upper Campanian	Alberta, Canada	lower Bearpaw Fm.	(Konishi et al., 2011)
				MP 2002.400.0001				
			70,2	SDSM 3393	Lower Maastrichian	South Dakota, USA	Virgin Creek Member, Upper Pierre Fm.	(Lingham- Soliar and Nolf, 1989)
<i>Romeosaurus</i> <i>fumanensis</i>		65,6	9,25	MPPS-45301	Lower Turonian– Lower Santonian	Fumane, Italy	Scaglia Rossa Veneta Fm. of Italy	(Palci et al., 2013)
<i>Tylosaurus bernardi</i>		22,1	21	IRScNB R23	Maastrichian	La Malogne, Belgium	Ciply Phosphatic Chalk	(Jimenez- Huidobro and

							Caldwell, 2016
<i>Tylosaurus kansasensis</i>	700	79,5	FHSM VP-2295	Coniacian	Ellis County	Smoky Hill Chalk Member	(Everhart, 2005)
<i>Tylosaurus nepaeolicus</i>		79	AMNH 124 e 134	Upper Coniacian-Lower Campanian	Kansas, USA	Smoky Hill Chalk member, Niobrara Chalk Fm.	(Everhart, 2002)
<i>Tylosaurus proriger</i>		15,71		Upper Coniacian-Lower Campanian	Kansas, USA	Smoky Hill Chalk member, Niobrara Chalk Fm.	(Nicholls & Callaway, 1997)
			AMNH 4909	Upper Coniacian-Lower Campanian	Kansas, USA	Smoky Hill Chalk member, Niobrara Chalk Fm.	(Everhart, 2002)
			USNM 8898	Upper Coniacian-Lower Campanian	Kansas, USA	Smoky Hill Chalk member, Niobrara Chalk Fm.	(Everhart, 2002)
	830		AMNH 221	Upper Coniacian-Lower Campanian	Kansas, USA	Smoky Hill Chalk member, Niobrara Chalk Fm.	(Everhart, 2002)
		101,6	FFHM 1997-10	Upper Coniacian-Lower Campanian	Kansas, USA	Smoky Hill Chalk member, Niobrara Chalk Fm.	(Everhart, 2002)
	880	108	FHSM VP-3	Upper Coniacian-Lower Campanian	Kansas, USA	Smoky Hill Chalk member, Niobrara Chalk Fm.	(Everhart, 2002)
		119,5	KUVP-1032	Upper Coniacian-Lower Campanian	Kansas, USA	Smoky Hill Chalk member, Niobrara Chalk Fm.	(Everhart, 2002)
<i>Tethysaurus nopcsai</i>		26,8	MNHN GOU1	Early Turonian	Goulmima, Morocco	Unit 4 of limestone bar	(Bardet et al., 2003)
<i>Yaguarasaurus columbianus</i>		55	BRV-68	Turonian	Magdalena River, Colombia	Villeta Fm.	(Taylor and Fonseca, 2009)

Supplementary Information S1- Table of contents depicting total body size, skull, femur and humerus lengths, associated geologic unit, age interval, geographic localities, and identification of the material.

REFERENCES

- Bardet, N., Suberbiola, X.P., Iarochene, M., Bouya, B., Amaghzaz, M., 2005. A new species of Halisaurus from the Late Cretaceous phosphates of Morocco, and the phylogenetical relationships of the Halisaurinae (Squamata: Mosasauridae). Zool. J. Linn. Soc. 143, 447–472. <https://doi.org/10.1111/j.1096-3642.2005.00152.x>
- Bardet, N., Suberbiola, X.P., Jalil, N.E., 2003. Un nouveau plésiosaure polycotylidé du Crétacé supérieur (Turonien) du Maroc. Comptes Rendus - Palevol 2, 307–315. [https://doi.org/10.1016/S1631-0683\(03\)00063-0](https://doi.org/10.1016/S1631-0683(03)00063-0)
- Camp, C. L. 1942. California mosasaurs. Memoirs of the University of California 13:1–68.
- Christiansen, P., Bonde, N., 2002. A new species of gigantic mosasaur from the Late Cretaceous of Israel. J. Vertebr. Paleontol. 22, 629–644. [https://doi.org/10.1671/0272-4634\(2002\)022\[0629:ANSOGM\]2.0.CO;2](https://doi.org/10.1671/0272-4634(2002)022[0629:ANSOGM]2.0.CO;2)
- Dutchak, A.R., Caldwell, M.W., 2006. Redescription of *Aigialosaurus dalmaticus* Kramberger, 1892, a Cenomanian mosasauroid lizard from Hvar Island, Croatia. Can. J. Earth Sci. 43, 1821–1834. <https://doi.org/10.1139/e06-086>
- Everhart, M.J., 2015. Elias Putnam West (1820–1892) - Lawyer, Attorney General, Militia Commander, Judge, Postmaster, Archaeologist, and Paleontologist. Trans. Kansas Acad. Sci. 118, 285–294. <https://doi.org/10.1660/062.118.0310>
- Everhart, M.J., 2005. *Tylosaurus kansensis*, a new species of tylosaurine (Squamata, Mosasauridae) from the Niobrara Chalk of western Kansas, USA. Geol. en Mijnbouw/Netherlands J. Geosci. 84, 231–240. <https://doi.org/10.1017/S0016774600021016>
- Everhart, M.J., 2002. New Data on Cranial Measurements and Body Length of the Mosasaur, *Tylosaurus nepaeolicus* (Squamata; Mosasauridae), from the Niobrara Formation of Western Kansas. Trans. Kansas Acad. Sci. 105, 33–43. <https://doi.org/10.1660/0022->

8443(2002)105[0033:NDOCMA]2.0.CO;2

Ikejiri, T., Lucas, S.G., 2014. Osteology and taxonomy of *Mosasaurus conodon* Cope 1881 from the Late Cretaceous of North America. *Geol. en Mijnbouw/Netherlands J. Geosci.* 94, 39–54. <https://doi.org/10.1017/njg.2014.28>

Jimenez-Huidobro, P., Caldwell, M.W., 2016. Reassessment and reassignment of the Early Maastrichtian mosasaur *Hainosaurus bernardi* Dollo, 1885, to *Tylosaurus Marsh*, 1872. *J. Vertebr. Paleontol.* 36. <https://doi.org/10.1080/02724634.2016.1096275>

Konishi, T., Brinkman, D., Massare, J.A., Caldwell, M.W., 2011. New exceptional specimens of *Prognathodon overtoni* (Squamata, Mosasauridae) from the Upper Campanian of Alberta, Canada, and the systematics and ecology of the genus. *J. Vertebr. Paleontol.* 31, 1026–1046. <https://doi.org/10.1080/02724634.2011.601714>

Konishi, T., Caldwell, M.W., 2016. Two New Plioplatecarpine (Squamata, Mosasauridae) Genera from the Upper Cretaceous of North America and a global phylogenetic analysis of Plioplatecarpines. *Journal of Vertebrate Paleontology* 31, 754–783.

Konishi, T., Caldwell, M.W., 2009. New Material of the Mosasaur *Plioplatecarpus nichollsae* Cuthbertson et al., 2007, Clarifies Problematic Features of the Holotype Specimen. *J. Vertebr. Paleontol.* 29, 417–436.

Konishi, T., Caldwell, M.W., 2007. New Specimens of *Platecarpus planifrons* (Cope, 1874) (Squamata: Mosasauridae) and a Revised Taxonomy of the Genus. *J. Vertebr. Paleontol.* 27, 59–72. [https://doi.org/10.1671/0272-4634\(2007\)27\[59:NSOPPC\]2.0.CO;2](https://doi.org/10.1671/0272-4634(2007)27[59:NSOPPC]2.0.CO;2)

Konishi, T., Lindgren, J., Caldwell, M.W., Chiappe, L., 2012. *Platecarpus tympaniticus* (Squamata, Mosasauridae): Osteology of an exceptionally preserved specimen and its insights into the acquisition of a streamlined body shape in mosasaurs. *J. Vertebr. Paleontol.* 32, 1313–1327. <https://doi.org/10.1080/02724634.2012.699811>

Konishi, T., Newbrey, M.G., Caldwell, M.W., 2014. A small, exquisitely preserved specimen of *Mosasaurus missouriensis* (Squamata, Mosasauridae) from the Upper Campanian of the Bearpaw Formation, western Canada, and the first stomach contents for the genus. *J. Vertebr. Paleontol.* 34, 802–819. <https://doi.org/10.1080/02724634.2014.838573>

Leblanc, A.R.H., Caldwell, M.W., Bardet, N., 2012. A new mosasaurine from the Maastrichtian (Upper Cretaceous) phosphates of Morocco and its implications for mosasaurine systematics. *J. Vertebr. Paleontol.* 32, 82–104. <https://doi.org/10.1080/02724634.2012.624145>

Lindgren, J., Caldwell, M.W., Jagt, J.W.M., 2008. New data on the postcranial anatomy of the California mosasaur *Plotosaurus bennisoni* (Camp, 1942) (Upper Cretaceous: Maastrichtian), and the taxonomic status of *P. tuckeri* (Camp, 1942). *J. Vertebr. Paleontol.* 28, 1043–1054. <https://doi.org/10.1671/0272-4634-28.4.1043>

- Lindgren, J., Everhart, M.J., Caldwell, M.W., 2011. Three-dimensionally preserved integument reveals hydrodynamic adaptations in the extinct marine lizard ectenosaurus (Reptilia, Mosasauridae). PLoS One 6. <https://doi.org/10.1371/journal.pone.0027343>
- Lingham-Soliar, T., 1995. Anatomy and functional morphology of the largest marine reptile known, *Mosasaurus hoffmanni* (Mosasauridae, Reptilia) from the Upper Cretaceous, Upper Maastrichtian of the Netherlands. Philos. Trans. R. Soc. B Biol. Sci. 347, 155–172. <https://doi.org/10.1098/rstb.1995.0019>
- Lingham-Soliar, T., Nolf, D., 1989. The mosasaur *Prognathodon* from the Upper Cretaceous of Belgium (Reptilia, Mosasauridae). Bull. l'Institut R. des Sci. Nat. Belgique 59, 137–190.
- Martin, J.E., 2007. A new species of the durophagous mosasaur *Globidens* (Squamata: Mosasauridae) from the Late Cretaceous Pierre Shale Group of central South Dakota, USA. Geol. Soc. Am. Spec. Pap. 427, 177–198. [https://doi.org/10.1130/2007.2427\(13\)](https://doi.org/10.1130/2007.2427(13)).
- Merriam, J.C. 1894. Ueber die Pythonomorphen der Kansas-Kreide. Palaeontographica 41: 1–39.
- Nicholls, E.L., Meckert, D., 2002. Marine reptiles from the Nanaimo Group (Upper Cretaceous) of Vancouver Island. Can. J. Earth Sci. 39, 1591–1603. <https://doi.org/10.1139/e02-075>
- Palci, A., Caldwell, M.W., Papazzoni, C.A., 2013. A new genus and subfamily of mosasaurs from the Upper Cretaceous of northern Italy. J. Vertebr. Paleontol. 33, 599–612. <https://doi.org/10.1080/02724634.2013.731024>
- Páramo Fonseca, M.E., 2014. *Eonatator coellensis* nov. sp. (Squamata: Mosasauridae), nueva especie del Cretacico Superior de Colombia. Rev. la Acad. Colomb. Ciencias 37, 499–518.
- Polcyni, M.J., Tchernov, E., Jacobsi, L.L., 1999. Of the Eastern Mediterranean with a description of a new basal Mosasauroid from in the eastern Mediterranean fauna. Proceedings of the Second Gondwanan Dinosaur symposium. 259–290.
- Russell, D. A. 1975. A new species of *Globidens* from South Dakota, and a review of globidentine mosasaurs. Fieldiana 33:235–256.
- Taylor, M. A. in Ancient Marine Reptiles (eds Callaway, J. M. & Nicholls, E. L.) xix–xlvi (Academic, San Diego, 1997).
- Taylor, P., Fonseca, M.E.P., 2009. Historical Biology : An International Journal of Mosasauridae, a primitive mosasaur from the Turonian (Upper Cretaceous) of Colombia *Yaguarasaurus columbianus* (Reptilia , Mosasauridae), a Primitive Mosasaur from the Turonian (Upper Cretaceous) of 37–41.

Williston, S.W., 1898. Upper Cretaceous of Kansas. Geol. Surv. Kansas 4, 3-587.

Supplementary Information S1- Nothosauria

Taxa	Total (cm)	Skull (cm)	Femur (cm)	Humerus (cm)	Material	Time interval	Localization	Geologic Unit	Reference
<i>Cymatosaurus fridericianus</i>	23,8					Lower Anisian	Saale, Germany	Lower Muschelkalk	(Rieppel, 1997)
<i>Cymatosaurus latifrons</i>	10,8				SMNS 10109	Lower Anisian	Silesia, Poland	Lower Muschelkalk	(Rieppel, 1997)
<i>Cymatosaurus latissimus</i>	27					Lower Anisian	Silesia, Poland	Lower Muschelkalk	(Rieppel, 1997)
<i>Germanosaurus schaefferi</i>	29,16				NHMW	Lower Anisian	Silesia, Poland	Lower Muschelkalk	(Rieppel, 1997)
<i>Lariosaurus balsami</i>			7,22		holotype	Upper Landinian	Perledo, Italy	Peledo-Varenna Fm.	(Rieppel, 1997)
	10,71		6,36		BSP ASI 802	Upper Landinian			(Rieppel, 1997)
<i>Lariosaurus buzzii</i>	9,16					Anisian-Landinian	Monte San Giorgio, Switzerland		(Storrs, 1993)
<i>Lariosaurus caicagnil</i>	14,9		8,47		MBS	Lower Landinian	Monte San Giorgio, Switzerland		(Rieppel, 1997)
<i>Lariosaurus curionii</i>	6,41		3,8		PVHR 1	Landinian	Pyrenees, France		(Rieppel, 1997)
<i>Lariosaurus hongguoensis</i>	10	4,2	3,11		GMPKU-P-1011	Anisian	Guizhou, China	Guanling Fm.	(Jiang et al., 2006)
<i>Lariosaurus valceresii</i>	13,33	5,95	6,43		P 500	Upper Landinian	Varese, Italy		(Rieppel, 1997)
<i>Lariosaurus xingylensis</i>	15,42				IVPP V 11866	Landinian	Guizhou Province, China	Zhuganpo Member , Falang Fm.	(Rieppel et al., 2003)
<i>Nothosaurus edingerae</i>	12,9				SMNS 59072	Late Triassic	Obersulm, Germany	Gipskeuper Fm.	(Jinling and Rieppel, 2004)
<i>Nothosaurus giganteus</i>	62,5				SMNS 18475	Landinian	Tiefenbach, Germany	Upper Muschelkalk	(Rieppel and Wild, 1996)

	51	SMNS 7162	Anisian	Hoheneck, Germany	Keuperdolomit	(Rieppel & Wild, 1996)
	60,8	SMF R-475	Anisian-Ladinian	Bayreuth, Germany	Upper Muschelkalk	(Rieppel & Wild, 1996)
	80	SMNS 18475	Anisian-Ladinian	Monte San Giorgio, Switzerland	Upper Muschelkalk	(Rieppel & Wild, 1996)
	30	SMNS 1797	Anisian-Ladinian	Schmalfelden, Germany	Upper Muschelkalk	(Rieppel & Wild, 1996)
	23	SIPB R 49	Anisian	Bavaria, Germany	Upper Muschelkalk	(Krahel et al., 2013)
<i>Nothosaurus haasi</i>	12,35	HUJ-Pal 2250	Upper Anisian- Lower Ladinian	Negev, Israel	Saharonim Fm.	(Rieppel, 1997)
	9,68	HUJ-Pal. 2049	Upper Anisian- Lower Ladinian	Negev, Israel	Saharonim Fm.	(Rieppel et al., 1999)
	75,5	HUJ-Pal. 2060	Upper Anisian- Lower Ladinian	Negev, Israel	Saharonim Fm.	(Rieppel et al., 1999)
	6,38	HUJ-Pal. 2174	Upper Anisian- Lower Ladinian	Negev, Israel	Saharonim Fm.	(Rieppel et al., 1999)
	5,98	HUJ-Pal. 3813	Upper Anisian- Lower Ladinian	Negev, Israel	Saharonim Fm.	(Rieppel et al., 1999)
	5,95	HUJ-Pal. 3798	Upper Anisian- Lower Ladinian	Negev, Israel	Saharonim Fm.	(Rieppel et al., 1999)
	5,73	HUJ-Pal. 2173	Upper Anisian- Lower Ladinian	Negev, Israel	Saharonim Fm.	(Rieppel et al., 1999)
	5,35	HUJ-Pal. 2045	Upper Anisian- Lower Ladinian	Negev, Israel	Saharonim Fm.	(Rieppel et al., 1999)
<i>Nothosaurus juvenilis</i>	12,6		Anisian	western Europe	Lower upper Muschelkalk	(Rieppel & Wild, 1996)
<i>Nothosaurus marchicus</i>	12,67	N MNHL-St4 45530	Lower Anisian	Winterswijk, Netherlands	Lower Wellenkalk layer 9	(Albers and Rieppel, 2003)
	10,14	TW480000375	Lower Anisian	Winterswijk, Netherlands	Lower Wellenkalk layer 9	(Albers, 2011)
	10,7	TW480000376	Lower Anisian	Winterswijk,	Lower Wellenkalk	(Albers, 2011)

					Netherlands	layer 9	
	10,7	NMNHL St 36375	Lower Anisian	Winterswijk, Netherlands	Lower Wellenkalk layer 10	(Albers, 2011)	
	16,5	Er 2302	Anisian-Landinian	Bad Sulza, Germany	Upper Muschelkalk, Bad Sulza Fm.	(Rieppel & Wild, 1996)	
	16	SMRF R-4572	Anisian-Landinian	Bayreuth, Germany	Upper Muschelkalk	(Rieppel & Wild, 1996)	
<i>Nothosaurus mirabilis</i>	20	SIPB R 54/2	Anisian	Winterswijk, Netherlands	Winterswijk Fm.	(Krahel et al., 2013)	
	16,5	SIPB R 54/1	Anisian	Winterswijk, Netherlands	Winterswijk Fm.	(Krahel et al., 2013)	
	14,66		Anisian-Landinian	Bayreuth, Germany	Upper Muschelkalk	(Krahel et al., 2013)	
	39,3		Landinian	Oberdorla, Germany	Muschelkalk	(Rieppel & Wild, 1996)	
	41,33	SMNS 16433	Landinian	Crailsheim, Germany	Upper Muschelkalk	(Rieppel & Wild, 1996)	
	22,8	MB I. 007/16	Landinian	Oberdorla, Germany	Muschelkalk	(Rieppel & Wild, 1996)	
	31,94	BMNH R-42829	Anisian-Landinian	Bayreuth, Germany	Upper Muschelkalk	(Rieppel & Wild, 1996)	
<i>Nothosaurus oldenburgi</i>	20,46	MB R.1	Anisian	Rudersdorf, Germany	Lower/Middle Muschelkalk	(Rieppel & Wild, 1996)	
<i>Nothosaurus procerus</i>	14,66	MB R.4	Anisian	Rudersdorf, Germany	Lower/Middle Muschelkalk	(Rieppel & Wild, 1996)	
	14	MB R.5	Anisian	Rudersdorf, Germany	Lower/Middle Muschelkalk	(Rieppel & Wild, 1996)	
<i>Nothosaurus raabi</i>	12,14	7,45	6,4	MB I. 007.18	Anisian	Rudersdorf, Germany	Lower/Middle Muschelkalk (Rieppel & Wild, 1996)
<i>Nothosaurus rostellatus</i>	21	9		IVPP V 14294	Anisian	Guizhou, China	Guanling Fm. (Shang, 2006)
	32			IVPP V 14301	Anisian	Guizhou, China	Guanling Fm. (Shang, 2006)

<i>Nothosaurus tchernovi</i>	31		HUJ-Pal. 3665	Upper Anisian-Lower Ladinian	Negev, Israel	Saharonim Fm.	(Rieppel <i>et al.</i> , 1999)		
	25,2		HUJ-Pal. 2055	Upper Anisian-Lower Ladinian	Negev, Israel	Saharonim Fm.	(Rieppel <i>et al.</i> , 1999)		
	24,5		HUJ-Pal. 3862	Upper Anisian-Lower Ladinian	Negev, Israel	Saharonim Fm.	(Rieppel <i>et al.</i> , 1999)		
<i>Nothosaurus zhangi</i>	65		LPV 20167	Anisian	Yunnan Province, China	Guanling Fm.	(Liu <i>et al.</i> , 2014)		
<i>Nothosaurus winkeihorsti</i>	4,65		NMNHL RGM 443825	Early Anisian	Winterswijk, The Netherlands	Vossenveld Fm., Lower Muschelkalk	(Klein and Albers, 2009)		
<i>Nothosaurus yangjuanensis</i>	34,8		GMPKU-P-1080	Middle Anisian	Guizhou, China	Guanling Fm.	(Jiang <i>et al.</i> , 2006)		
<i>Nothosaurus youngi</i>	16		IVPP V 13590	Landinian	Xingyi , Guizhou, China	Zhuganpo Member , Falang Fm.	(Ji <i>et al.</i> , 2014)		
	127	16,9	11,99	11,08	WS-30-R24	Landinian	Guizhou Province, China	Zhuganpo Member , Falang Fm.	(Ji <i>et al.</i> , 2014)
<i>Sanchiaosaurus dengi</i>	20,3	14,1	11,2	IVPP V3228	Anisian	Guizou, China		(Rieppel, 1999)	
<i>Simosaurus guilielmi</i>	25		SMNS 167000	Upper Landinian	Lettenkeuper, Germany	Upper Muschelkalk	(Rieppel, 1994)		
	19,16			Upper Landinian	Lower Gipskeuper of Obersontheim		(Rieppel, 1994)		
	20,65		10360	Upper Landinian			(Rieppel, 1994)		

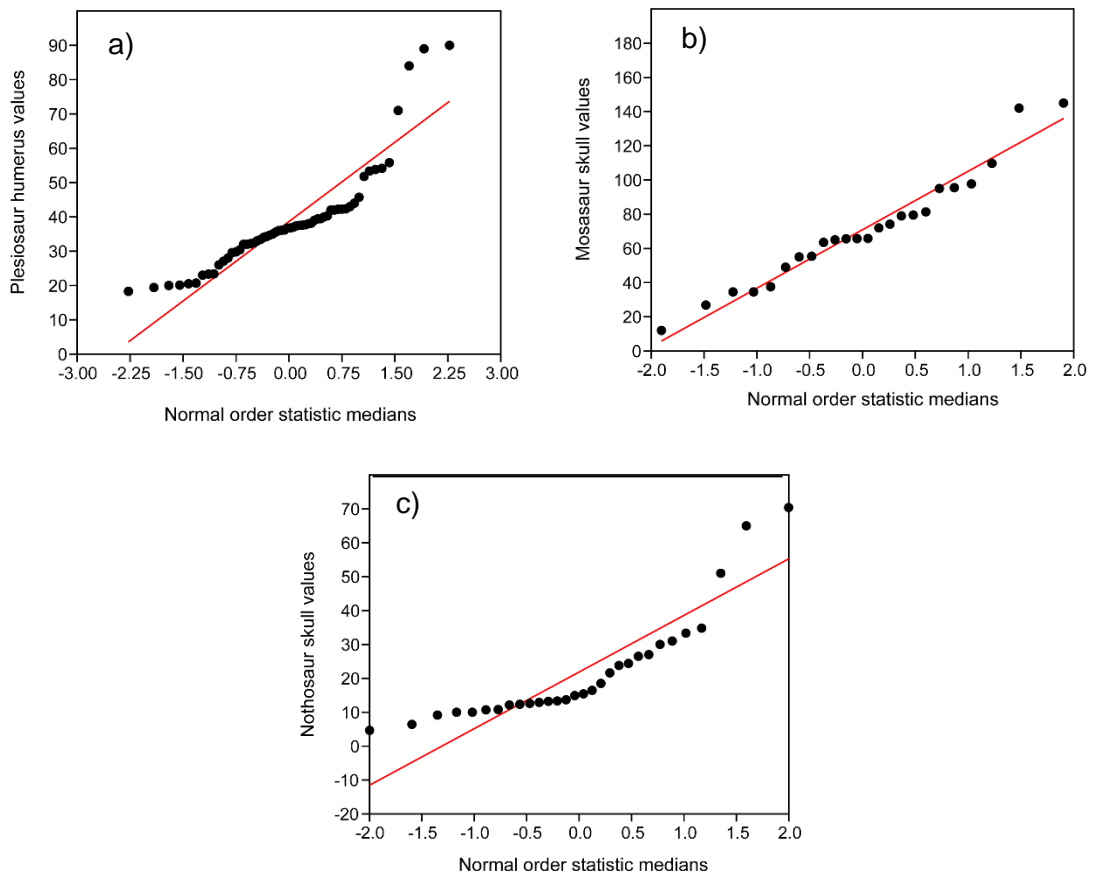
Supplementary Information S1- Table of contents depicting total body size, skull, femur and humerus lengths, associated geologic unit, age interval, geographic localities, and identification of the material.

REFERENCES

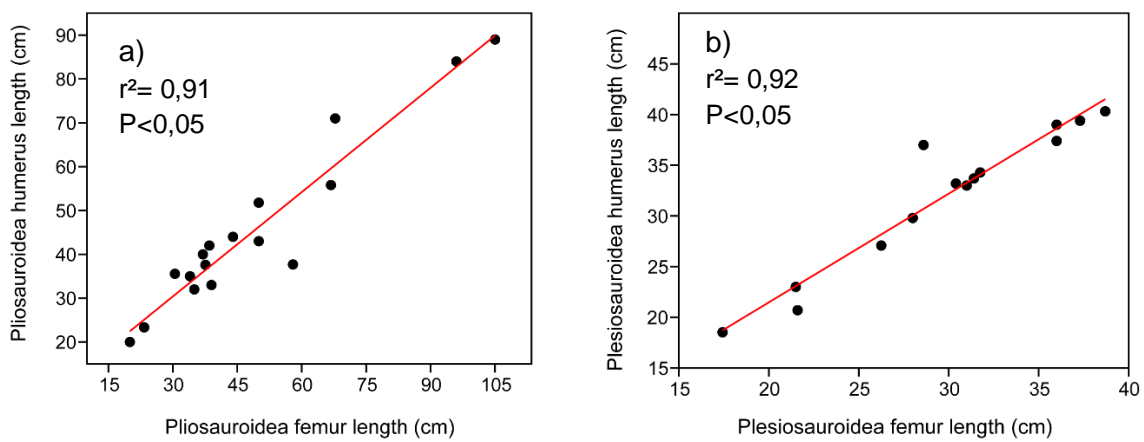
- Albers, P.C.H., 2011. New Nothosaurus skulls from the Lower Muschelkalk of the Western Lower Saxony Basin (Winterswijk, the Netherlands) shed new light on the status of *Nothosaurus winterswijkensis*. *Geol. en Mijnbouw/Netherlands J. Geosci.* 90, 15–21. <https://doi.org/10.1017/S0016774600000639>
- Albers, P.C.H., Rieppel, O., 2003. a New Species of the Sauropterygian Genus Nothosaurus From the Lower Muschelkalk of Winterswijk, the Netherlands. *J. Paleontol.* 77, 738–744. [https://doi.org/10.1666/0022-3360\(2003\)077<0738:ANSOTS>2.0.CO;2](https://doi.org/10.1666/0022-3360(2003)077<0738:ANSOTS>2.0.CO;2)
- Ji, C., Jiang, D.Y., Rieppel, O., Motani, R., Tintori, A., Sun, Z.Y., 2014. A new specimen of *Nothosaurus youngi* from the Middle Triassic of Guizhou, China. *J. Vertebr. Paleontol.* 34, 465–470. <https://doi.org/10.1080/02724634.2013.808204>
- Jiang, D.-Y., Maisch, M.W., Sun, Z.-Y., Sun, Y., Hao, W., 2006. A new species of Lariosaurus (Reptilia, Sauropterygia) from the Middle Anisian (Middle Triassic) of Southwestern China. *Neues Jahrb. für Geol. und Paläontologie Abhandlungen* 242, 19–42. <https://doi.org/10.1142/9789812774484>
- Jinling, L., Rieppel, O., 2004. A new Nothosaur from middle Triassic of Guizou, China. *Vertebr. Pal Asiat.* 42, 1–42.
- Klein, N., Albers, P.C.H., 2009. A New Species of the Sauropsid Reptile *Nothosaurus* from the Lower Muschelkalk of the Western Germanic Basin, Winterswijk, the Netherlands. *Acta Palaeontol. Pol.* 54, 589–598. <https://doi.org/10.4202/app.2008.0083>
- Krahl, A., Klein, N., Sander, P.M., 2013. Evolutionary implications of the divergent long bone histologies of Nothosaurus and Pistosaurus (Sauropterygia, Triassic). *BMC Evol. Biol.* 13. <https://doi.org/10.1186/1471-2148-13-123>
- Liu, J., Hu, S.X., Rieppel, O., Jiang, D.Y., Benton, M.J., Kelley, N.P., Aitchison, J.C., Zhou, C.Y., Wen, W., Huang, J.Y., Xie, T., Lv, T., 2014. A gigantic nothosaur (Reptilia: Sauropterygia) from the Middle Triassic of SW China and its implication for the Triassic biotic recovery. *Sci. Rep.* 4, 1–9. <https://doi.org/10.1038/srep07142>
- Rieppel, O., 1999. The sauropterygian genera Chinchenia, Kwangsisaurus, and Sanchiaosaurus from the Lower and Middle Triassic of China. *J. Vertebr. Paleontol.* 19, 321–337. <https://doi.org/10.1080/02724634.1999.10011144>
- Rieppel, O., Mazin, J.-M., Tchernov, E., 1999. Sauropterygia from the Middle Triassic of Makhtesh Ramon, Negev, Israel. *Fieldiana Geol.* 40, 1–85.

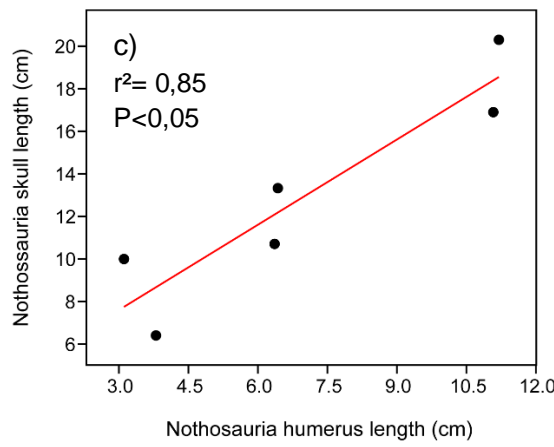
- Rieppel, O., Wild, R., 1996. A Revision of the Genus *Nothosaurus* (Reptilia: Sauropterygia) from the Germanic Triassic, with Comments on the Status of *Conchiosaurus clavatus*. *Fieldiana Geol.* 2–98.
- Rieppel, O.C., 1997. Revision of the Sauropterygian Reptiles genus *Cymatosaurus* v. Fritsch, 1894, and the relationships of the *Germanosaurus Nopcsa*, 1928, from the Middle Triassic of Europe. *Fieldiana Geol.* 36, 1–38.
- Rieppel, O.C., 1994. Osteology of *Simosaurus gaillardotii* and the Relationships of Stem-Group Sauropterygia. *Fieldiana Geol.* 28, 1–85. <https://doi.org/10.1017/CBO9781107415324.004>
- Rieppel, O.C., Jinling, L., Jun, L., 2003. *Lariosaurus xingyiensis* (Reptilia: Sauropterygia) from the Triassic of China. *Can. J. Earth Sci.* 40, 621–634. <https://doi.org/10.1139/e02-067>
- Shang, Q.H., 2006. A new species of *Nothosaurus* from the early middle Triassic of Guizhou, China. *Vertebr. Pal Asiat.* 1–249.
- Storrs, G.W., 1993. The systematic position of *Silvestrosaurus* and a classification of Triassic sauropterygians (Neodiapsida). *Palaeontologische Zeitschrift*, 67(1-2), pp.177—191.

Informação Suplementar S2

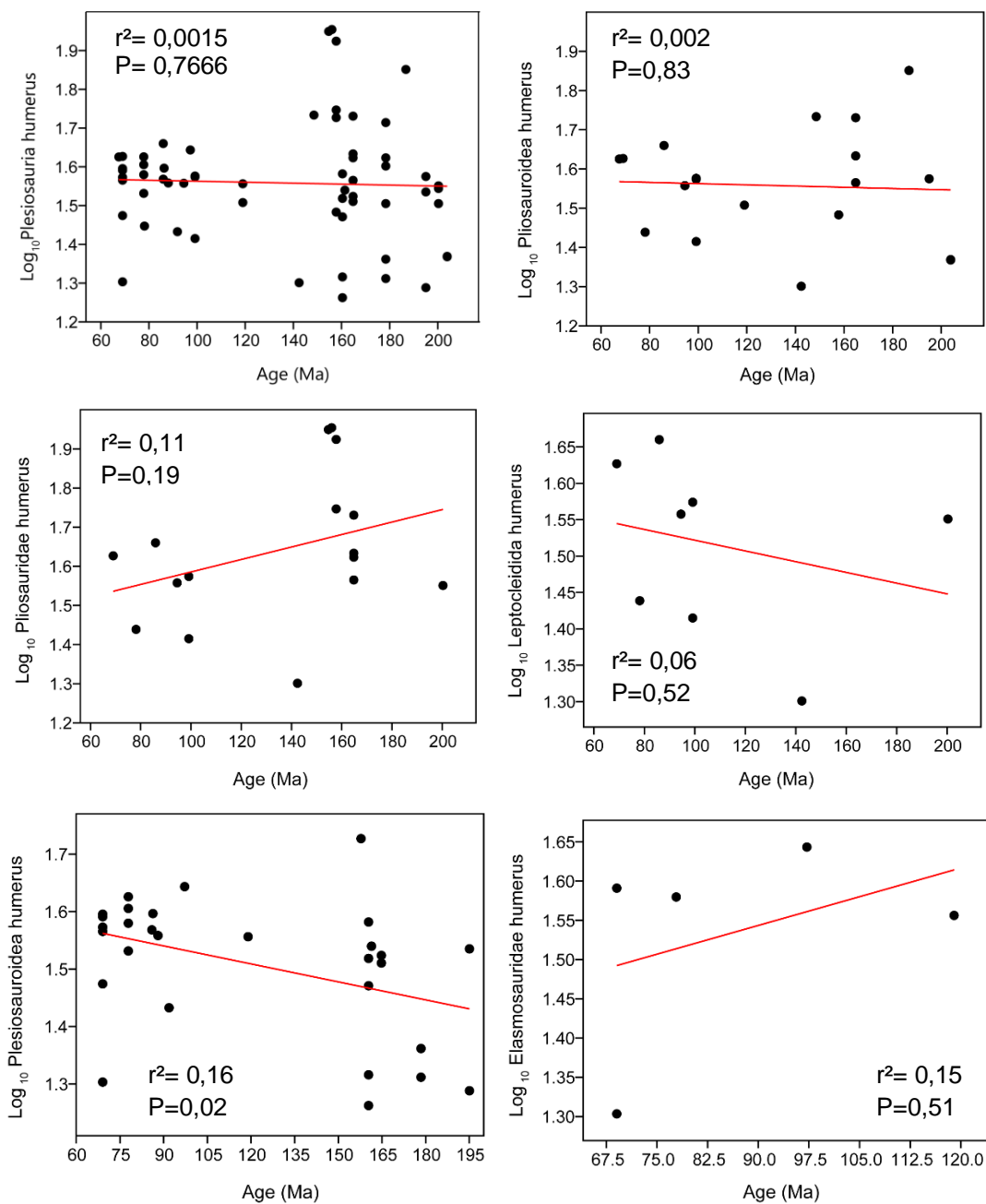


A-Normal probability plot (Shapiro-Wilk test) of: a) Plesiosaur humerus values, b) Mosasaur skull values, c) Nothosaurus skull values.

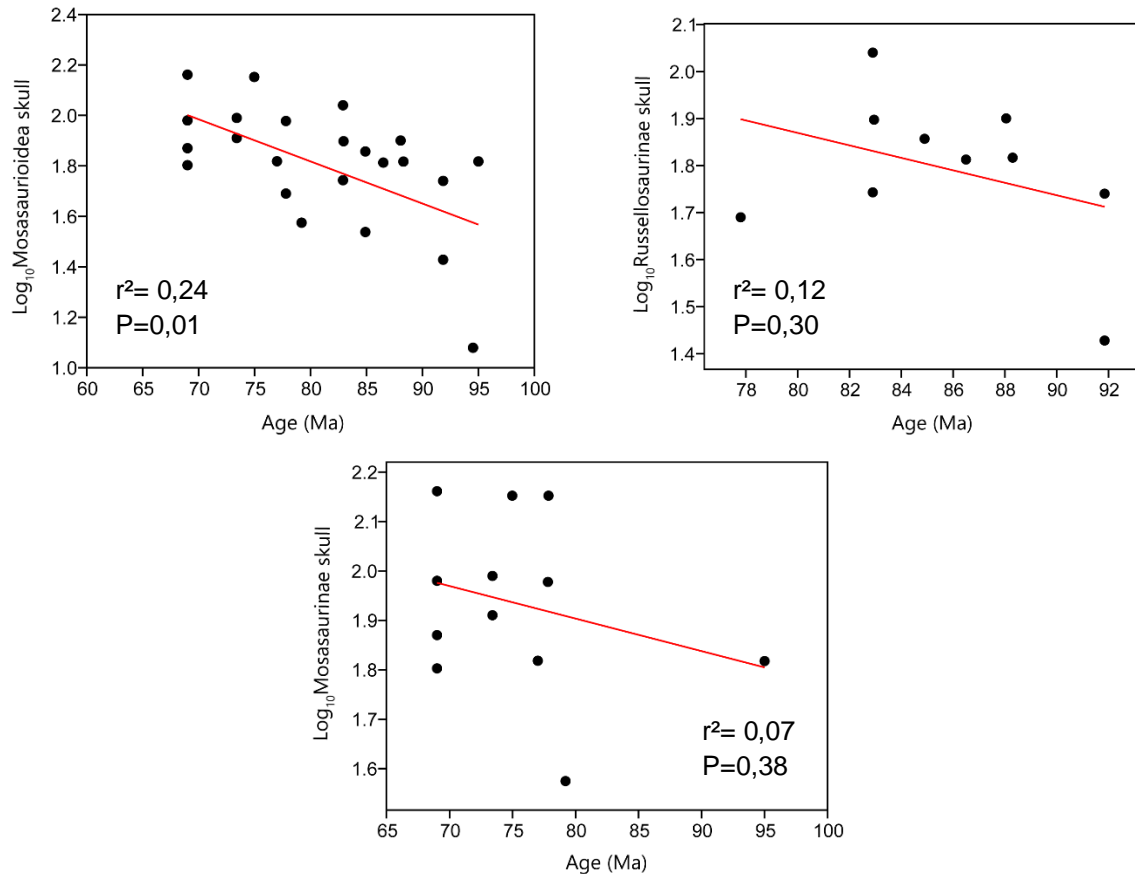




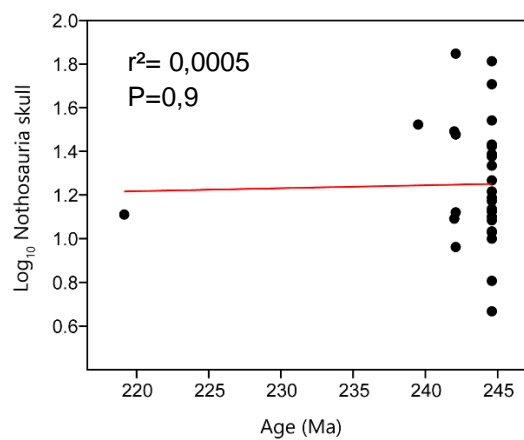
B- a) Linear regression of humeral length (y-axis, in centimeters) against femoral length (x-axis, in centimeters) for Pliosauroidea (regression line is $y = 0,7936x + 6,576$), b) Linear regression of humeral length (y-axis, in centimeters) against femoral length (x-axis, in centimeters) for Plesiosauroida ($y = 1,0723x + 0,0282$), c) Linear regression of skull length (y-axis, in centimeters) against humerus length (x-axis, in centimeters) for Nothosaura ($y = 1,3347x + 3,6032$). Each pair of humerus and femur; skull and femur values refers to the same specimens being that in some species the average of the sizes was used (see Table 1 Supplementary material).



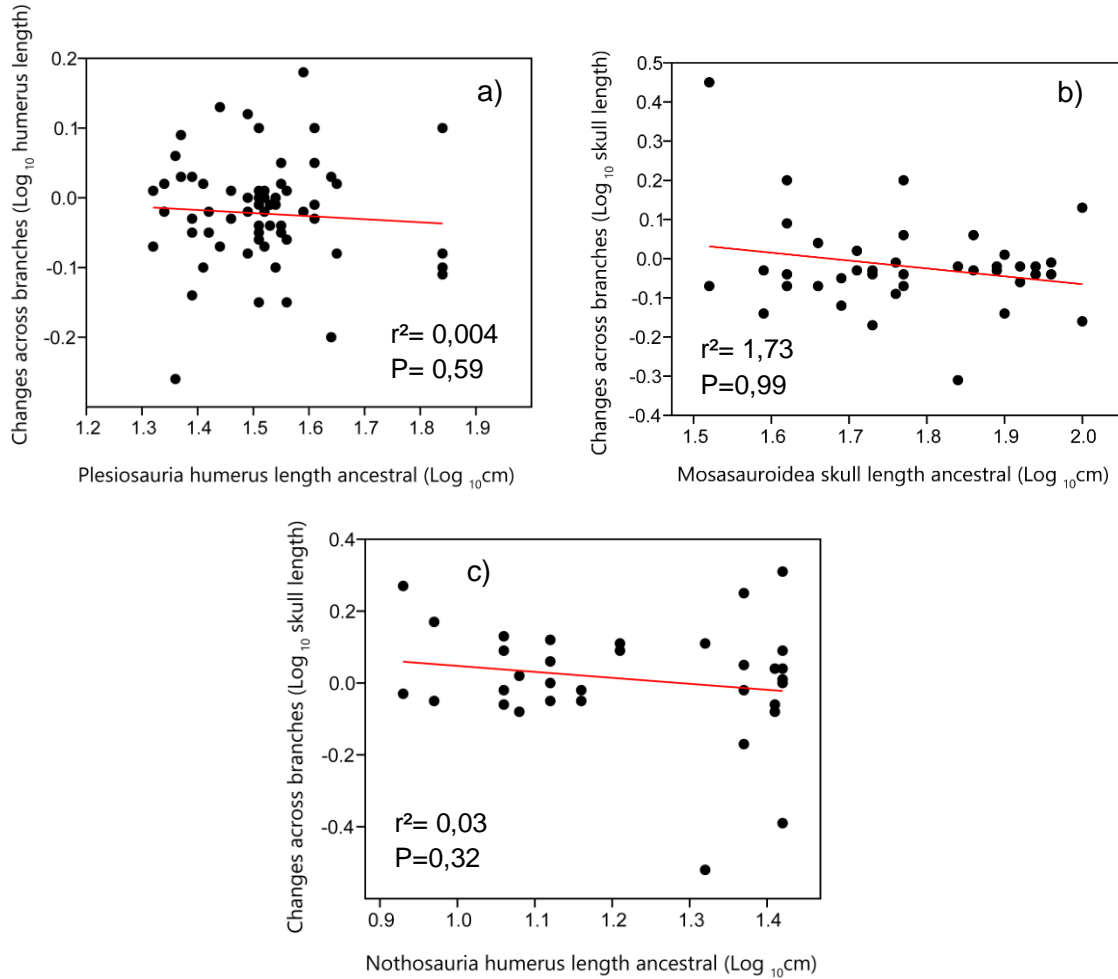
C- Scatter plot comparing log₁₀ humerus length (y-axis, proxy for body mass) against age (x-axis, Ma) for some plesiosaurs subclades. The age assigned to each taxon was calculated as the mid-point of its total stratigraphic range.



D- Scatter plot comparing log10 skull length (y-axis, proxy for body mass) against age (x-axis, Ma) for some mosasaurs subclades. The age assigned to each taxon was calculated as the mid-point of its total stratigraphic range.



E- Scatter plot comparing log10 skull length (y-axis, proxy for body mass) against age (x-axis, Ma) for Nothosaur. The age assigned to each taxon was calculated as the mid-point of its total stratigraphic range.

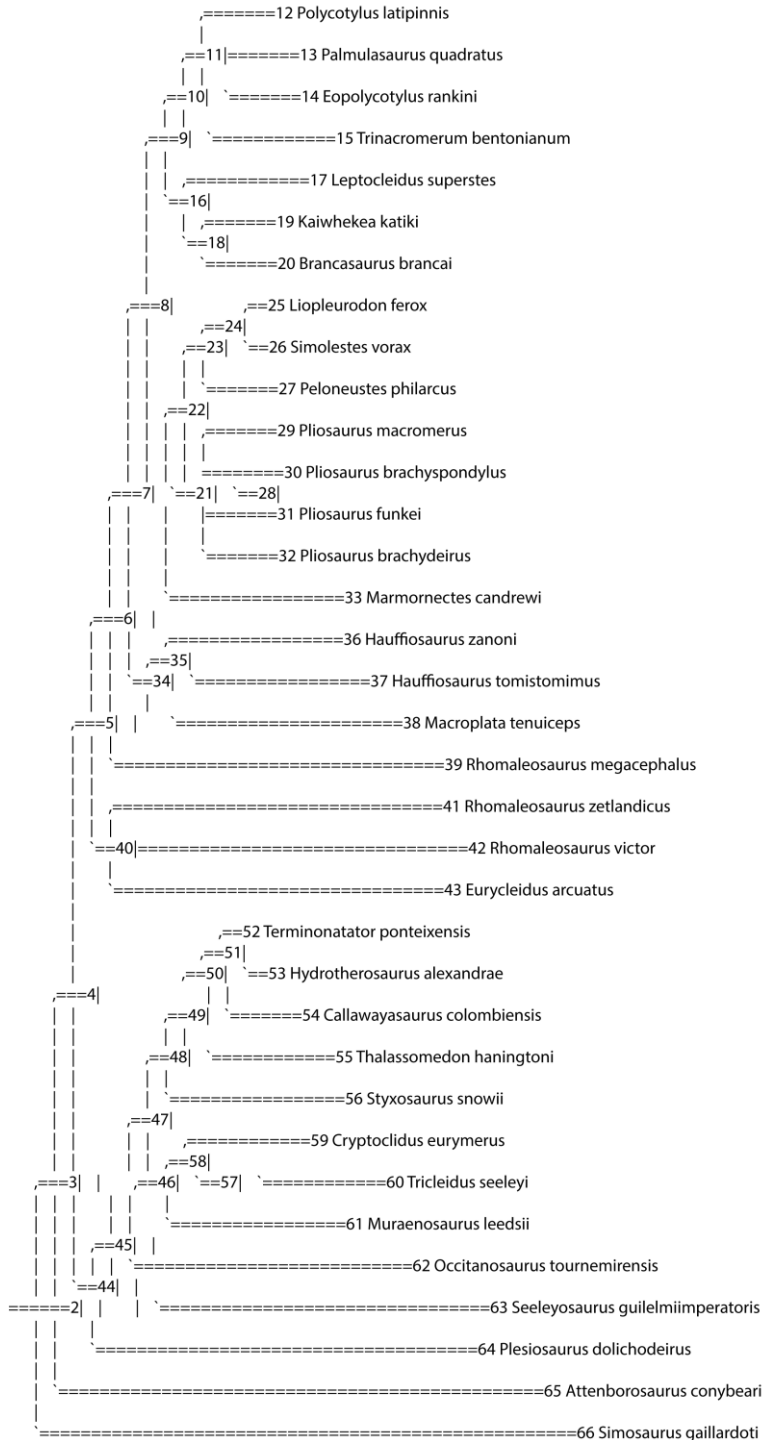


F- Changes between ancestor and descendants. Scatter plot comparing ancestral size at nodes in the supertree (log10 size length, y-axis) against calculated changes through the branches (log10 size length, x-axis) for: a) Plesiosauria, b) Mosasauroidea, c) Nothosauaria.

Informação Suplementar S3- Plesiosauroidea

Tree Description: (((((((((Polycotylus_latipinnis:28,Palmulasaurus_quadratus:11,Eopolycotylus_rankini:11):3,Trinacromerum_bentonianum:14):46,(Leptocleidus_superstes:22,Kaiwhekea_katiki:77,Brancasaurus_brancai:5):3):3):30,(((Liopleurodon_ferox,Simolestes_vorax),Peloneutes_philarcus:3),(Pliosaurus_macromerus:12,Pliosaurus_brachyspondylus:12,Pliosaurus_funkei:9,Pliosaurus_brachydeirus:12):12):3,Marmornectes_candrewi:1):3):25,((Hauffiosaurus_zanoni:9,Hauffiosaurus_tomistomimus:4.5):18,Macropelta_tenuiceps:3):6):3,Rhomaleosaurus_megacephalus:12):3,(Rhomaleosaurus_zetlandicus:28,Rhomaleosaurus_victor:28,Eurycleidus_arcuatus:3):12):3,((((Terminonator_ponteixensis:11,Hydrotherosaurus_alexandriae:18):41,Callawayasaurus_colombiensis:6):3,Thalassomedon_haningtoni:3):3,Styxosaurus_snowii:59):40,((Cryptoclidus_eurymerus:3,Tricleidus_seeleyi:8):3,Muraenosaurus_leedsii:1):3):5,Occitanosaurus_tournemirensis:5,Seeleyosaurus_guilelmiimperatoris:5):19,Plesiosaurus_dolichodeirus:19):20):3,Attenborosaurus_conybeari:30):14,Simosaurus_gaillardoti:5):3;

Tree with node numbers:



Supertree com os valores de cada táxon de Plesiosauria e os valores ancestrais de cada nó interno construída no programa Mesquite versão 3.40.

----- Trace Character History -----

Character 1: humerus

Parsimony reconstruction (Squared) [Squared length: 0.03444434]

node 2: 1.46218648

node 3: 1.49630861

node 4: 1.49625136

node 5: 1.51477559

node 6: 1.52178988

node 7: 1.52425164

node 8: 1.5909063

node 9: 1.41928913

node 10: 1.51856957

node 11: 1.51830929

node 12: 1.66

node 13: 1.41

node 14: 1.57

node 15: 1.55

node 16: 1.3956526

node 17: 1.44

node 18: 1.3659687

node 19: 1.62

node 20: 1.3

node 21: 1.61606657

node 22: 1.64031914

node 23: 1.61338652

node 24: 1.65779551

node 25: 1.73

node 26: 1.63

node 27: 1.56

node 28: 1.84505984

node 29: 1.92

node 30: 1.94

node 31: 1.95

node 32: 1.74

node 33: 1.62

node 34: 1.51317803

node 35: 1.55902543

node 36: 1.5

node 37: 1.6

node 38: 1.5

node 39: 1.54

node 40: 1.56081534

node 41: 1.71

node 42: 1.62

node 43: 1.55

node 44: 1.37237481

node 45: 1.3470669

node 46: 1.32747383

node 47: 1.39524991

node 48: 1.53968025

node 49: 1.54897084

node 50: 1.54945216

node 51: 1.55228661

node 52: 1.53

node 53: 1.59

node 54: 1.55

node 55: 1.64

node 56: 1.57

node 57: 1.42508329

node 58: 1.44266665

node 59: 1.51

node 60: 1.31

node 61: 1.47

node 62: 1.31

node 63: 1.36

node 64: 1.28
 node 65: 1.57
 node 66: 1.45

#NEXUS

[written Thu Jul 19 13:08:20 BRT 2018 by Mesquite version 3.40 (build 877) at DESKTOP-M9K2NNB/192.168.0.10]

BEGIN TAXA;

TITLE Untitled_Block_of_Taxa;

DIMENSIONS NTAX=35;

TAXLABELS

Polycotylus_latipinnis	Palmulasaurus_quadratus	Eopolycotylus_rankini
Trinacromerum_bentonianum	Leptocleidus_superstes	Kaiwhekea_katiki
Simolestes_vorax	Peloneustes_philarcus	Brancasaurus_brancai
Pliosaurus_brachydeirus	Pliosaurus_macromerus	Liopleurodon_ferox
Marmornectes_candrewi	Pliosaurus_brachyspondylus	Pliosaurus_funkei
Macroplata_tenuiceps	Hauffiosaurus_zanoni	Hauffiosaurus_tomistomimus
Rhomaleosaurus_megacephalus	Rhomaleosaurus_zetlandicus	Rhomaleosaurus_victor
Eurycleidus_arcuatus	Cryptoclidus_eurymerus	Callawayasaurus_colombiensis
Thalassomedon_haningtoni	Styxosaurus_snowii	Occitanosaurus_tournemirensis
Seeleyosaurus_guilemiimperatoris	Cryptocephalus_eurymerus	Attenborosaurus_dolichodeirus
Plesiosaurus_dolichodeirus	Tricleidus_seeleyi	Attenborosaurus_conybeari
Attenborosaurus_conybeari	Muraenosaurus_leedsii	Simosaurus_gaillardoti

;

END;

BEGIN CHARACTERS;

TITLE Character_Matrix;

DIMENSIONS NCHAR=1;

FORMAT DATATYPE = CONTINUOUS GAP = - MISSING = ?;

CHARSTATELABELS

1 humerus ;	
MATRIX	
Polycotylus_latipinnis	1.66
Palmulasaurus_quadratus	1.41
Eopolycotylus_rankini	1.57
Trinacromerum_bentonianum	1.55
Leptocleidus_superstes	1.44
Kaiwhekea_katiki	1.62
Brancasaurus_brancai	1.3
Liopleurodon_ferox	1.73
Simolestes_vorax	1.63
Peloneustes_philarcus	1.56
Pliosaurus_macromerus	1.92
Pliosaurus_brachyspondylus	1.94
Pliosaurus_funkei	1.95
Pliosaurus_brachydeirus	1.74
Marmornectes_candrewi	1.62
Hauffiosaurus_zanoni	1.5
Hauffiosaurus_tomistomimus	1.6
Macroplata_tenuiceps	1.5
Rhomaleosaurus_megacephalus	1.54
Rhomaleosaurus_zetlandicus	1.71
Rhomaleosaurus_victor	1.62
Eurycleidus_arcuatus	1.55
Terminonatator_ponteixensis	1.53
Hydrotherosaurus_alexandrae	1.59
Callawayasaurus_colombiensis	1.55
Thalassomedon_haningtoni	1.64
Styxosaurus_snowii	1.57
Cryptoclidus_eurymerus	1.51
Tricleidus_seeleyi	1.31
Muraenosaurus_leedsii	1.47
Occitanosaurus_tournemirensis	1.31
Seeleyosaurus_guilemiimperatoris	1.36
Plesiosaurus_dolichodeirus	1.28
Attenborosaurus_conybeari	1.57

```

Simosaurus_gaillardotii      1.45

;

END;
BEGIN TREES;
    Title 'Trees from "plesiosaur.tree"';
    ID 015f92395fc81;
    LINK Taxa = Untitled_Block_of_Taxa;
    TRANSLATE
[0]        1 Polycotylus_latipinnis,
[1]        2 Palmulasaurus_quadratus,
[2]        3 Eopolycotylus_rankini,
[3]        4 Trinacromerum_bentonianum,
[4]        5 Leptocleidus_superstes,
[5]        6 Kaiwhekea_katiki,
[6]        7 Brancasaurus_brancai,
[7]        8 Liopleurodon_ferox,
[8]        9 Simolestes_vorax,
[9]        10 Peloneustes_philarcus,
[10]       11 Pliosaurus_macromerus,
[11]       12 Pliosaurus_brachyspondylus,
[12]       13 Pliosaurus_funkei,
[13]       14 Pliosaurus_brachydeirus,
[14]       15 Marmorectes_candrewi,
[15]       16 Hauffiosaurus_zanoni,
[16]       17 Hauffiosaurus_tomistomimus,
[17]       18 Macroplata_tenuiceps,
[18]       19 Rhomaleosaurus_megacephalus,
[19]       20 Rhomaleosaurus_zetlandicus,
[20]       21 Rhomaleosaurus_victor,
[21]       22 Eurycleidus_arcuatus,
[22]       23 Terminonatator_ponteixensis,
[23]       24 Hydrotherosaurus_alexandrae,
[24]       25 Callawayasaurus_colombiensis,
[25]       26 Thalassomedon_haningtoni,
[26]       27 Styxosaurus_snowii,
[27]       28 Cryptoclidus_eurymerus,
[28]       29 Tricleidus_seeleyi,
[29]       30 Muraenosaurus_leedsii,
[30]       31 Occitanosaurus_tournemirensis,
[31]       32 Seeleyosaurus_guilelmiimperatoris,
[32]       33 Plesiosaurus_dolichodeirus,
[33]       34 Attenborosaurus_conybeari,
[34]       35 Simosaurus_gaillardotii;

    TREE 'PAUP_1'=
((((((1,2,3),4),(5,(6,7))),(((8,9),10),(11,12,13,14)),15),((16,17),18)),19),(20,21,22),((((((23,24),25),26),27),((28,29),30)),31),32),33),34),35);

END;

BEGIN ASSUMPTIONS;
    TYPESET * UNTITLED = Squared: 1;
END;

BEGIN MESQUITECHARMODELS;
    ProbModelSet * UNTITLED = Brownian_default: 1;
END;

Begin MESQUITE;
    MESQUITESCRIPTVERSION 2;
    TITLE AUTO;
    tell ProjectCoordinator;
    timeSaved 1532016500573;
    getEmployee #mesquite.minimal.ManageTaxa.ManageTaxa;

```

```

tell It;
    setID 0 4935789195780038782;
endTell;
getEmployee #mesquite.charMatrices.ManageCharacters.ManageCharacters;
tell It;
    setID 0 9175578767526856009;
    mqVersion 340;
    checksumv 0 3 1142165859 null numChars 1 numItems 1 min 1.28 max 1.95
sumSquares 86.72420000000001 NumFiles 1 NumMatrices 1;
    mqVersion;
endTell;
getWindow;
tell It;
    suppress;
    setResourcesState false false 108;
    setPopoutState 300;
    setExplanationSize 0;
    setAnnotationSize 0;
    setFontIncAnnot 0;
    setFontIncExp 0;
    setSize 1366 649;
    setLocation -8 -8;
    setFont SanSerif;
    setFontSize 10;
    getToolPalette;
tell It;
endTell;
desuppress;
endTell;
getEmployee #mesquite.trees.BasicTreeWindowCoord.BasicTreeWindowCoord;
tell It;
makeTreeWindow #4935789195780038782
#mesquite.trees.BasicTreeWindowMaker.BasicTreeWindowMaker;
tell It;
    suppressEPCResponse;
    setTreeSource #mesquite.trees.StoredTrees.StoredTrees;
tell It;
    setTreeBlock 1;
    setTreeBlockID 015f92395fc81;
    toggleUseWeights off;
endTell;
setAssignedID 951.1509988117149.4318598956301169906;
getTreeWindow;
tell It;
    setExplanationSize 30;
    setAnnotationSize 20;
    setFontIncAnnot 0;
    setFontIncExp 0;
    setSize 1258 577;
    setLocation -8 -8;
    setFont SanSerif;
    setFontSize 10;
    getToolPalette;
tell It;
    setTool
mesquite.trees.BasicTreeWindowMaker.BasicTreeWindow.arrow;
endTell;
showPage 1;
 setActive;
getTreeDrawCoordinator
#mesquite.trees.BasicTreeDrawCoordinator.BasicTreeDrawCoordinator;
tell It;
suppress;
setTreeDrawer #mesquite.trees.SquareTree.SquareTree;
tell It;
    setNodeLocs
#mesquite.trees.NodeLocsStandard.NodeLocsStandard;

```

```

        tell It;
            branchLengthsToggle off;
            toggleScale on;
            toggleBroadScale off;
            toggleCenter off;
            toggleEven off;
            setFixedTaxonDistance 0;
        endTell;
        setEdgeWidth 6;
        orientUp;
        setCornerMode Right_Angle 50;
    endTell;
    setBackground White;
    setBranchColor Black;
    showNodeNumbers on;
    showBranchColors on;
    labelBranchLengths off;
    centerBrLenLabels on;
    showBrLensUnspecified on;
    showBrLenLabelsOnTerminals on;
    setBrLenLabelColor 0 0 255;
    setNumBrLenDecimals 6;
    desuppress;
    getEmployee
#mesquite.trees.BasicDrawTaxonNames.BasicDrawTaxonNames;
tell It;
    setColor Black;
    toggleColorPartition off;
    toggleColorAssigned on;
    toggleShadePartition off;
    toggleShowFootnotes on;
    toggleNodeLabels on;
    toggleCenterNodeNames off;
    toggleShowNames on;
    namesAngle ?>;
endTell;
endTell;
setTreeNumber 1;
setTree
'((((((((((1:28,2:11,3:11):3,4:14):46,(5:22,(6:77,7:5):3):3):30,(((8,9),10):3,(11:12,12:12,13:9,14:12):12):3,15:13):3):2
5,((16:9,17:4.5):18,18:(3):6):3,19:12):3,(20:28,21:28,22:3):12):3,((((((23:11,24:18):41,25:6):3,26:31):3,27:59):40,(((
28:3,29:8):3,30:11):3):5,31):5,32:5):19,33:19):20):3,34:30):14,35:5):3:';
setDrawingSizeMode 0;
toggleLegendFloat on;
scale 0;
toggleTextOnTree off;
togglePrintName on;
showWindow;
newAssistant
#mesquite.ancstates.TraceCharacterHistory.TraceCharacterHistory;
tell It;
suspend ;
setDisplayMode
#mesquite.ancstates.ShadeStatesOnTree.ShadeStatesOnTree;
tell It;
        toggleLabels off;
        togglePredictions off;
        toggleGray off;
endTell;
setHistorySource
#mesquite.ancstates.RecAncestralStates.RecAncestralStates;
tell It;
        getCharacterSource
#mesquite.charMatrices.CharSrcCoordObed.CharSrcCoordObed;
tell It;
        setCharacterSource
#mesquite.charMatrices.StoredCharacters.StoredCharacters;

```

```

                tell It;
                dataSet #9175578767526856009;
                endTell;
                endTell;
                setMethod
#mesquite.parsimony.ParsAncestralStates.ParsAncestralStates;
                tell It;
                setModelSource
#mesquite.parsimony.CurrentParsModels.CurrentParsModels;
                toggleMPRsMode off;
                getEmployee
#mesquite.parsimony.ParsimonySquared.ParsimonySquared;
                tell It;
                toggleWeight on;
                endTell;
                endTell;
                toggleShowSelectedOnly off;
                endTell;
                setCharacter 1;
                setMapping 1;
                toggleShowLegend on;
                setColorMode 0;
                toggleWeights on;
                setInitialOffsetX 4;
                setInitialOffsetY -309;
                setLegendWidth 142;
                setLegendHeight 132;
                resume ;
                endTell;
newAssistant #mesquite.trees.ValuesAtNodes.ValuesAtNodes;
                tell It;
                suppress;
                setNumForNodes #mesquite.cont.MapContinuous.MapContinuous;
                tell It;
                getCharacterSource
#mesquite.charMatrices.CharSrcCoordObed.CharSrcCoordObed;
                tell It;
                setCharacterSource
#mesquite.charMatrices.StoredCharacters.StoredCharacters;
                tell It;
                dataSet #9175578767526856009;
                endTell;
                endTell;
                setCharacter 1;
                setItem 0;
                getEmployee
#mesquite.parsimony.ParsAncestralStates.ParsAncestralStates;
                tell It;
                setModelSource
#mesquite.parsimony.CurrentParsModels.CurrentParsModels;
                toggleMPRsMode off;
                getEmployee
#mesquite.parsimony.ParsimonySquared.ParsimonySquared;
                tell It;
                toggleWeight on;
                endTell;
                endTell;
                endTell;
                setDisplay
#mesquite.trees.ShadeNumbersOnTree.ShadeNumbersOnTree;
                tell It;
                toggleLabels on;
                toggleLabelTerminals on;
                toggleColor on;
                toggleShade on;
                toggleRectangle off;
                toggleLog off;

```

```

        toggleDisplayPercentage off;
        setDigits 4;
    endTell;
    desuppress;
endTell;
newAssistant #mesquite.trees.ValuesAtNodes.ValuesAtNodes;
tell It;
suppress;
setNumForNodes #mesquite.cont.MapContinuous.MapContinuous;
tell It;
getCharacterSource
#mesquite.charMatrices.CharSrcCoordObed.CharSrcCoordObed;
tell It;
setCharacterSource
#mesquite.charMatrices.StoredCharacters.StoredCharacters;
tell It;
setDataSet #9175578767526856009;
endTell;
endTell;
setCharacter 1;
setItem 0;
getEmployee
#mesquite.parsimony.ParsAncestralStates.ParsAncestralStates;
tell It;
setModelSource
#mesquite.parsimony.CurrentParsModels.CurrentParsModels;
toggleMPRsMode off;
getEmployee
#mesquite.parsimony.ParsimonySquared.ParsimonySquared;
tell It;
toggleWeight on;
endTell;
endTell;
endTell;
setDisplay
#mesquite.trees.ShadeNumbersOnTree.ShadeNumbersOnTree;
tell It;
toggleLabels off;
toggleLabelTerminals on;
toggleColor on;
toggleShade on;
toggleRectangle off;
toggleLog off;
toggleDisplayPercentage off;
setDigits 4;
endTell;
desuppress;
endTell;
endTell;
desuppressEPCResponse;
getEmployee #mesquite.trees.ColorBranches.ColorBranches;
tell It;
setColor Red;
removeColor off;
endTell;
getEmployee #mesquite.ornamental.BranchNotes.BranchNotes;
tell It;
setAlwaysOn off;
endTell;
getEmployee
#mesquite.ornamental.ColorTreeByPartition.ColorTreeByPartition;
tell It;
colorByPartition off;
endTell;
getEmployee
#mesquite.ornamental.DrawTreeAssocDoubles.DrawTreeAssocDoubles;
tell It;

```

```

        setOn on;
        toggleShow consensusFrequency;
        toggleShow posteriorProbability;
        toggleShow bootstrapFrequency;
        toggleShow consensusFrequency;
        toggleShow posteriorProbability;
        toggleShow bootstrapFrequency;
        setDigits 4;
        setThreshold ?>;
        writeAsPercentage off;
        toggleCentred off;
        toggleHorizontal off;
        toggleWhiteEdges on;
        toggleShowOnTerminals on;
        setFontSize 10;
        setOffset 0 0;
    endTell;
    getEmployee
#mesquite.ornamental.DrawTreeAssocStrings.DrawTreeAssocStrings;
    tell It;
        setOn on;
        toggleCentred on;
        toggleHorizontal on;
        setFontSize 10;
        setOffset 0 0;
        toggleShowOnTerminals on;
    endTell;
    getEmployee #mesquite.trees.TreeInfoValues.TreeInfoValues;
    tell It;
        panelOpen false;
    endTell;
endTell;
getEmployee #mesquite.charMatrices.BasicDataWindowCoord.BasicDataWindowCoord;
tell It;
    showDataWindow #9175578767526856009
#mesquite.charMatrices.BasicDataWindowMaker.BasicDataWindowMaker;
    tell It;
        getWindow;
        tell It;
            setExplanationSize 30;
            setAnnotationSize 20;
            setFontIncAnnot 0;
            setFontIncExp 0;
            setSize 1258 577;
            setLocation -8 -8;
            setFont SanSerif;
            setFontSize 10;
            getToolPalette;
            tell It;
                setTool
mesquite.charMatrices.BasicDataWindowMaker.BasicDataWindow.ibeam;
        endTell;
        setTool
mesquite.charMatrices.BasicDataWindowMaker.BasicDataWindow.ibeam;
        colorCells #mesquite.charMatrices.NoColor.NoColor;
        colorRowNames
#mesquite.charMatrices.TaxonGroupColor.TaxonGroupColor;
        colorColumnNames
#mesquite.charMatrices.CharGroupColor.CharGroupColor;
        colorText #mesquite.charMatrices.NoColor.NoColor;
        setBackground White;
        toggleShowNames on;
        toggleShowTaxonNames on;
        toggleTight off;
        toggleThinRows off;
        toggleShowChanges on;

```

```

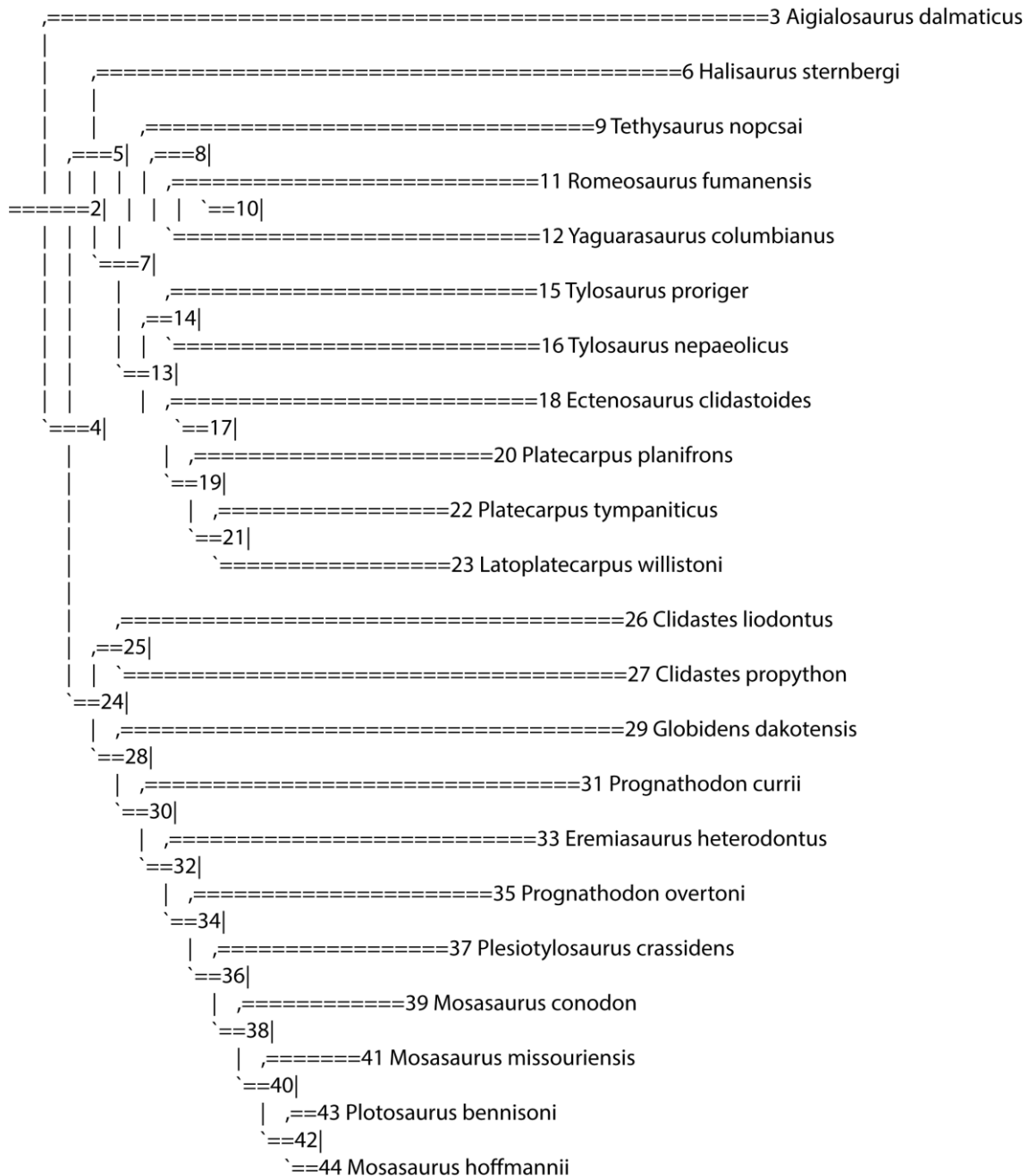
        toggleSeparateLines off;
        toggleShowStates on;
        toggleAutoWCharNames on;
        toggleAutoTaxonNames off;
        toggleShowDefaultCharNames off;
        toggleConstrainCW on;
        toggleBirdsEye off;
        toggleShowPaleGrid off;
        toggleShowPaleCellColors off;
        toggleShowPaleExcluded off;
        togglePaleInapplicable on;
        toggleShowBoldCellIText off;
        toggleAllowAutosize on;
        toggleColorsPanel off;
        toggleLinkedScrolling on;
        toggleScrollLinkedTables off;
    endTell;
    showWindow;
    getWindow;
    tell It;
        forceAutosize;
    endTell;
    getEmployee #mesquite.charMatrices.AlterData.AlterData;
    tell It;
        toggleBySubmenus off;
    endTell;
    getEmployee #mesquite.charMatrices.ColorByState.ColorByState;
    tell It;
        setStateLimit 9;
        toggleUniformMaximum on;
    endTell;
    getEmployee #mesquite.charMatrices.ColorCells.ColorCells;
    tell It;
        setColor Red;
        removeColor off;
    endTell;
    getEmployee #mesquite.charMatrices.AnnotPanel.AnnotPanel;
    tell It;
        togglePanel off;
    endTell;
    getEmployee
#mesquite.charMatrices.CharReferenceStrip.CharReferenceStrip;
    tell It;
        showStrip off;
    endTell;
    getEmployee #mesquite.charMatrices.SelSummaryStrip.SelSummaryStrip;
    tell It;
        showStrip off;
    endTell;
    getEmployee
#mesquite.cont.ItemsEditorForInfoPanel.ItemsEditorForInfoPanel;
    tell It;
        panelOpen false;
    endTell;
endTell;
endTell;
end;

```

Informação Suplementar S3- Mosasauroidea

Tree Description: (Aigialosaurus_dalmaticus:17,((Halisaurus_sternbergi:21,((Tethysaurus_nopcsai:6,(Romeosaurus_fumanensis:8,Yaguarasaurus_columbianus:4):3):6,((Tylosaurus_proriger:10,Tylosaurus_nepaeolicus:10):13,(Ectenosaurus_clidastoides:15,(Platecarpus_planifrons:5,(Platecarpus_tympaniticus:11,Latoplatecarpus_willistoni:5):13):3):3):3):3,((Clidastes_liodontus:15,Clidastes_propython:22):10,(Globidens_dakotensis:22,(Prognathodon_currii:19,(Eremiasaurus_heterodontus:25,(Prognathodon_overtoni:20,(Plesiotylosaurus_crassidens:21,(Mosasaurus_conodon:17,(Mosasaurus_missouriensis:11,(Plotosaurus_bennisoni:6,Mosasaurus_hoffmannii:6):11):3):3):3):3):3):3):8):3);

Tree with node numbers:



Supertree com os valores de cada táxon de Mosasauroidea e os valores ancestrais de cada nó interno construída no programa Mesquite versão 3.40.

----- Trace Character History -----

Character 1: Skull

Parsimony reconstruction (Squared) [Squared length: 0.05355828]

node 2: 1.52042771

node 3: 1.07

node 4: 1.59991496

node 5: 1.62752268

node 6: 1.53

node 7: 1.66906222

node 8: 1.62027034

node 9: 1.42

node 10: 1.69600957

node 11: 1.81

node 12: 1.74

node 13: 1.7349977

node 14: 1.90111047

node 15: 2.04

node 16: 1.89

node 17: 1.76259946

node 18: 1.85

node 19: 1.77272111

node 20: 1.81

node 21: 1.71965651

node 22: 1.74

node 23: 1.69

node 24: 1.73826034

node 25: 1.77617987

node 26: 1.81

node 27: 1.81

node 28: 1.77876399

node 29: 1.57

node 30: 1.84773547

node 31: 2.15

node 32: 1.86898096

node 33: 1.8

node 34: 1.89850417

node 35: 1.91

node 36: 1.92630301

node 37: 1.98

node 38: 1.94643085

node 39: 1.98

node 40: 1.96063472

node 41: 1.97

node 42: 2.0033503

node 43: 1.87

node 44: 2.16

#NEXUS

[written Wed May 30 21:33:17 BRT 2018 by Mesquite version 3.40 (build 877) at DESKTOP-M9K2NNB/192.168.0.10]

BEGIN TAXA;

TITLE Taxa;

DIMENSIONS NTAX=22;

TAXLABELS

Plotosaurus_bennisoni Mosasaurus_hoffmannii Mosasaurus_missouriensis Mosasaurus_conodon
 Plesiotylosaurus_crassidens Prognathodon_overtoni Eremiasaurus_heterodontus Prognathodon_currii
 Globidens_dakotensis Clidastes_liodontus Clidastes_propython Tethysaurus_nopcsai Romeosaurus_fumanensis
 Yaguarasaurus_columbianus Platecarpus_tympaniticus Latoplatecarpus_willistoni Platecarpus_planifrons
 Ectenosaurus_clidastoides Tylosaurus_proriger Tylosaurus_nepaeolicus Halisaurus_sternbergi
 Aigialosaurus_dalmaticus

;

END;

BEGIN CHARACTERS;

TITLE Character_Matrix;
 DIMENSIONS NCHAR=20;
 FORMAT DATATYPE = STANDARD GAP = - MISSING = ? SYMBOLS = " 0 1";
 MATRIX

Plotosaurus_bennisoni	11111111010000000001
Mosasaurus_hoffmannii	11111111010000000001
Mosasaurus_missouriensis	01111111010000000001
Mosasaurus_conodon	00111111010000000001
Plesiotylosaurus_crassidens	00011111010000000001
Prognathodon_overtoni	00001111010000000001
Eremiasaurus_heterodontus	00000111010000000001
Prognathodon_currii	00000011010000000001
Globidens_dakotensis	00000001010000000001
Clidastes_liodontus	00000000110000000001
Clidastes_propython	00000000110000000001
Tethysaurus_nopcsai	00000000000100000111
Romeosaurus_fumanensis	00000000001100000111
Yaguarasaurus_columbianus	00000000001100000111
Platecarpus_tympaniticus	00000000000011101111
Latoplatecarpus_willistoni	00000000000011101111
Platecarpus_planifrons	00000000000001101111
Ectenosaurus_clidastoides	00000000000000101111
Tylosaurus_proriger	00000000000000011111
Tylosaurus_nepaeolicus	00000000000000011111
Halisaurus_sternbergi	00000000000000000011
Aigialosaurus_dalmaticus	00000000000000000001

;

END;

BEGIN CHARACTERS;

TITLE Character_Matrix3;
 DIMENSIONS NCHAR=1;
 FORMAT DATATYPE = CONTINUOUS GAP = - MISSING = ?;
 CHARSTATELABELS

1	Skull	;
MATRIX		
Plotosaurus_bennisoni	1.87	
Mosasaurus_hoffmannii	2.16	
Mosasaurus_missouriensis	1.97	
Mosasaurus_conodon	1.98	
Plesiotylosaurus_crassidens	1.98	
Prognathodon_overtoni	1.91	
Eremiasaurus_heterodontus	1.8	

Prognathodon_currii	2.15
Globidens_dakotensis	1.57
Clidastes_liodontus	1.81
Clidastes_propython	1.81
Tethysaurus_nopcsai	1.42
Romeosaurus_fumanensis	1.81
Yaguarasaurus_columbianus	1.74
Platecarpus_tympaniticus	1.74
Latoplatecarpus_willistoni	1.69
Platecarpus_planifrons	1.81
Ectenosaurus_clidastoides	1.85
Tylosaurus_proriger	2.04
Tylosaurus_nepaeolicus	1.89
Halisaurus_sternbergi	1.53
Aigialosaurus_dalmaticus	1.07

;

END;

BEGIN ASSUMPTIONS;

TYPESET * UNTITLED (CHARACTERS = Character_Matrix) = unord: 1 - 20;

TYPESET * UNTITLED (CHARACTERS = Character_Matrix2) = unord: 1;

TYPESET * UNTITLED (CHARACTERS = Character_Matrix3) = Squared: 1;

END;

BEGIN MESQUITECHARMODELS;

ProbModelSet * UNTITLED (CHARACTERS = Character_Matrix) = 'Mk1 (est.)': 1 - 20;

ProbModelSet * UNTITLED (CHARACTERS = Character_Matrix2) = 'Mk1 (est.)': 1;

ProbModelSet * UNTITLED (CHARACTERS = Character_Matrix3) = Brownian_default: 1;

END;

BEGIN TREES[!Parameters: Tree search criterion: minimize Tree value using character matrix];

Title 'Trees from Mesquite's heuristic search';

ID 0163a698a5651;

LINK Taxa = Taxa;

TRANSLATE

[0]	1 Plotosaurus_bennisoni,
[1]	2 Mosasaurus_hoffmannii,
[2]	3 Mosasaurus_missouriensis,
[3]	4 Mosasaurus_conodon,
[4]	5 Plesiotylosaurus_crassidens,
[5]	6 Prognathodon_overtoni,
[6]	7 Eremiasaurus_heterodontus,
[7]	8 Prognathodon_currii,
[8]	9 Globidens_dakotensis,
[9]	10 Clidastes_liodontus,
[10]	11 Clidastes_propython,
[11]	12 Tethysaurus_nopcsai,
[12]	13 Romeosaurus_fumanensis,
[13]	14 Yaguarasaurus_columbianus,
[14]	15 Platecarpus_tympaniticus,
[15]	16 Latoplatecarpus_willistoni,
[16]	17 Platecarpus_planifrons,
[17]	18 Ectenosaurus_clidastoides,
[18]	19 Tylosaurus_proriger,
[19]	20 Tylosaurus_nepaeolicus,
[20]	21 Halisaurus_sternbergi,

[21] 22 Aigialosaurus_dalmaticus;

BEGIN TREES[!Parameters: Tree search criterion: minimize Tree value using character matrix];

Title Trees from Mesquite's heuristic search';

ID 0163a7eac1cd4;

LINK Taxa = Taxa;

TRANSLATE

- [0] 1 Plotosaurus_bennisoni,
- [1] 2 Mosasaurus_hoffmannii,
- [2] 3 Mosasaurus_missouriensis,
- [3] 4 Mosasaurus_conodon,
- [4] 5 Plesiotylosaurus_crassidens,
- [5] 6 Prognathodon_overtoni,
- [6] 7 Eremiasaurus_heterodontus,
- [7] 8 Prognathodon_currii,
- [8] 9 Globidens_dakotensis,
- [9] 10 Clidastes_liodontus,
- [10] 11 Clidastes_propython,
- [11] 12 Tethysaurus_nopcsai,
- [12] 13 Romeosaurus_fumanensis,
- [13] 14 Yaguarasaurus_columbianus,
- [14] 15 Platecarpus_tympaniticus,
- [15] 16 Latoplatecarpus_willistoni,
- [16] 17 Platecarpus_planifrons,
- [17] 18 Ectenosaurus_clidastoides,
- [18] 19 Tylosaurus_proriger,
- [19] 20 Tylosaurus_nepaeolicus,
- [20] 21 Halisaurus_sternbergi,
- [21] 22 Aigialosaurus_dalmaticus;

BEGIN TREES[!Parameters: Tree search criterion: minimize Tree value using character matrix];

Title Trees from Mesquite's heuristic search';

ID 0163acf9d8dd4;

LINK Taxa = Taxa;

TRANSLATE

- [0] 1 Plotosaurus_bennisoni,
- [1] 2 Mosasaurus_hoffmannii,
- [2] 3 Mosasaurus_missouriensis,
- [3] 4 Mosasaurus_conodon,
- [4] 5 Plesiotylosaurus_crassidens,
- [5] 6 Prognathodon_overtoni,
- [6] 7 Eremiasaurus_heterodontus,
- [7] 8 Prognathodon_currii,
- [8] 9 Globidens_dakotensis,
- [9] 10 Clidastes_liodontus,
- [10] 11 Clidastes_propython,
- [11] 12 Tethysaurus_nopcsai,
- [12] 13 Romeosaurus_fumanensis,
- [13] 14 Yaguarasaurus_columbianus,
- [14] 15 Platecarpus_tympaniticus,
- [15] 16 Latoplatecarpus_willistoni,
- [16] 17 Platecarpus_planifrons,
- [17] 18 Ectenosaurus_clidastoides,
- [18] 19 Tylosaurus_proriger,
- [19] 20 Tylosaurus_nepaeolicus,
- [20] 21 Halisaurus_sternbergi,

[21] 22 Aigialosaurus_dalmaticus;

BEGIN TREES[!Parameters: Tree search criterion: minimize Tree value using character matrix];

Title Trees from Mesquite's heuristic search';

ID 0163acf89267;

LINK Taxa = Taxa;

TRANSLATE

[0] 1 Plotosaurus_bennisoni,
[1] 2 Mosasaurus_hoffmannii,
[2] 3 Mosasaurus_missouriensis,
[3] 4 Mosasaurus_conodon,
[4] 5 Plesiotylosaurus_crassidens,
[5] 6 Prognathodon_overtoni,
[6] 7 Eremiasaurus_heterodontus,
[7] 8 Prognathodon_currii,
[8] 9 Globidens_dakotensis,
[9] 10 Clidastes_liodontus,
[10] 11 Clidastes_propython,
[11] 12 Tethysaurus_nopcsai,
[12] 13 Romeoosaurus_fumanensis,
[13] 14 Yaguarasaurus_columbianus,
[14] 15 Platecarpus_tympaniticus,
[15] 16 Latoplatecarpus_willistoni,
[16] 17 Platecarpus_planifrons,
[17] 18 Ectenosaurus_clidastoides,
[18] 19 Tylosaurus_proriger,
[19] 20 Tylosaurus_nepaeolicus,
[20] 21 Halisaurus_sternbergi,
[21] 22 Aigialosaurus_dalmaticus;

BEGIN TREES[!Parameters: Tree search criterion: minimize Tree value using character matrix];

Title Trees from Mesquite's heuristic search';

ID 0163b0ec32e86;

LINK Taxa = Taxa;

TRANSLATE

[0] 1 Plotosaurus_bennisoni,
[1] 2 Mosasaurus_hoffmannii,
[2] 3 Mosasaurus_missouriensis,
[3] 4 Mosasaurus_conodon,
[4] 5 Plesiotylosaurus_crassidens,
[5] 6 Prognathodon_overtoni,
[6] 7 Eremiasaurus_heterodontus,
[7] 8 Prognathodon_currii,
[8] 9 Globidens_dakotensis,
[9] 10 Clidastes_liodontus,
[10] 11 Clidastes_propython,
[11] 12 Tethysaurus_nopcsai,
[12] 13 Romeoosaurus_fumanensis,
[13] 14 Yaguarasaurus_columbianus,
[14] 15 Platecarpus_tympaniticus,
[15] 16 Latoplatecarpus_willistoni,
[16] 17 Platecarpus_planifrons,
[17] 18 Ectenosaurus_clidastoides,
[18] 19 Tylosaurus_proriger,
[19] 20 Tylosaurus_nepaeolicus,

[20] [21]

```
Begin MESQUITE;
MESQUITESCRIPTVERSION 2;
TITLE AUTO;
tell ProjectCoordinator;
timeSaved 1527726798141;
getEmployee #mesquite.minimal.ManageTaxa.ManageTaxa;
tell It;
    setID 0 468229581651728023;
endTell;
getEmployee #mesquite.charMatrices.ManageCharacters.ManageCharacters;
tell It;
    setID 0 7368728090070061898;
    mqVersion 340;
    checksumv 0 3 2327643616 null getNumChars 20 numChars 20 getNumTaxa 22
numTaxa 22 short true bits 3 states 3 sumSquaresStatesOnly 800.0 sumSquares 800.0 longCompressibleToShort
false usingShortMatrix true NumFiles 1 NumMatrices 3;
    mqVersion;
    setID 1 3038392112874669912;
    mqVersion 340;
    checksumv 1 3 2999280832 null getNumChars 1 numChars 1 getNumTaxa 22
numTaxa 22 short true bits 258 states 258 sumSquaresStatesOnly 66564.0 sumSquares 66564.0
longCompressibleToShort false usingShortMatrix true NumFiles 1 NumMatrices 3;
    mqVersion;
    setID 2 3412301690423095127;
    mqVersion 340;
    checksumv 2 3 1075056615 null numChars 1 numItems 1 min 1.07 max 2.16
sumSquares 72.53380000000001 NumFiles 1 NumMatrices 3;
    mqVersion;
endTell;
getWindow;
tell It;
    suppress;
    setResourcesState false false 4;
    setPopoutState 300;
    setExplanationSize 0;
    setAnnotationSize 0;
    setFontIncAnnot 0;
    setFontIncExp 0;
    setSize 679 640;
    setLocation 672 0;
    setFont SanSerif;
    setFontSize 10;
    getToolPalette;
    tell It;
    endTell;
    desuppress;
endTell;
getEmployee #mesquite.trees.BasicTreeWindowCoord.BasicTreeWindowCoord;
tell It;
    makeTreeWindow #468229581651728023
#mesquite.trees.BasicTreeWindowMaker.BasicTreeWindowMaker;
tell It;
    suppressEPCResponse;
    setTreeSource #mesquite.trees.StoredTrees.StoredTrees;
    tell It;
```

```

        setTreeBlock 5;
        setTreeBlockID 0163b0ec32e86;
        toggleUseWeights off;
    endTell;
    setAssignedID 1134.1527681750367.1367327869104515855;
    getTreeWindow;
    tell It;
        setExplanationSize 30;
        setAnnotationSize 20;
        setFontIncAnnot 0;
        setFontIncExp 0;
        setSize 675 568;
        setLocation 672 0;
        setFont SanSerif;
        setFontSize 10;
        getToolPalette;
        tell It;
            setTool
mesquite.trees.BranchLengthsAdjust.AdjustToolExtra.adjustor;
    endTell;
    showPage 1;
    getTreeDrawCoordinator
#mesquite.trees.BasicTreeDrawCoordinator.BasicTreeDrawCoordinator;
    tell It;
        suppress;
        setTreeDrawer #mesquite.trees.SquareLineTree.SquareLineTree;
        tell It;
            setNodeLocs
#mesquite.trees.NodeLocsStandard.NodeLocsStandard;
    tell It;
        branchLengthsToggle off;
        toggleScale on;
        toggleBroadScale off;
        toggleCenter on;
        toggleEven on;
        setFixedTaxonDistance 0;
    endTell;
    setEdgeWidth 4;
    showEdgeLines on;
    orientUp;
endTell;
setBackgroundColor White;
setBranchColor Black;
showNodeNumbers off;
showBranchColors on;
labelBranchLengths off;
centerBrLenLabels on;
showBrLensUnspecified on;
showBrLenLabelsOnTerminals on;
setBrLenLabelColor 0 0 255;
setNumBrLenDecimals 6;
desuppress;
getEmployee
#mesquite.trees.BasicDrawTaxonNames.BasicDrawTaxonNames;
tell It;
    setColor Black;
    toggleColorPartition off;
    toggleColorAssigned on;

```

```

        toggleShadePartition off;
        toggleShowFootnotes on;
        toggleNodeLabels on;
        toggleCenterNodeNames off;
        toggleShowNames on;
        namesAngle ?;
    endTell;
endTell;
setTreeNumber 1;
setTree
'(22:17,((21:21,((12:6,(13:8,14:4):3):6,((19:10,20:10):13,(18:15,(17:5,(15:11,16:5):13):3):3):3):3,((10:15,11:22):10
,(9:22,(8:19,(7:25,(6:20,(5:21,(4:17,(3:11,(1:6,2:6):11):3):3):3):3):3):8):3);"
        setDrawingSizeMode 0;
        toggleLegendFloat on;
        scale 0;
        toggleTextOnTree off;
        togglePrintName on;
        showWindow;
        newAssistant
#mesquite.ancstates.TraceCharacterHistory.TraceCharacterHistory;
    tell It;
        suspend ;
        setDisplayMode
#mesquite.ancstates.ShadeStatesOnTree.ShadeStatesOnTree;
    tell It;
        toggleLabels off;
        togglePredictions off;
        toggleGray off;
    endTell;
    setHistorySource
#mesquite.ancstates.RecAncestralStates.RecAncestralStates;
    tell It;
        getCharacterSource
#mesquite.charMatrices.CharSrcCoordObed.CharSrcCoordObed;
    tell It;
        setCharacterSource
#mesquite.charMatrices.StoredCharacters.StoredCharacters;
    tell It;
        setDataSet #3412301690423095127;
    endTell;
    setMethod
#mesquite.parsimony.ParsAncestralStates.ParsAncestralStates;
    tell It;
        setModelSource
#mesquite.parsimony.CurrentParsModels.CurrentParsModels;
        toggleMPRsMode off;
        getEmployee
#mesquite.parsimony.ParsimonySquared.ParsimonySquared;
    tell It;
        toggleWeight on;
    endTell;
    toggleShowSelectedOnly off;
endTell;
setCharacter 1;
setMapping 1;
toggleShowLegend on;

```

```

        setColorMode 0;
        toggleWeights on;
        setInitialOffsetX 4;
        setInitialOffsetY -308;
        setLegendWidth 142;
        setLegendHeight 308;
        resume ;
    endTell;
    endTell;
    desuppressEPCResponse;
    getEmployee #mesquite.trees.ColorBranches.ColorBranches;
    tell It;
        setColor Red;
        removeColor off;
    endTell;
    getEmployee #mesquite.ornamental.BranchNotes.BranchNotes;
    tell It;
        setAlwaysOn off;
    endTell;
    getEmployee
#mesquite.ornamental.ColorTreeByPartition.ColorTreeByPartition;
    tell It;
        colorByPartition off;
    endTell;
    getEmployee
#mesquite.ornamental.DrawTreeAssocDoubles.DrawTreeAssocDoubles;
    tell It;
        setOn on;
        toggleShow consensusFrequency;
        toggleShow bootstrapFrequency;
        toggleShow posteriorProbability;
        toggleShow consensusFrequency;
        toggleShow posteriorProbability;
        toggleShow bootstrapFrequency;
        setDigits 4;
        setThreshold ?>;
        writeAsPercentage off;
        toggleCentred off;
        toggleHorizontal on;
        toggleWhiteEdges on;
        toggleShowOnTerminals on;
        setFontSize 10;
        setOffset 0 0;
    endTell;
    getEmployee
#mesquite.ornamental.DrawTreeAssocStrings.DrawTreeAssocStrings;
    tell It;
        setOn on;
        toggleCentred on;
        toggleHorizontal on;
        setFontSize 10;
        setOffset 0 0;
        toggleShowOnTerminals on;
    endTell;
    getEmployee #mesquite.trees.TreeInfoValues.TreeInfoValues;
    tell It;
        panelOpen false;
endTell;

```

```
        endTell;
    endTell;
    getEmployee #mesquite.charMatrices.BasicDataWindowCoord.BasicDataWindowCoord;
    tell It;
        showDataWindow #7368728090070061898
#mesquite.charMatrices.BasicDataWindowMaker.BasicDataWindowMaker;
    tell It;
        getWindow;
    tell It;
        getTable;
    tell It;
        rowNamesWidth 156;
    endTell;
    setExplanationSize 30;
    setAnnotationSize 20;
    setFontIncAnnot 0;
    setFontIncExp 0;
    setSize 675 568;
    setLocation 672 0;
    setFont SanSerif;
    setFontSize 10;
    getToolPalette;
    tell It;
        setTool
mesquite.charMatrices.BasicDataWindowMaker.BasicDataWindow.ibeam;
    endTell;
    setTool
mesquite.charMatrices.BasicDataWindowMaker.BasicDataWindow.ibeam;
    colorCells #mesquite.charMatrices.NoColor.NoColor;
    colorRowNames
#mesquite.charMatrices.TaxonGroupColor.TaxonGroupColor;
    colorColumnNames
#mesquite.charMatrices.CharGroupColor.CharGroupColor;
    colorText #mesquite.charMatrices.NoColor.NoColor;
    setBackground White;
    toggleShowNames on;
    toggleShowTaxonNames on;
    toggleTight off;
    toggleThinRows off;
    toggleShowChanges on;
    toggleSeparateLines off;
    toggleShowStates on;
    toggleAutoWCharNames on;
    toggleAutoTaxonNames off;
    toggleShowDefaultCharNames off;
    toggleConstrainCW on;
    toggleBirdsEye off;
    toggleShowPaleGrid off;
    toggleShowPaleCellColors off;
    toggleShowPaleExcluded off;
    togglePaleInapplicable on;
    toggleShowBoldCellText off;
    toggleAllowAutosize on;
    toggleColorsPanel off;
    toggleDiagonal on;
    setDiagonalHeight 80;
    toggleLinkedScrolling on;
    toggleScrollLinkedTables off;
```

```

        endTell;
        showWindow;
        getWindow;
        tell It;
            forceAutosize;
        endTell;
        getEmployee #mesquite.charMatrices.AlterData.AlterData;
        tell It;
            toggleBySubmenus off;
        endTell;
        getEmployee #mesquite.charMatrices.ColorByState.ColorByState;
        tell It;
            setStateLimit 9;
            toggleUniformMaximum on;
        endTell;
        getEmployee #mesquite.charMatrices.ColorCells.ColorCells;
        tell It;
            setColor Red;
            removeColor off;
        endTell;
        getEmployee #mesquite.categ.StateNamesStrip.StateNamesStrip;
        tell It;
            showStrip off;
        endTell;
        getEmployee #mesquite.charMatrices.AnnotPanel.AnnotPanel;
        tell It;
            togglePanel off;
        endTell;
        getEmployee
#mesquite.charMatrices.CharReferenceStrip.CharReferenceStrip;
        tell It;
            showStrip off;
        endTell;
        getEmployee #mesquite.charMatrices.QuickKeySelector.QuickKeySelector;
        tell It;
            autotabOff;
        endTell;
        getEmployee #mesquite.charMatrices.SelSummaryStrip.SelSummaryStrip;
        tell It;
            showStrip off;
        endTell;
        getEmployee
#mesquite.categ.SmallStateNamesEditor.SmallStateNamesEditor;
        tell It;
            panelOpen true;
        endTell;
        endTell;
        showDataWindow #3038392112874669912
#mesquite.charMatrices.BasicDataWindowMaker.BasicDataWindowMaker;
        tell It;
            getWindow;
            tell It;
                setExplanationSize 30;
                setAnnotationSize 20;
                setFontIncAnnot 0;
                setFontIncExp 0;
                setSize 675 568;
                setLocation 672 0;

```

```

setFont SanSerif;
setFontSize 10;
getToolPalette;
tell It;
        setTool
mesquite.charMatrices.BasicDataWindowMaker.BasicDataWindow.ibeam;
        endTell;
        setTool
mesquite.charMatrices.BasicDataWindowMaker.BasicDataWindow.ibeam;
        colorCells #mesquite.charMatrices.NoColor.NoColor;
        colorRowNames
#mesquite.charMatrices.TaxonGroupColor.TaxonGroupColor;
        colorColumnNames
#mesquite.charMatrices.CharGroupColor.CharGroupColor;
        colorText #mesquite.charMatrices.NoColor.NoColor;
        setBackground White;
        toggleShowNames on;
        toggleShowTaxonNames on;
        toggleTight off;
        toggleThinRows off;
        toggleShowChanges on;
        toggleSeparateLines off;
        toggleShowStates on;
        toggleAutoWCharNames on;
        toggleAutoTaxonNames off;
        toggleShowDefaultCharNames off;
        toggleConstrainCW on;
        toggleBirdsEye off;
        toggleShowPaleGrid off;
        toggleShowPaleCellColors off;
        toggleShowPaleExcluded off;
        togglePaleInapplicable on;
        toggleShowBoldCellText off;
        toggleAllowAutosize on;
        toggleColorsPanel off;
        toggleDiagonal on;
        setDiagonalHeight 80;
        toggleLinkedScrolling on;
        toggleScrollLinkedTables off;
endTell;
getWindow;
tell It;
        forceAutosize;
endTell;
hideWindow;
getEmployee #mesquite.charMatrices.AlterData.AlterData;
tell It;
        toggleBySubmenus off;
endTell;
getEmployee #mesquite.charMatrices.ColorByState.ColorByState;
tell It;
        setStateLimit 9;
        toggleUniformMaximum on;
endTell;
getEmployee #mesquite.charMatrices.ColorCells.ColorCells;
tell It;
        setColor Red;
        removeColor off;

```

```

        endTell;
        getEmployee #mesquite.categ.StateNamesStrip.StateNamesStrip;
        tell It;
            showStrip off;
        endTell;
        getEmployee #mesquite.charMatrices.AnnotPanel.AnnotPanel;
        tell It;
            togglePanel off;
        endTell;
        getEmployee
#mesquite.charMatrices.CharReferenceStrip.CharReferenceStrip;
        tell It;
            showStrip off;
        endTell;
        getEmployee #mesquite.charMatrices.QuickKeySelector.QuickKeySelector;
        tell It;
            autotabOff;
        endTell;
        getEmployee #mesquite.charMatrices.SelSummaryStrip.SelSummaryStrip;
        tell It;
            showStrip off;
        endTell;
        getEmployee
#mesquite.categ.SmallStateNamesEditor.SmallStateNamesEditor;
        tell It;
            panelOpen true;
        endTell;
        endTell;
        showDataWindow #3412301690423095127
#mesquite.charMatrices.BasicDataWindowMaker.BasicDataWindowMaker;
        tell It;
            getWindow;
        tell It;
            getTable;
        tell It;
            rowNamesWidth 110;
        endTell;
        setExplanationSize 30;
        setAnnotationSize 20;
        setFontInAnnot 0;
        setFontInExp 0;
        setSize 675 568;
        setLocation 672 0;
        setFont SanSerif;
        setFontSize 10;
        getToolPalette;
        tell It;
            setTool
mesquite.charMatrices.BasicDataWindowMaker.BasicDataWindow.ibeam;
        endTell;
        setActive;
        setTool
mesquite.charMatrices.BasicDataWindowMaker.BasicDataWindow.ibeam;
        colorCells #mesquite.charMatrices.NoColor.NoColor;
        colorRowNames
#mesquite.charMatrices.TaxonGroupColor.TaxonGroupColor;
        colorColumnNames
#mesquite.charMatrices.CharGroupColor.CharGroupColor;

```

```

        colorText #mesquite.charMatrices.NoColor.NoColor;
        setBackground White;
        toggleShowNames on;
        toggleShowTaxonNames on;
        toggleTight off;
        toggleThinRows off;
        toggleShowChanges on;
        toggleSeparateLines off;
        toggleShowStates on;
        toggleAutoWCharNames on;
        toggleAutoTaxonNames off;
        toggleShowDefaultCharNames off;
        toggleConstrainCW on;
        toggleBirdsEye off;
        toggleShowPaleGrid off;
        toggleShowPaleCellColors off;
        toggleShowPaleExcluded off;
        togglePaleInapplicable on;
        toggleShowBoldCellText off;
        toggleAllowAutosize on;
        toggleColorsPanel off;
        toggleLinkedScrolling on;
        toggleScrollILinkedTables off;
    endTell;
    showWindow;
    getWindow;
    tell It;
        forceAutosize;
    endTell;
    getEmployee #mesquite.charMatrices.AlterData.AlterData;
    tell It;
        toggleBySubmenus off;
    endTell;
    getEmployee #mesquite.charMatrices.ColorByState.ColorByState;
    tell It;
        setStateLimit 9;
        toggleUniformMaximum on;
    endTell;
    getEmployee #mesquite.charMatrices.ColorCells.ColorCells;
    tell It;
        setColor Red;
        removeColor off;
    endTell;
    getEmployee #mesquite.charMatrices.AnnotPanel.AnnotPanel;
    tell It;
        togglePanel off;
    endTell;
    getEmployee
#mesquite.charMatrices.CharReferenceStrip.CharReferenceStrip;
    tell It;
        showStrip off;
    endTell;
    getEmployee #mesquite.charMatrices.SelSummaryStrip.SelSummaryStrip;
    tell It;
        showStrip off;
    endTell;
    getEmployee
#mesquite.cont.ItemsEditorForInfoPanel.ItemsEditorForInfoPanel;

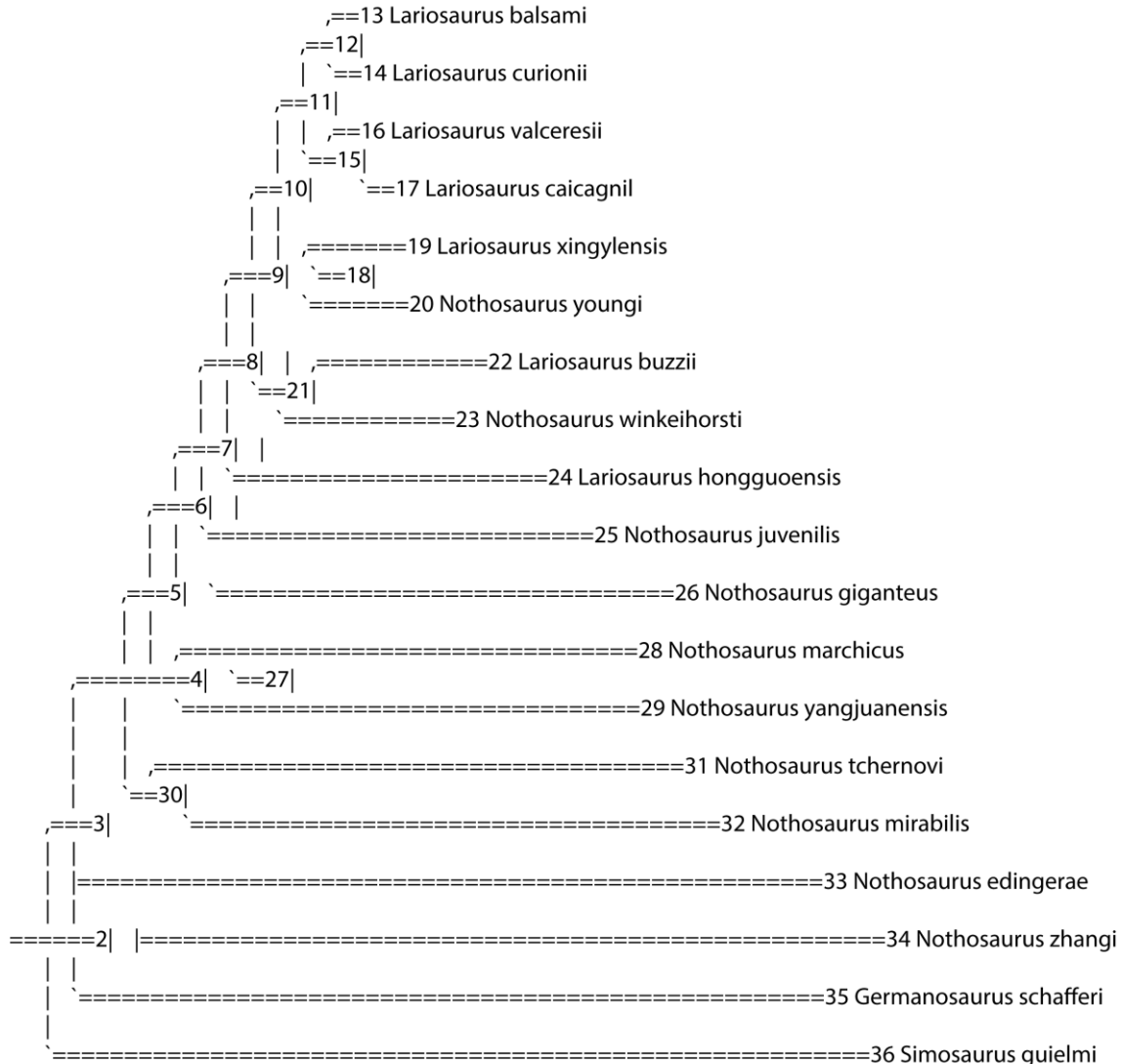
```

```
    tell It;
        panelOpen false;
    endTell;
endTell;
endTell;
end;
```

Informação Suplementar S3- Nothosauria

Tree Description: (((((((Lariosaurus_balsami:5,Lariosaurus_curionii:5):3,(Lariosaurus_valceresii,Lariosaurus_caicagnil:2.5):3):3,(Lariosaurus_xingylensis:5,Nothosaurus_youngi:5):6):3,(Lariosaurus_buzzii:10,Nothosaurus_winkeihorsti:10):5):3,Lariosaurus_hongguoensis:13):3,Nothosaurus_juvenilis:19):3,Nothosaurus_giganteus:25):3,(Nothosaurus_marchicus:10,Nothosaurus_yangjuanensis:5):17):3,(Nothosaurus_tchernovi:7,Nothosaurus_mirabilis:10):21),Nothosaurus_edingerae,Nothosaurus_zhangi,Germanosaurus_schafferi):3,Simosaurus_guielmi:37);

Tree with node numbers:



Supertree com os valores de cada táxon de Nothosauria e os valores ancestrais de cada nó interno construída no programa Mesquite versão 3.40.

----- Trace Character History -----

Character 1: Character 1

Parsimony reconstruction (Squared) [Squared length: 0.30753119]

node 2: 1.42118305

node 3: 1.42857627

node 4: 1.4167695

node 5: 1.37358629
node 6: 1.32650597
node 7: 1.21780637
node 8: 1.12770777
node 9: 1.0670802
node 10: 1.08357669
node 11: 1.0607473
node 12: 0.9785215
node 13: 1.02
node 14: 0.8
node 15: 1.12014371
node 16: 1.12
node 17: 1.17
node 18: 1.16222844
node 19: 1.18
node 20: 1.21
node 21: 0.9385401
node 22: 0.96
node 23: 0.66
node 24: 1
node 25: 1.1
node 26: 1.84
node 27: 1.39566988
node 28: 1.12
node 29: 1.54
node 30: 1.47110975
node 31: 1.49
node 32: 1.47
node 33: 1.11
node 34: 1.81
node 35: 1.38
node 36: 1.33

NEXUS

[written Thu Jul 19 13:09:22 BRT 2018 by Mesquite version 3.40 (build 877) at DESKTOP-M9K2NNB/192.168.0.10]

BEGIN TAXA;

TITLE Untitled_Block_of_Taxa;
DIMENSIONS NTAX=19;
TAXLABELS
Lariosaurus_balsami
Lariosaurus_curionii Lariosaurus_valceresii Lariosaurus_caicagnil Lariosaurus_xingylensis Nothosaurus_youngi
Lariosaurus_buzzii Nothosaurus_winkeihorsti Lariosaurus_hongguoensis Nothosaurus_juvenilis
Nothosaurus_giganteus Nothosaurus_marchicus Nothosaurus.yangjuanensis Nothosaurus_tchernovi
Nothosaurus_mirabilis Nothosaurus_edingerae Nothosaurus_zhangi Germanosaurus_schafferi Simosaurus_guielmi
;

END;

BEGIN CHARACTERS;

TITLE Character_Matrix;
DIMENSIONS NCHAR=1;
FORMAT DATATYPE =

CONTINUOUS GAP = - MISSING = ?;

MATRIX
Lariosaurus_balsami 1.02

```

Lariosaurus_curionii      0.8
Lariosaurus_valceresii    1.12
Lariosaurus_caicagnil     1.17
Lariosaurus_xingylensis   1.18
Nothosaurus_youngi        1.21
Lariosaurus_buzzii        0.96
Nothosaurus_winkeihorsti  0.66
Lariosaurus_hongguoensis  1.0
Nothosaurus_juvenilis     1.1
Nothosaurus_giganteus    1.84
Nothosaurus_marchicus    1.12
Nothosaurus.yangjuanensis 1.54
Nothosaurus_tchernovi     1.49
Nothosaurus_mirabilis    1.47
Nothosaurus_edingerae    1.11
Nothosaurus_zhangi        1.81
Germanosaurus_schafferi   1.38
Simosaurus_guielmi        1.33
;

END;
BEGIN TREES;
"filogenianotossauros.tree";

```

```

Title Trees from
ID 015f58ede7ef1;
LINK Taxa = Untitled_Block_of_Taxa;
TRANSLATE
[0] 1 Lariosaurus_balsami,
[1] 2 Lariosaurus_curionii,
[2] 3 Lariosaurus_valceresii,
[3] 4 Lariosaurus_caicagnil,
[4] 5 Lariosaurus_xingylensis,
[5] 6 Nothosaurus_youngi,
[6] 7 Lariosaurus_buzzii,
[7] 8 Nothosaurus_winkeihorsti,
[8] 9 Lariosaurus_hongguoensis,
[9] 10 Nothosaurus_juvenilis,
[10] 11 Nothosaurus_giganteus,
[11] 12 Nothosaurus_marchicus,
[12] 13 Nothosaurus.yangjuanensis,
[13] 14 Nothosaurus_tchernovi,
[14] 15 Nothosaurus_mirabilis,
[15] 16 Nothosaurus_edingerae,
[16] 17 Nothosaurus_zhangi,
[17] 18 Germanosaurus_schafferi,
[18] 19 Simosaurus_guielmi;
TREE 'PAUP_1' =
((((((((((1,2),(3,4)),(5,6)),(7,8)),9),10),11),(12,13)),(14,15)),16,17,18),19);

```

```

END;

```

```

BEGIN ASSUMPTIONS;

```

```

TYPESET * UNTITLED = Squared:
1;

```

```

END;

```

```

BEGIN MESQUITECHARMODELS;
ProbModelSet * UNTITLED =
Brownian_default: 1;
END;

Begin MESQUITE;
MESQUITESCRIPTVERSION 2;
TITLE AUTO;
tell ProjectCoordinator;
timeSaved 1532016563023;
getEmployee

#mesquite.minimal.ManageTaxa.ManageTaxa;
tell It;
setID 0

3575276788517179732;
endTell;
getEmployee

#mesquite.charMatrices.ManageCharacters.ManageCharacters;
tell It;
setID 0

6206891594224781980;
mqVersion 340;
checksumv 0 3 2629811336

null numChars 1 numItems 1 min 0.66 max 1.84 sumSquares 30.30149999999994 NumFiles 1 NumMatrices
1;
mqVersion;
endTell;
getWindow;
tell It;
suppress;
setResourcesState false false

17;
setPopoutState 300;
setExplanationSize 0;
setAnnotationSize 0;
setFontIncAnnot 0;
setFontIncExp 0;
setSize 1366 649;
 setLocation -8 -8;
setFont SanSerif;
setFontSize 10;
getToolPalette;
tell It;
endTell;
desuppress;

#mesquite.trees.BasicTreeWindowCoord.BasicTreeWindowCoord;
endTell;
getEmployee

#mesquite.trees.BasicTreeWindowCoord.BasicTreeWindowCoord;
tell It;
makeTreeWindow

#3575276788517179732 #mesquite.trees.BasicTreeWindowMaker.BasicTreeWindowMaker;
tell It;

suppressEPCResponse;
setTreeSource

#mesquite.trees.StoredTrees.StoredTrees;
tell It;

```

```
setTreeBlock 1;

setTreeBlockID 015f58ede7ef1;

toggleUseWeights off;
endTell;
setAssignedID

951.1509025517989.2167087018468276849;
getTreeWindow;
tell It;

setExplanationSize 30;

setAnnotationSize 20;

setFontIncAnnot 0;

setFontIncExp 0;
setSize

1349 577;
setLocation -8 -8;
setFont

SanSerif;
setFontSize 10;

getToolPalette;
tell It;

setTool
mesquite.trees.BasicTreeWindowMaker.BasicTreeWindow.arrow;
endTell;

showPage 1;

setActive;

getTreeDrawCoordinator
#mesquite.trees.BasicTreeDrawCoordinator.BasicTreeDrawCoordinator;
tell It;
suppress;

setTreeDrawer
#mesquite.trees.SquareLineTree.SquareLineTree;
tell It;

setNodeLocs
#mesquite.trees.NodeLocsStandard.NodeLocsStandard;
tell It;

branchLengthsToggle off;

toggleScale on;

toggleBroadScale off;
```

```
        toggleCenter on;  
        toggleEven on;  
        setFixedTaxonDistance 0;  
        endTell;  
        setEdgeWidth 4;  
        showEdgeLines on;  
        orientUp;  
        endTell;  
  
        setBackground White;  
        setBranchColor Black;  
        showNodeNumbers on;  
        showBranchColors on;  
        labelBranchLengths off;  
        centerBrLenLabels on;  
        showBrLensUnspecified on;  
        showBrLenLabelsOnTerminals on;  
        setBrLenLabelColor 0 0 255;  
        setNumBrLenDecimals 6;  
        desuppress;  
        getEmployee  
#mesquite.trees.BasicDrawTaxonNames.BasicDrawTaxonNames;  
        tell It;  
  
        setColor Black;  
        toggleColorPartition off;  
        toggleColorAssigned on;  
        toggleShadePartition off;  
        toggleShowFootnotes on;  
        toggleNodeLabels on;  
        toggleCenterNodeNames off;  
        toggleShowNames on;
```

```

namesAngle ?;
    endTell;
endTell;

setTreeNumber 1;
    setTree
'((((((((((1:5,2:5):3,(3,4:2.5):3):3,(5:5,6:5):6):3,(7:10,8:10):5):3,9:13):3,10:19):3,11:25):3,(12:10,13:5):17):3,(14:7,15
:10):21),16,17,18):3,19:37);;

setDrawingSizeMode 0;
    toggleLegendFloat on;
        scale 0;

toggleTextOnTree off;
    togglePrintName on;
    showWindow;
    newAssistant
    tell It;
        suspend ;

setDisplayMode
    tell It;

toggleLabels off;
    togglePredictions off;
    toggleGray off;
        endTell;

setHistorySource
    tell It;

getCharacterSource
    tell It;

setCharacterSource
    tell It;
        dataSet #6206891594224781980;

endTell;
endTell;

```

```

setMethod
#mesquite.parsimony.ParsAncestralStates.ParsAncestralStates;

tell It;

setModelSource
#mesquite.parsimony.CurrentParsModels.CurrentParsModels;

toggleMPRsMode off;

getEmployee
#mesquite.parsimony.ParsimonySquared.ParsimonySquared;

tell It;

toggleWeight on;

endTell;
endTell;

toggleShowSelectedOnly off;
endTell;

setCharacter 1;

setMapping 1;

toggleShowLegend on;

setColorMode 0;

toggleWeights on;

setInitialOffsetX 4;

setInitialOffsetY -343;

setLegendWidth 110;

setLegendHeight 308;
resume ;
endTell;

newAssistant
#mesquite.trees.ValuesAtNodes.ValuesAtNodes;

tell It;
suppress;

setNumForNodes
#mesquite.cont.MapContinuous.MapContinuous;

tell It;

getCharacterSource
#mesquite.charMatrices.CharSrcCoordObed.CharSrcCoordObed;

tell It;

```

```
        setCharacterSource
#mesquite.charMatrices.StoredCharacters.StoredCharacters;

        tell It;

        setDataSet #6206891594224781980;

        endTell;

        endTell;

        setCharacter 1;

        setItem 0;

        getEmployee

#mesquite.parsimony.ParsAncestralStates.ParsAncestralStates;

        tell It;

        setModelSource

#mesquite.parsimony.CurrentParsModels.CurrentParsModels;

        toggleMPRsMode off;

        getEmployee

#mesquite.parsimony.ParsimonySquared.ParsimonySquared;

        tell It;

        toggleWeight on;

        endTell;

        endTell;

        endTell;

#mesquite.trees.ShadeNumbersOnTree.ShadeNumbersOnTree;

        setDisplay

        tell It;

        toggleLabels on;

        toggleLabelTerminals on;

        toggleColor on;

        toggleShade on;

        toggleRectangle on;

        toggleLog off;

        toggleDisplayPercentage off;

        setDigits 4;

        endTell;
```

```

        setInitialOffsetX 77;
        setInitialOffsetY -254;
        desuppress;
            endTell;
            endTell;

        desuppressEPCResponse;
            getEmployee
            tell It;
            setColor

#mesquite.trees.ColorBranches.ColorBranches;
    Red;
        removeColor off;
            endTell;
            getEmployee
            tell It;

        setAlwaysOn off;
            endTell;
            getEmployee
            tell It;

        colorByPartition off;
            endTell;
            getEmployee
            tell It;
            setOn on;

#mesquite.ornamental.BranchNotes.BranchNotes;
#mesquite.ornamental.ColorTreeByPartition.ColorTreeByPartition;
#mesquite.ornamental.DrawTreeAssocDoubles.DrawTreeAssocDoubles;
    4;
        toggleShow consensusFrequency;
        toggleShow posteriorProbability;
        toggleShow bootstrapFrequency;
        toggleShow consensusFrequency;
        toggleShow posteriorProbability;
        toggleShow bootstrapFrequency;
            setDigits
            setThreshold ?;
            writeAsPercentage off;
            toggleCentred off;
            toggleHorizontal on;
            toggleWhiteEdges on;

```

```

        toggleShowOnTerminals on;

        setFontSize 10;
        setOffset
0 0;
        endTell;
        getEmployee

#mesquite.ornamental.DrawTreeAssocStrings.DrawTreeAssocStrings;
        tell It;
        setOn on;

        toggleCentred on;

        toggleHorizontal on;

        setFontSize 10;
        setOffset
0 0;
        endTell;
        getEmployee

#mesquite.trees.TreeInfoValues.TreeInfoValues;
        tell It;

        panelOpen false;
        endTell;
        endTell;
        endTell;
        getEmployee

#mesquite.charMatrices.BasicDataWindowCoord.BasicDataWindowCoord;
        tell It;
        showDataWindow
#6206891594224781980 #mesquite.charMatrices.BasicDataWindowMaker.BasicDataWindowMaker;
        tell It;
        getWindow;
        tell It;

        setExplanationSize 30;

        setAnnotationSize 20;

        setFontIncAnnot 0;

        setFontIncExp 0;
        setSize
1349 577;
        setLocation -8 -8;
        setFont
SanSerif;

        setFontSize 10;

        getToolPalette;
        tell It;

```

```
        setTool
mesquite.charMatrices.BasicDataWindowMaker.BasicDataWindow.ibeam;
                                endTell;
                                setTool
mesquite.charMatrices.BasicDataWindowMaker.BasicDataWindow.ibeam;

                                colorCells
#mesquite.charMatrices.NoColor.NoColor;

                                colorRowNames
#mesquite.charMatrices.TaxonGroupColor.TaxonGroupColor;

                                colorColumnNames
#mesquite.charMatrices.CharGroupColor.CharGroupColor;
                                colorText
#mesquite.charMatrices.NoColor.NoColor;

                                setBackground White;
                                toggleShowNames on;
                                toggleShowTaxonNames on;
                                toggleTight off;
                                toggleThinRows off;
                                toggleShowChanges on;
                                toggleSeparateLines off;
                                toggleShowStates on;
                                toggleAutoWCharNames on;
                                toggleAutoTaxonNames off;
                                toggleShowDefaultCharNames off;
                                toggleConstrainCW on;
                                toggleBirdsEye off;
                                toggleShowPaleGrid off;
                                toggleShowPaleCellColors off;
                                toggleShowPaleExcluded off;
                                togglePaleInapplicable on;
                                toggleShowBoldCellText off;
                                toggleAllowAutosize on;
                                toggleColorsPanel off;
```

```
        toggleLinkedScrolling on;
        toggleScrollLinkedTables off;
            endTell;
            showWindow;
            getWindow;
            tell It;

        forceAutosize;
            endTell;
            getEmployee
            tell It;

        toggleBySubmenus off;
            endTell;
            getEmployee
            tell It;

        setStateLimit 9;

        toggleUniformMaximum on;
            endTell;
            getEmployee
            tell It;
            setColor

#mesquite.charMatrices.AlterData.AlterData;
    Red;
    removeColor off;
        endTell;
        getEmployee
        tell It;

#mesquite.charMatrices.AnnotPanel.AnnotPanel;
    togglePanel off;
        endTell;
        getEmployee
        tell It;

#mesquite.charMatrices.CharReferenceStrip.CharReferenceStrip;
    showStrip off;
        endTell;
        getEmployee
        tell It;

#mesquite.charMatrices.SelSummaryStrip.SelSummaryStrip;
    showStrip off;
        endTell;
        getEmployee
        tell It;

#mesquite.cont.ItemsEditorForInfoPanel.ItemsEditorForInfoPanel;
    panelOpen false;
        endTell;
        endTell;
```

```
end;  
endTell;  
endTell;
```